Review

Metal Nanozymes: New Horizons in Cellular Homeostasis Regulation

Hanna Lewandowska [1,*] , Karolina Wójciuk [2] and Urszula Karczmarczyk [3,*]

1. Institute of Nuclear Chemistry and Technology, 16 Dorodna St., 03-195 Warsaw, Poland
2. National Centre for Nuclear Research, Andrzeja Soltana 7, 05-400 Otwock, Poland; karolina.wojciuk@ncbj.gov.pl
3. Radioisotope Centre POLATOM, National Centre for Nuclear Research, Andrzeja Sołtana 7, 05-400 Otwock, Poland
* Correspondence: h.lewandowska@ichtj.waw.pl (H.L.); urszula.karczmarczyk@polatom.pl (U.K.)

Abstract: Nanomaterials with enzyme-like activity (nanozymes) have found applications in various fields of medicine, industry, and environmental protection. This review discusses the use of nanozymes in the regulation of cellular homeostasis. We also review the latest biomedical applications of nanozymes related to their use in cellular redox status modification and detection. We present how nanozymes enable biomedical advances and demonstrate basic design strategies to improve diagnostic and therapeutic efficacy in various diseases. Finally, we discuss the current challenges and future directions for developing nanozymes for applications in the regulation of the redox-dependent cellular processes and detection in the cellular redox state changes.

Keywords: metals; metal oxides; metal nanozymes; homeostasis; oxidative stress

1. Introduction

Nanomaterials with enzyme-like activity, generally referred to as "nanozymes", have innumerable potential in various fields of biomedicine. Nanoparticles that can functionally mimic the activity of cellular antioxidant enzymes are of great interest because of their possible therapeutic potential in oxidative stress-related disorders.

Since natural enzymes are proteins, their production and storage are difficult and expensive. Their instability during transfer, modification, and, very often, incompatibility with desired activity conditions limits their use. In addition, there are more and more new needs related to the development of medical knowledge. Meanwhile, designing ab initio a new protein structure that would meet the expected steric and catalytic requirements is beyond the possibilities of modern science. After systematically examining the structure-function relationship of natural enzymes, researchers hypothesized that the rational assembly of functional atoms or molecules could generate similar catalytic activities on enzyme substrates and represent a self-assembled system that mimics the enzyme [1–3]. Recent advances in nanotechnology have given rise to developments in this direction and have allowed scientists' access to an ever-evolving set of artificial enzymes. The nanozyme concept has revolutionized our basic understanding of biology and chemistry, facilitating many applications in the fields of biodetection, biology, and medicine (Figure 1) [4–6]. Nanoenzymes have also found numerous applications as catalysts for chemical reactions in the industry [7], wastewater treatment [8], diagnostics [9,10], and others [11].

This review discusses the use of nanozymes in regulating the cellular redox status and thus cell signaling pathways modulation. We also review the latest biomedical applications of nanozymes related to their use in cellular redox status modification and detection. We present how nanozymes enable biomedical advances and demonstrate basic design strategies to improve diagnostic and therapeutic efficacy in various diseases. We discuss the current challenges and future directions in developing nanozymes for regulation of the

redox-dependent cellular processes and detection in the cellular redox state changes. It should be noted that the purpose of this review is not to exhaustively cover all the work performed to date in the field of nanozymes in cellular applications. It would be very difficult at present, due to the large amount of work in this field, which is constantly growing exponentially. The authors aimed only to outline the most promising and surprising directions of research that allow discovering the potential hidden in these seemingly simple structures, which are nanoparticles of metals and their oxides.
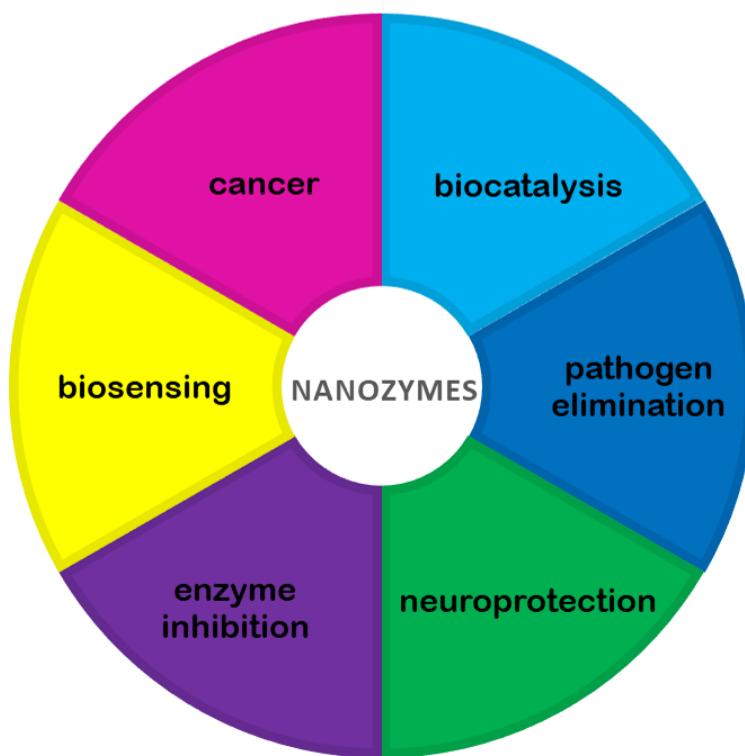

Figure 1. The emerging roles of nanozymes in cellular biology.

2. A Short History of Nanozymes

The term "artificial enzyme" was used by Ronald Breslow in 1970 for a chemical structure combining a metal catalytic group and a hydrophobic binding cavity of a polysaccharide [12], while the term "nanozyme" was first used in 2004 by Manea et al. for triazacyclonane-functionalized gold nanoparticles that have been used as catalysts for phosphate ester transphosphorylation [13]. The essence of the catalytic action of this enzyme boils down to the interaction of Zn^{2+} ions on the surface of gold nanoparticles and inspired researchers in this developing field. Another example of using catalytic systems with an activity similar to the enzyme is described in 2007 by Gao et al. [14], where the intrinsic enzyme peroxidase-like activity of magnetic nanoparticles (Fe_3O_4) was utilized in an immunoassay. This discovery used the same element atoms with different valences on the nanoparticle surface for catalytic reactions. In addition, numerous studies have revealed that various metal and metal oxide nanoparticles (such as iron, cerium, and gold oxide nanoparticles), carbon nanomaterials (including carbon nanotubes and graphene oxide), and many organometallic structures exhibit excellent catalytic properties by mimicking structures or functions of natural enzymes [4,15,16]. Together, these nanozyme systems offer higher catalytic stability, ease of modification, and lower production costs in a variety of biomedical applications compared to natural enzymes (see, e.g., [4,15,17,18]).

Nanozymes can be divided into three categories according to material types: metal-based nanozymes (e.g., gold, platinum, and cobalt), metal oxides or metal sulfide nanozymes (e.g., ferric oxide, cerium dioxide, vanadiumpentoxide, and iron sulfide), and carbon-based

nanozymes, (e.g., fullerenes, graphene, and carbon dots). Herein, according to the keynote of the special edition, we focus on the metal- and metal-oxide-based nanozymes. The catalytic reaction of nanozymes is like that of natural enzymes, which conforms to the kinetic curve of Michaelis–Menten equation. Kinetics analysis performed by researchers [19–23] indicated that nanozymes showed typical Michaelis−Menten behavior toward H_2O_2, TMB (3,3,5,5-tetramethylbenzidine) glucose and other substrates. The selected examples of the K_m (Michaelis–Menten constant) values and V_{max} (maximum rate) of the reaction for certain substrates are shown in Table 1 (see also [19]).

Table 1. Comparison of the Km and Vmax of selected nanozymes.

Nanozymes	Substrate	K_m (mM)	Vmax (M $\times$ s^{-1})	Ref.
V$_2$O$_5$	TMB	0.738	1.85×10^{-5}	[21]
	H$_2$O$_2$	0.232	1.29×10^{-5}	
Fe$_3$O$_4$ MNPs	TMB	0.434	10.00×10^{-8}	[21]
	H$_2$O$_2$	154	9.78×10^{-8}	
MOF(Co/2Fe0)	TMB	0.25	0.38×10^{-7}	[20]
	H$_2$O$_2$	4.22	0.49×10^{-7}	
AuNPs	glucose	0.41	0.10×10^{-6}	[22]
ZnO	starch	0.022	1.81×10^{-6}	[23]
GOx-Fe^0@EM-A	H$_2$O$_2$	29.59	3.81×10^{-8}	[24]

TMB—3,3,5,5-tetramethylbenzidine, K_m—Michaelis–Menten constant, V_{max}—maximum rate.

The redox properties of metal and metaloxide nanozymes are mainly responsible for their regulatory action, analogous to natural enzymes containing metal centers. Recently, however, the possibility of regulating their auxiliary properties, such as lipophilicity, stereospecificity, and the ability to respond to destination-specific stimuli, has gained increasing importance. Similar to natural enzymes, the activities of nanozymes can be tuned by many factors, such as pH [25,26], temperature [26], surrounding environment [27], and the type of the metal ion [26]. One class of such easily tunable substances are organometallic frameworks (MOFs). They are a class of coordination polymers containing metal ions/clusters linked by coordination bonds with organic ligands organized into a repeating structure and have aroused great interest in researchers over the past decades. It must be mentioned that the particular interest in MOFs is not only due to their catalytic activity but also to their regulated structures and morphologies, excellent surface areas, high porosity and crystallinity, high loading capacity, thermal/chemical stability, and tunable affinity, which makes them functionally even more similar to natural enzymes. Studies of activities mimicking the enzymes of catalytic nanoparticles based on metals and their oxides gained popularity in the last decade and are currently in the phase of exponential growth (Figure 2).
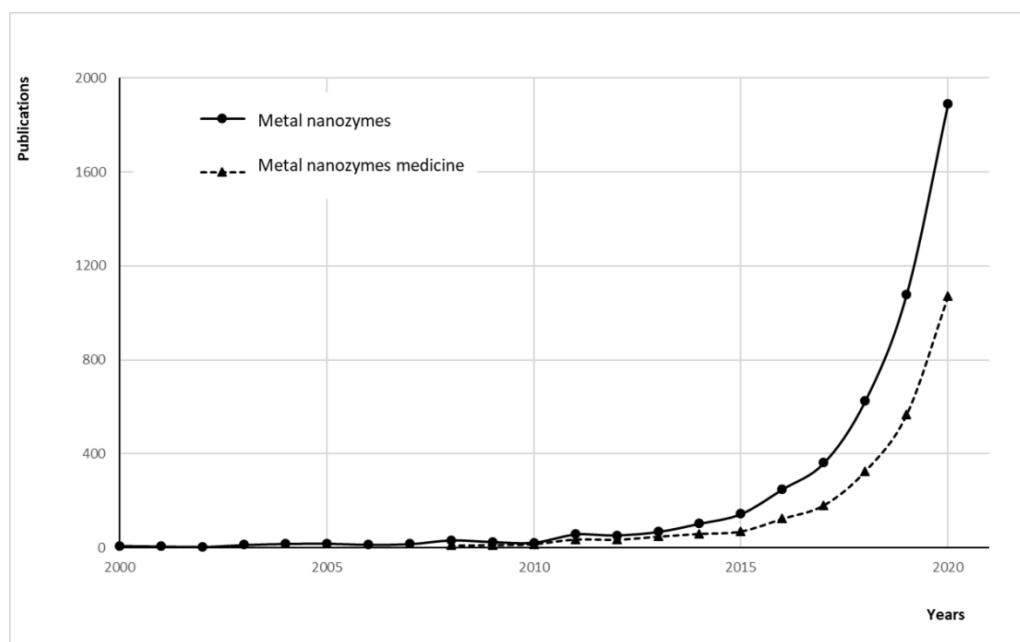
Figure 2. Studies of activities mimicking the enzymes of catalytic nanoparticles based on metals and their oxides gain popularity. The graph denotes the number of publications on 'metal nanozymes' and 'metal nanozymes medicine' cited in Google Scholar by year.

3. Mechanisms of Pro-Oxidative and Antioxidant Action of Nanozymes

Reactive oxygen species (ROS) such as $O_2^{\bullet-}$, $^{\bullet}OH$, and H_2O_2 are natural byproducts of cellular metabolism [28]. Low ROS levels can serve as important transmitters in cell signaling and participate in many signaling processes [29]. However, overexpression of ROS leads to many undesirable effects, such as oxidative damage to lipids, proteins, DNA, and other biological molecules. Moreover, ROS can induce caspase to activate cell apoptosis [30–34]. Therefore, ROS overexpression is associated with many pathological conditions such as neurodegeneration, cancer, diabetes, atherosclerosis, arthritis, and kidney disease [35], contributing to aging and death. Therefore, the regulation of ROS levels is of great importance in maintaining intracellular redox homeostasis.

It is assumed that the cytotoxicity of nanoparticles results from oxidative stress induction. Its mechanisms are well known and described in the literature. Nanomaterials can generate and induce ROS production through various mechanisms. Radicals such as $O_2^{\bullet-}$, $^{\bullet}OH$, $SiO^{\bullet}$, or $TiO^{\bullet}$ may be present on the surface of the nanomaterial. These, in turn, can generate secondary ROS. The nanomaterial surface may also contain structural defects inducing the formation of reactive groups [36], as well as transition metals that can generate ROS by Fenton and Haber–Weiss type reactions [37]. In addition, environmental oxidants such as ozone, semiquinones, and NO can adsorb to the nanomaterial surface and enter cells through the so-called "Trojan horse effect" [37]. Nanomaterials may also indirectly enable the production of ROS by triggering cellular mechanisms. For example, damage to or activation of mitochondria can lead to the release of ROS produced by the mitochondrial electron transport chain [38], structural damage, activation of nicotinamide adenine dinucleotide phosphate (NADPH) oxidase-like enzyme activity, and via irreversible membrane potential loss in the mitochondria [39,40]. The native NADPH oxidase can also be activated by nanomaterials, as shown for ZnO NP [41]. This membrane-bound enzyme is highly expressed in neutrophils and macrophages, where it induces the so-called oxygen burst, designed to kill invading microorganisms by producing ROS. Nanomaterials can activate inflammatory cells, inducing oxygen burst in the absence of pathogens [42]. Macrophage activation is a particularly important mechanism for ROS production by the so-called long aspect ratio nanomaterials, as long, thin, and biopersistent fibers can lead

to 'frustrated phagocytosis' [43]. This mechanism led to the sustained release of oxidants and proinflammatory mediators and was first described as explaining the toxicity of asbestos but has since also been observed in carbon nanotubes (CNTs) [44]. The involvement of NADPH oxidase in the toxicity of CeO_2 and CoCr NP has also been demonstrated, for example, in fibroblasts [45]. Nanomaterials can also inhibit repair mechanisms that eliminate ROS-damaged molecules, enhancing their toxicity [46,47]. Another indirect mechanism by which nanomaterials induce oxidative stress is depletion or inhibition of antioxidants, leading to an imbalance of redox homeostasis in the cell. For example, Au@Pt nanorods have been shown to oxidize ascorbic acid [48]. There are numerous reports and reviews concerning the oxidative stress-related mechanisms and effects induced by metallic nanoparticles. At the same time, there are several strategies to overcome this: not always desired property of nanoparticles or even giving nanoparticles the antioxidant properties [49,50]. There are attempts to achieve this by combining, quenching, or coating nanoparticles with classic chain-breaking antioxidants, such as tocopherols (vitamin E) [51], flavonoids [52,53], ascorbate (vitamin C [54,55]), aromatic amines [56], and nitroxides [57]. Some other nanomaterials could by themselves scavenge radicals on their surface or exert antioxidant properties (e.g., Au, Ag, CeO_2, and Pl NPs).

The antioxidant activity of metal-based nanoparticles can be related to those of natural enzymes. There are several types of antioxidant enzymes in the cellular system, such as catalase (CAT), superoxide dismutase (SOD), glutathione peroxidase (GPX), peroxiredoxin, etc. [58]. These antioxidant enzymes play an important role in maintaining cellular redox balance. Many nanomaterials have catalytic effects similar to those of antioxidant enzymes. This interesting antioxidant property of some nanomaterials is intended to be used in nanomedical applications (Colon et al., 2010, Rehman et al., 2012). As reviewed by Qu et al. [26], among the various antioxidant nanoparticles reported to date, metal oxide nanozymes have proven to be effective candidates in mimicking the antioxidant activities of first-line enzymes, i.e., SOD, CAT, and GPX.

Based on the reaction mechanism, nanozymes can be divided into two main families: 4 (i) the oxidoreductase family and (ii) the hydrolase family. The oxidoreductase mimetic nanozymes catalyze the oxidation reaction in which reducing agents and oxidants act as electron donors and acceptors, respectively. Among the metallic nanoparticles that exhibit oxidoreductase activity are nanoparticles of platinum [59], cerium oxide [60], iron oxide [61], and others. Hydrolase nanozymes catalyze the hydrolysis reaction by cleaving chemical bonds. In this process, the larger molecule dissociates into two smaller molecules. For example, gold nanoparticles are widely used as common nanoenzymes of hydrolases to catalyze the hydrolysis reaction [62–64].

Nanozymes can also be classified into (i) antioxidants and (ii) pro-oxidants [65]. In biological systems, the pro-oxidant induces oxidative stress by producing free radicals. For example, the presence of a transition metal can generate a hydroxyl radical ($HO^\bullet$) by Fenton chemistry [66]. Antioxidant nanozymes clean or scavenge free radicals using CAT-like or SOD-like actions. Superoxide ($OO^-\cdot$) decays at a low pH as the result of the reaction between its protonated and deprotonated form (Equation (1), k = 8.9×10^7 M^{-1} s^{-1} in H_2O), while at low pH and in organic solvents, decisive is the reaction between two molecules of the protonated form (Equation (2), k = 7.6×10^5 M^{-1} s^{-1} in H_2O).

$$O_2^{\bullet-} + HOO^\bullet + H^+ \rightarrow O_2 + H_2O_2, \tag{1}$$

$$HOO^\bullet + HOO^\bullet \rightarrow O_2 + H_2O_2, \tag{2}$$

The self-decomposition of peroxide is thus highly pH-dependent, with a maximum rate at pH = 4.5, and becomes slower with increasing pH. At physiological pH = 7.4, this reaction has an apparent rate constant of 2×10^5 M^{-1} s^{-1}. Meanwhile, even a small amount of $HOO^\bullet$ can initiate lipid peroxidation and cause radical damage to biomolecules. Thus, the SOD activity is important, catalyzing the decomposition of the dangerous reactive peroxide radical. The SOD mimetic catalyzes the dismutation of superoxide anions to

hydrogen peroxide, which in turn can be converted to molecular oxygen and water by a catalase-like nanozyme. On the other hand, peroxidase mimetic can convert hydrogen peroxide into hydroxyl free radicals. Peroxidase-like activity is demonstrated, among others, by iron oxide nanocomposites [67–70] and iron-containing nanomaterials [71]. These materials are widely used for glucose detection [72,73]. Figure 3 summarizes the classification of nanozymes based on the reaction mechanism and the generation/scavenging of free radicals.
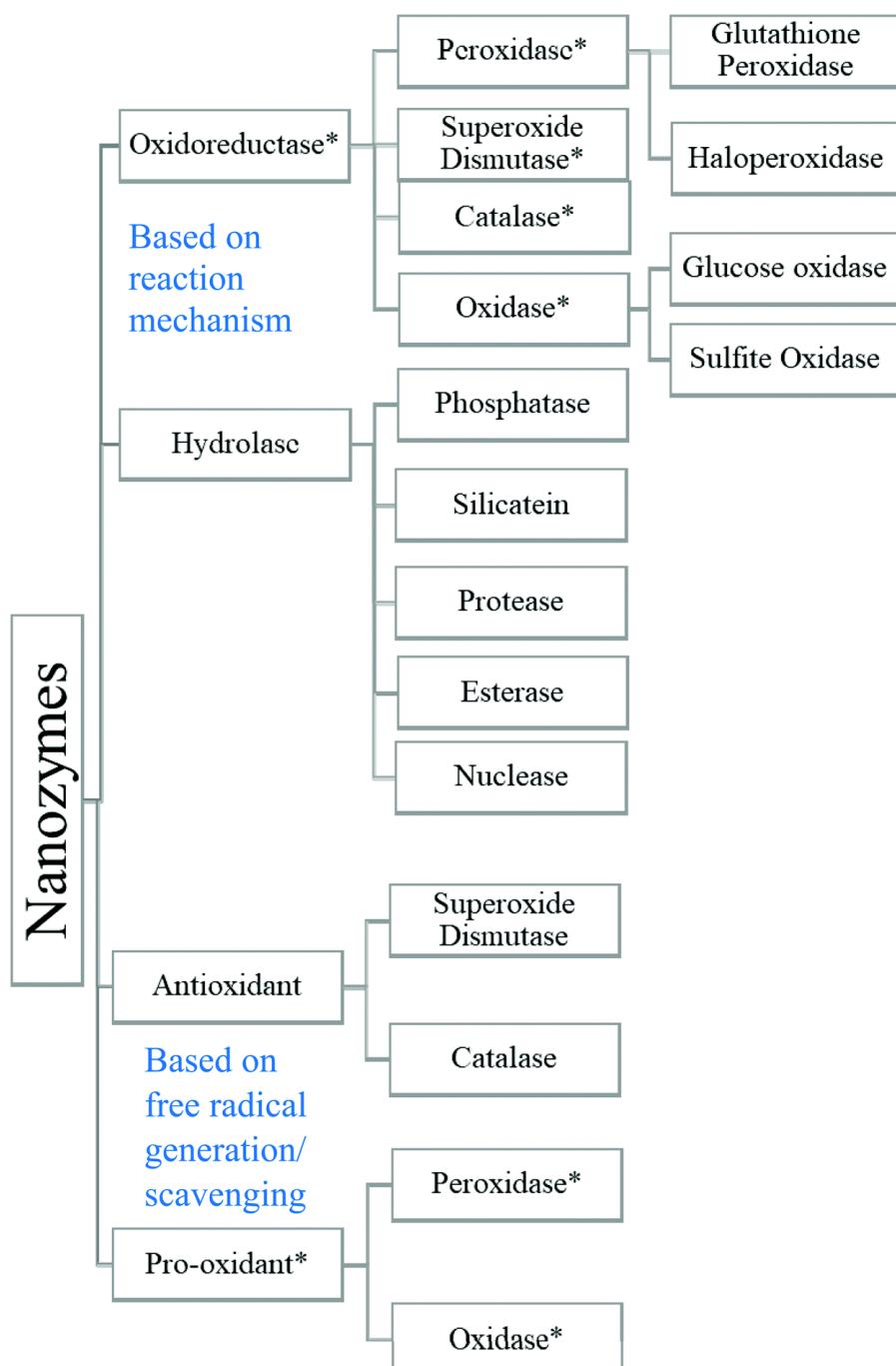

Figure 3. Classification of nanozymes [26,65,74]. (*) Mark represents the nanozymes commonly used for electrochemical biosensors. Reprinted from [75] with the permission of the Royal Society of Chemistry.

4. Strategies in the Quest for New Nanozymes

Almost all of the metals and their oxides in block d (and many of block f) of the periodic table are useful as redox catalysts mimicking natural enzymes. The important quality in the research seems to consist not so much in proving the catalytic abilities of subsequent metallic nanoparticles and metaloxides but in the use of a set of structural solutions in experimental design (Figure 4). This brings particularly interesting effects that inspire new approaches to nanozyme catalysis, allowing very selective activities of nanozymes, as was the case in an interesting work of Parac-Vogt et al. [76] on discrete hafnium metal-oxo cluster $[Hf_{18}O_{10}(OH)_{26}(SO_4)_{13} \bullet (H_2O)_{33}]$ (Hf_{18}), centered by the hexamer motif found in many MOFs. This water-insoluble nanoparticle acts as a heterogeneous catalyst for the efficient hydrolysis of horse heart myoglobin (HHM), inducing a strictly selective cleavage at directed protein sites. Among 154 amino acids present in the sequence of HHM, cleavage at only six solvent-accessible aspartate residues was observed. The hydrolytic activity was likely derived from the actuation of Hf^{IV} Lewis acidic sites and the Brønsted acidic surface of Hf_{18}, by a heterogeneous reaction. The selective hydrolysis of proteins by nonenzymatic catalysis is difficult to achieve, yet it is crucial for applications in biotechnology and proteomics.
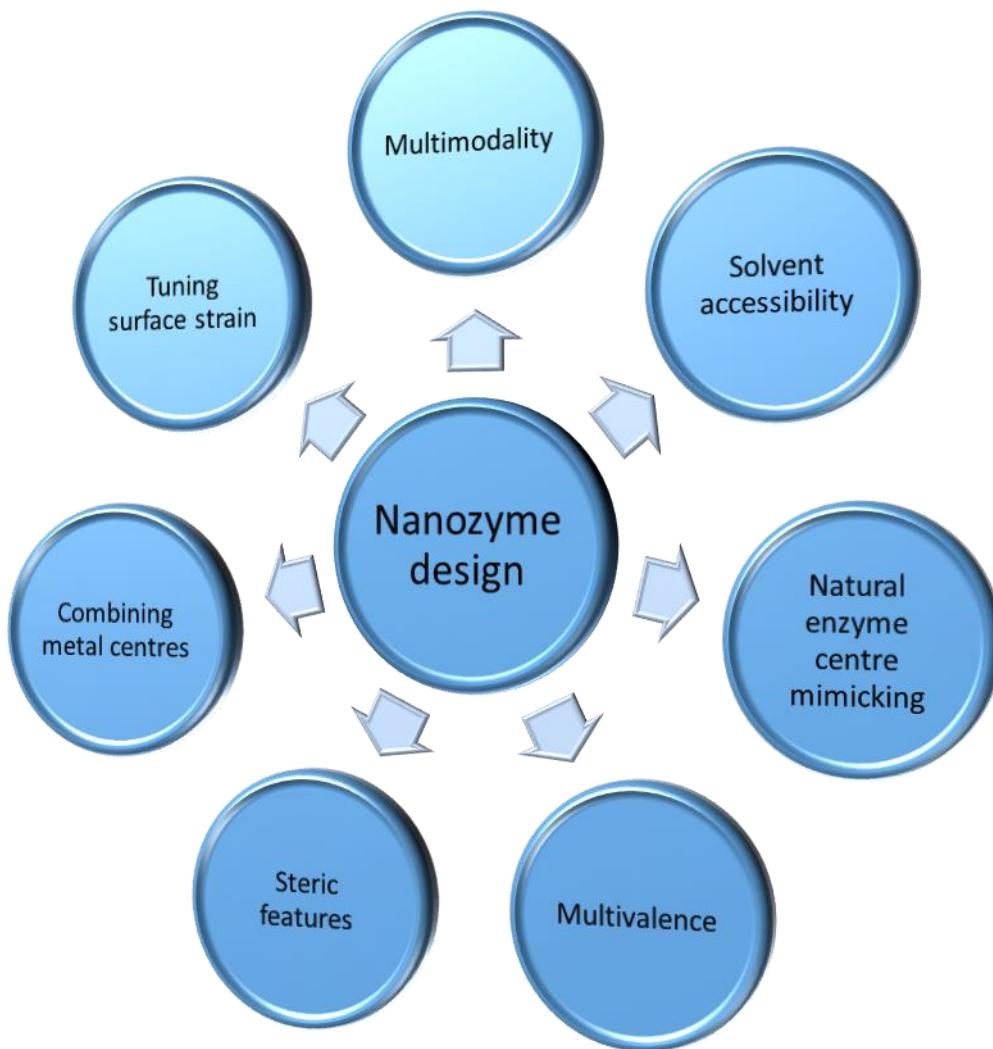

Figure 4. Approaches in the design of new nanozymes.

An important aspect of searching for new catalytic nanoparticles is careful observation and inspiration with naturally occurring processes. For example, one of the reasons why

natural enzymes contain mostly d-block metals is the valence flexibility of the latter. Therefore, bioinspired nanomaterials that show great potential for constructing novel nanozyme catalysts are those based on molybdenum. The main valence states of Mo include Mo (0), Mo (III), Mo (IV), Mo (V), and Mo (VI). No wonder then that this extremely valence-flexible metal is an essential trace element and nutrient in bacteria, plants, and animals serving as a cofactor for various Mo-based enzymes such as xanthine dehydrogenase, aldehyde oxidase, sulfite oxidase (SuOx), and nitrate reductase (NRase) [77]. The classes of bioinspired Mo-based nanozymes so far include molybdenum disulfide (MoS_2) [78,79] molybdenum selenide ($MoSe_2$) [80] molybdenum oxide (MoO_x, $2 \leq x \leq 3$) [81], molybdenum carbide (Mo_2C) [82,83], and hybrid Mo-based nanomaterials ($TiO2@MoS_2/CoFe_2O_4$, Au–Pd/MoS_2, MoS_2/GO, MoS_2:CeO_2, etc.) [84–87]. The MoO_x NPs were first reported to have oxidase (OXD)-like catalytic activity, and the MoS_2 NSs were reported to have peroxidase-like activity [78,88]. $MoSe_2$ and hybrid Mo-based nanozymes were then found to possess various enzyme-like activities, including POD, OXD, CAT, SOD, and RNase [80,81,89,90]. Li, Zhang, et al. [91] successfully used cysteine-protected nanodots MoS_2 with CAT and SOD catalytic properties for protection against ionizing radiation. The electrochemical measurements of cysteine-protected MoS_2 dots evidenced their strong in vitro catalytic activities in H_2O_2 and oxygen reduction reactions. Viabilities of mouse fibroblast cells treated with MoS_2 dots in different doses under exposure to gamma rays were significantly increased. The in vivo experiments showed that the surviving fractions of mice can be significantly increased with exposure to gamma rays (7.5 Gy; 76% survival at the dose of 50 mg/kg vs. 0% for non-treated irradiated mice).

The oxidation state of the metal is a decisive factor influencing the nanozyme activity, as shown in the research of Wang et al. [92]. The authors obtained the porous $LaNiO_3$ nanocubes. The 3+ oxidation state of Ni was shown to be superior to Ni^0 and Ni^{2+} for the nanozymes' catalytic activities. Specifically, the peroxidase-mimicking activity of the porous $LaNiO_3$ nanocubes with Ni^{3+} was, respectively, about 58-fold and 22-fold higher than that of NiO with Ni^{2+} and Ni nanoparticles with Ni^0. The oxidation state was very important for cerium oxides' [93,94] and iron oxides' [95] enzyme mimicking activities.

Fe_3O_4 nanoparticles are one of the most classic nanozymes showing peroxidase and catalase-like activity [14]. Enzyme-mimicking iron-oxide-based nanomaterials can be synthesized in various conformations, yet the decisive factor that allows one to fully reveal the iron oxide catalytic potential seems to rely on the application of the proper ligand environment. Again, the observation of nature prompts the application of the amino acid ligand entourage. For example, distal histidine, highly conserved in nearly all globins and all heme peroxidases, is important in tuning the affinity of these proteins ligands. In globins, the distal His stabilizes O_2 binding and has possible subsidiary functions of preventing autoxidation and discrimination against CO binding to the heme Fe. In peroxidases, the distal His has the nearly opposite role of activating bound H_2O_2 for heterolytic bond cleavage [96]. Indeed, as shown by Fan et al. [97], covalently modifying the histidine residues on the Fe_3O_4 surface resulted in nanozymes having a significantly higher affinity for H_2O_2 than that of unmodified Fe_3O_4. As in the case of many other metaloxide nanozymes, the presence of metal in two different oxidation states on the surface of the nanozyme is crucial for enzymatic activity of Fe_3O_4-based nanozymes. Such a multivalent system brings the nanozymes functionally closer to the systems present in the active centers of various proteins, for example, those containing heme [98] or iron–sulfur clusters [5,99,100]. Prussian Blue (PB) nanoparticles and their analogues are organometallic structures (MOFs) composed of alternately arranged Fe^{2+} and Fe^{3+} atoms coordinated with cyanides. Due to this multivalent structure, they exhibit activity resembling those of catalytic sites in metals. Moreover, they possess other important properties such as highly porous structure and biocompatibility [101]. The property of PB nanoparticles to scavenge ROS is due to their affinity for hydroxyl radicals and their ability to mimic three enzymes: SOD, CAT, and peroxidase. Different oxidation states are responsible for the unique multicatalytic properties of these enzymes, which can be changed by the

regulation of external potentials (PB has a low redox potential). The HRP-like (horseradish peroxidase) catalytic activity of PB is mainly due to the presence of ferrous ions [95]. For another instance, cerium (IV) oxide nanoparticles have been shown to exhibit SOD properties due to their mixed valence (Ce^{3+} and Ce^{4+}) [102]. Interestingly, the ability of nanoceria to scavenge superoxide is directly related to higher cerium (III) concentrations at the surface of the particle, while the CAT mimetic activity correlates with a reduced level of cerium in the +3 state, in favor of the 4+ [93,94]. Concluding, the catalytic mode of the nanozyme can be tuned by changing the oxidation state of the nanoparticle's surface.

Another observation of nature implicates that the choice of the metal according to the observed natural effects can be useful in tuning the catalytic potential of nanozymes. For example, the research showed that natural Mn SOD works better than Cu/Zn SOD and Fe SOD [103], which suggests that it should also be similar in regard to manganese nanozymes. Indeed, Yao et al. [104] obtained Mn_3O_4 nanozymes, which dismutated superoxide anion radicals, hydrogen peroxide, and hydroxyl radicals in vitro and protected live mice from ROS-induced ear-inflammation in vivo.

Specific steric features of the matrix of the nanozymes with active metallic centers can bring other effects allowing for targeted selectivity of the obtained nanoparticles. For example, upon being entrapped on the amine-terminated PAMAM dendrimer (AuNCs-NH$_2$), gold nanoclusters unexpectedly lost their peroxidase-like activity while still retaining their CAT-like activity in physiological conditions [105]. The possible mechanism was proposed that the enrichment of polymeric $3°$-amine on the surface of AuNCs-NH$_2$ (or AuNCs-OH) provided sufficient suppression of the critical mediator $^\bullet$OH, which is responsible for the peroxidase-like activity. Because their CAT-like activity was superior to that of AuNCs-OH and their hidden peroxidase-like activity diminished cytotoxic effects, AuNCs-NH$_2$ were further chosen for H_2O_2-mediated cytotoxicity tests in primary neuronal cells. Testing indicated a potential for the use of AuNCs-NH$_2$ in protecting primary neuronal cells against H_2O_2-induced toxicity.

Many metallic NPs can display multienzymatic activity, as it is in the case of Pt nanoparticles, which serve as both CAT and SOD mimics [59,106–108]. Simultaneous expression of multiple antioxidant enzymes is more effective than single or double expression in combating oxidative stress [109]. It has been reported that CAT-GPx cooperativity is important for the proper control of H_2O_2 levels under pathophysiological conditions. While CAT is responsible for the removal of excess H_2O_2 during oxidative stress, GPx is known to fine-tune the concentration of H_2O_2 for cell signaling. Unlike CAT activity that is common for many metal and metal oxide materials, GPX is a selenium-based enzyme. GPx is a GSH-dependent antioxidant enzyme that can catalyze peroxides such as H_2O_2 to form nontoxic products in the presence of gluthatione (GSH) [110,111]. Thus, it plays an important role in the maintenance of intracellular redox homeostasis. Until recently, mimicking GPx has mainly focused on designing selenium-based organic molecules [112]. However, these molecules can have disadvantages such as complicated preparation process, high toxicity, low cycle efficiency, etc. Therefore, the development of new and biocompatible GPx mimics is of great importance [113–116]. Mugesh, D'Silva, and colleagues also discovered that V_2O_5 nanowires could as well mimic GPx activity by using cellular GSH [115]. Although bulk V_2O_5 is known to be toxic to the cells, the property is altered when converted into a nanomaterial form. The vanadium-based nanozymes were readily internalized into mammalian cells and fully restored the redox balance without perturbing the cellular antioxidant defense. The potential of the biocompatible V_2O_5 nanowires in the treatment of aging, heart disease, and many neurological diseases was thus shown. This work was a breakthrough in mimicking GPXs by the non-selenium-based materials. Mugesh, D'Silva, et al. [116] reported that Mn_3O_4 nanoparticles with flower-like morphology (Mnf) could potentially exhibit the activities of all three primary antioxidant enzymes namely SOD, CAT, and GPX. They studied the GPx-like activity of Mnf using the classical coupled assay system involving glutathione reductase (GR) and NADPH to confirm the formation of GSSG. The catalytic properties of Mnf, investigated using steady-state kinetics

by independently varying the concentrations of H_2O_2 (0–1.8 mm) and GSH (0–5.0 mm), followed the Michaelis–Menten kinetics. A proportional dependence of the initial rate corresponding to the first-order kinetics was observed as the concentration of Mnf was varied by keeping the concentration of other reactants constant. Interestingly, Mnf was found to be highly specific to H_2O_2 as there was a significant decrease in the activity when cumene hydroperoxide or t-butyl hydroperoxide was used as substrates. The observed selectivity was attributed to the availability of active sites on the surface specific to small molecule H_2O_2 and not bulky organic peroxides.

In turn, in ceria-vanadium systems, a combination of the surface composition involves vanadium species (polymeric VOx and CeO_2 acting as Lewis acid sites, whereas $CeVO_4$ act like Brønsted acid sites). Hence, Peng et al. [117] suggested that the duality of both V-containing species (i.e., VOx and $CeVO_4$) can explain synergetic effects and can widen the operating window. A cerium vanadate ($CeVO_4$) nanozyme can substitute the function of superoxide dismutase 1 and 2 (SOD1 and SOD2) in the neuronal cells even when the natural enzyme is downregulated by specific gene silencing. The nanozyme prevents the mitochondrial damage in SOD1- and SOD2-depleted cells by regulating the superoxide levels and restores the physiological levels of the antiapoptotic Bcl-2 family proteins [118].

Combining different oxides gives additional catalytic potential. Qu et al. [119] constructed a manganese oxide composite with V_2O_5 nanowires decorated with MnO_2. V_2O_5 nanowire served as GPX mimic, while MnO_2 nanoparticle was used to mimic SOD and CAT. To assemble V_2O_5 nanowires with MnO_2 nanoparticles, polydopamine (pDA) was used to combine two nanomaterials. In this way, the obtained V_2O_5@pDA@MnO_2 nanocomposites could serve as a multinanozyme model to mimic the intracellular enzyme-based antioxidative process. Moreover, pDA can also serve as an antioxidant to remove ROS [120]. Thus, by combining the antioxidant capacity of nanozymes and pDA, the V_2O_5@pDA@MnO_2 nanocomposites exhibited a synergistic ROS-scavenging effect that would protect cell components from oxidative damage. To further explore the potential of nanocomposites, a mouse model of phorbol 12-myristate 13-acetate (PMA)-induced otitis was designed. The results showed that V_2O_5@pDA@MnO_2 nanocomposites can be effective in lowering ROS levels as well as ameliorating the adverse effects caused by inflammation in mice.

More recently, Hyeon et al. [84] followed the idea of oxidative protection in cells designing CeO_2 conjugated with Mn_3O_4 nanoparticles. The authors presented a very interesting emerging insight into the principles governing the structural physico-chemistry of nanomaterials. Namely, they managed to use the possibility of tuning the surface strain of metallic nanoparticles to modify their redox potential. Manganese ions deposition on the surface of CeO_2 nanocrystals caused the formation of strained layers of Mn_3O_4 islands, increasing the number of oxygen vacancies in the CeO_2 phase. This feature enhanced the efficiency of oxygen adsorption on the surface of the nanocrystals, allowing for more effective removal of ROS. As a result, nanoparticles administered in vitro to hematopoietic intestinal stem cells protected them from radiation-induced ROS damage. In the mouse model, CeO_2/Mn_3O_4 nanocrystals prevented radiation-induced multiorgan damage in vivo and improved survival after total body irradiation.

An important issue concerning metallic particles is their stabilization and biocompatibility. One method is the use of surfactants such as poly(acrylic acid) (PAA) [121]. Citrate-capped PtNPs were also shown to have SOD, CAT, and peroxidase-like properties that can reduce intracellular increased ROS levels in genetic model hyperoxia (krit1-ko MEF cells), protecting cell components from oxidative stress [122]. Similarly, citrate-capped nanocrystals of Pd can serve as both CAT and SOD mimics [123]. Nevertheless, other, more sophisticated coating methods can be applied, providing additional bioinspired features of the nanomaterials. For example, Nie et al. used apoferritin (apoFt) as a nanocarrier for the in situ synthetized Pt nanostructures [124]. Apoferritin was treated with K_2PtCl_4 salt at pH 8.5 to increase the electrostatic interaction between Pt ions and the interior surface of the protein. Pt ions were reduced, resulting in PtNPs trapped inside the FT shell. The

obtained platinum ferritin nanoparticles were bioactive, nontoxic, and stable, with an excellent CAT-like activity [124].

Many interesting designs with multimodal effects are being developed as part of the research that extends the similarity of metaloxide NPs to naturally occurring enzymes. For example, Qu et al. constructed a bifunctional ROS control and Cu^{2+} chelation system based on the CeO_2 NPs [125]. The system consisted of a mesoporous nanoparticle functionalized with a derivative of phenylboronic acid (MSN-BA). It is used to design glucose-responsive materials due to its unique reversible covalent interactions with the cis-diol moiety in glucose to form cyclic boronate moieties [126]. Such modified CeO_2NPs behave like reservoirs with pore blockers to prevent the premature release of the encapsulated drug at unwanted sites in the organism. The release mechanism depends on a redox reaction involving the presence of H_2O_2 to which the arylboronic esters are oxidized to phenols [127]. The complete breakage of arylboronic esters results in the release of CeO_2NPs and their payload after that. Due to the catalytic ability of CeO_2 nanocomposites similar to the antioxidant enzyme, the authors proposed this nanocomposite for the treatment of Alzheimer's disease (AD) in an in vitro mouse model on PC12 cells. As an additional charge to the antioxidant function, preventing the oxidative aggregation of amyloid plaque, 5-chloro-7-iodo-8-hydroxyquinoline (CQ) was chosen as a guest molecule, as described below in the section devoted to AD. As a result, a cooperative effect of chelation and ROS enzymatic decomposition was found. Similarly, a noteworthy cooperative multimodal system containing nanovalves was also designed and applied in multimodal imaging in the work of Yang et al. [128].

The abovementioned discoveries of the multienzymatic antioxidant activity of the metaloxide-based nanoenzymes are of great importance for potential medical applications. Gu et al. discovered that PB nanoparticles with multienzyme-like properties can effectively lower intracellular ROS levels and achieve excellent cytoprotection efficacy [95]. In vivo experiments showed their anti-inflammatory activity in a mouse model of lipopolysaccharide-induced hepatitis [101]. The results demonstrated their unique characteristics in inflammation and ROS-related damage. PBNPs and their analogues are gathering an increasing research interest [129].

5. Metal Nanozymes as Enzyme Inhibitors

In addition to biocatalytic functions, nanozymes can be used to selectively bind various enzymes and inhibit their activity [130]. This is related to their abovementioned features: a developed surface that is easy to modify and functionalize, and their architecture, which can be highly ordered and often has features important from the point of view of biocatalysis, such as chirality [131].

Protein surface recognition is an important issue in biomedical and biomaterial research. In addition to its use in immunoimaging methods, it is necessary for the specific inhibition of enzymes [132]. Until recently, small molecules, such as polypeptides or metal complexes, have been used as structures recognizing the active sites of enzymes [133], but the complicated geometry of enzyme active sites often requires structurally complex inhibitors difficult to precisely design. The required large receptor-protein contact surfaces and the inherent complexity of protein surfaces, the need to consider the hydrophobic nature of the active electrostatic center, and hydrogen bonds are still a challenge for modern biochemistry [131]. To obtain functional nanomaterials compatible with protein surfaces, You et al. [132] constructed carboxylic acid-functionalized gold nanoparticles with various L-amino acids and investigated their effect on the rate of R-chymotrypsin (ChT) catalyzed N-succinyl-L-alanine-p-nitroanilide (SPNA) hydrolysis. The authors observed an explicit charge-dependent inhibition of the enzyme. In the presence of negatively charged amino acid-modified gold nanoparticles, the rate of ChT-catalyzed SPNA hydrolysis was reduced, while the positively charged amino-acid-modified gold nanoparticles had no obvious effect on ChT activity. This is well following the fact that the ChT active site is surrounded by cationic residues. Circular dichroism (CD) analysis showed conformation changes depen-

dent on the side chains of negatively charged amino acids with which the nanoparticles were decorated. At the same time, in the presence of gold particles with a hydrophobic side chain of the NP-L-Leu amino acid, almost no changes in the CD ChT spectrum were observed. In addition, the hydrophobicity was postulated decisively for the observed inhibition effect: After 24 h incubation with nanoparticles, hydrophilic NP_L-Asp induced approximately 90% denaturation of ChT, while hydrophobic NP_L-Leu induced only 20% denaturation. Moving on, You et al. showed that the interaction between nanoparticles and protein influences both the catalytic constants and Michaelis constant values, resulting in the modulation of the association/dissociation processes. The recognition of the ChT surface by charged nanoparticles opens up new horizons for research into the affinity of protein-active centers [132,134].

As mentioned, apart from electrostatic interactions, the surface geometry is also of great importance for the interaction with the active center of the enzyme. This situation has been observed by VanEpps, Kotov et al. [135], who showed that small zinc oxide nanoparticles (ZnO NP), pyramids, plates, and spheres, can inhibit the activity of β-galactosidase (GAL), a proteolytic enzyme, the upregulation of which is usually associated with primary ovarian cancer and cell aging. The inhibition of enzymes by ZnO nanoparticles is reversible and strongly depends on their geometry [135].

Pandit et al. [136] synthesized several functionalized two-dimensional molybdenum disulfide (2D-MoS_2) nanomaterials capable of inhibiting penicillinase, also known as β-lactamase, which is responsible for penicillin-resistance bacterial strains [137]. The authors showed that carboxylate-functionalized negatively charged MoS_2 effectively blocked the β-lactamase active site and exhibited a competitive inhibitory effect. The inhibition mechanism was attributed both to electrostatic and non-covalent interactions with the β-lactamase center surrounded by cationic residues (lysine and arginine), as well as to geometry and steric blockade between the enzyme and the inhibitor.

Table 2 summarizes the above-described inhibition mechanisms and their potential applications in enzyme regulation.

Table 2. Nanozymes inhibit natural enzymes by various interaction modes.

Nanozyme	Ref.	Target Enzyme	Enzyme-Nanozyme Interaction Type	Application
AuNPs	[132]	ChT	electrostatic interactions	Protein interaction
ZnONPs	[135]	Beta-Gal	Hydrogen bonding, Van der Vaals, molecular shape	Ovarian cancer, cell aging
2DMoS2	[138]	β-Gal, ChT	electrostatic interactions	diagnosis, treatment
2DMoS2	[136]	β-lactamase	electrostatic interactions, steric hindrance	overcoming penicillin resistance

Abbreviations: AuNPs, gold nanoparticles; ZnONPs, ZnO nanoparticles; ChT, R-chymotrypsin β-Gal, beta-galactosidase.

6. Metal Nanozymes as Cellular Probes for Biosensing

Over the past decade, nanozymes have proved to be excellent providers of high-performance and ultra-sensitive biosensors, including colorimetric, fluorometric, chemi-luminescent, surface-enhanced Raman scattering, and electrochemical assays [139]. Due to their oxidase-like activity, metallic, metaloxide, and metal-organic nanoparticles are used for colorimetric and fluorimetric sensing of H_2O_2, O_2 and H_2S, glucose, ascorbic acid, cysteine, GSH, and other bio-thiols, cholesterol, uric acid, dopamine, epinephrine, phenol, Hg^{2+}, cancer cells, thrombin, ALP, HIV DNA, sulfadimethoxine, xanthine, bacteria, heavy metal ions, and many others (a detailed review on analytical applications of MOF-based nanozymes can be found in [79]; Detailed reviews on metal nanozyme biosensors can be found in [19,140]).

Colorimetric detection provides a quick response (color change), often allowing the naked eye to evaluate the sample parameters and subsequent quantification in UV-VIS. The advantage of naked-eye detection is that it can be used as a first-pass screening test for rapid disease diagnosis. This feature of colorimetric sensors makes them suitable for

developing fast and inexpensive screening tools in medicine (i.e., detection of disease-specific molecules, proteins, and cells), biotechnology, and environmental sciences.

Nanozymes can oxidize a variety of chromogenic substrates, such as (e.g., TMB), 2,2′-azino-bis(3-ethylbenzthiazoline-6-sulfonic acid) (ABTS), 3,3′-diaminobenzidine (DAB), and *o*-phenylenediamine dihydrochloride (OPD)) in the presence of hydrogen peroxide (H_2O_2) and produce a distinguishable color. The analytical determination of hydrogen peroxide is of considerable importance for medical diagnosis because H_2O_2 is formed as an intermediate product in a large number of important detection processes (Equations (3) and (4), Figure 5). Nanozymes can easily replace peroxidase in conventional assays, often extending the field of application of tests by, e.g., a larger pH range. This makes them interesting for the investigation of combined multienzyme assays with oxidases that require a narrower pH range for their optimum activity, as shown for the glucose/glucose oxidase catalytic test [141].
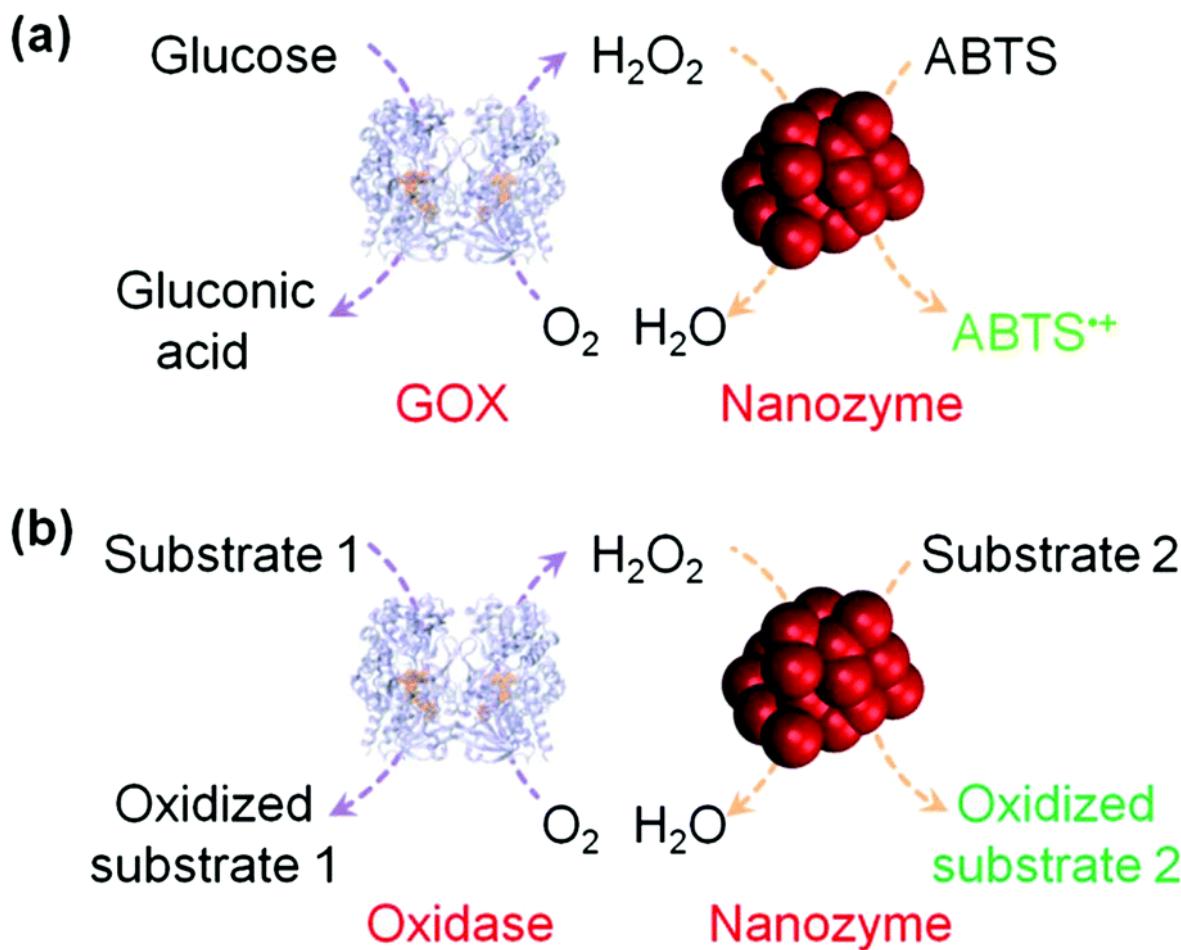
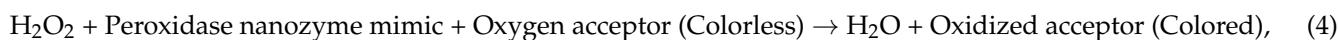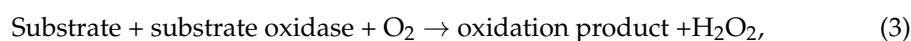$$\text{Substrate + substrate oxidase} + O_2 \rightarrow \text{oxidation product} + H_2O_2, \tag{3}$$

$$H_2O_2 + \text{Peroxidase nanozyme mimic + Oxygen acceptor (Colorless)} \rightarrow H_2O + \text{Oxidized acceptor (Colored)}, \tag{4}$$

Figure 5. *Cont.*

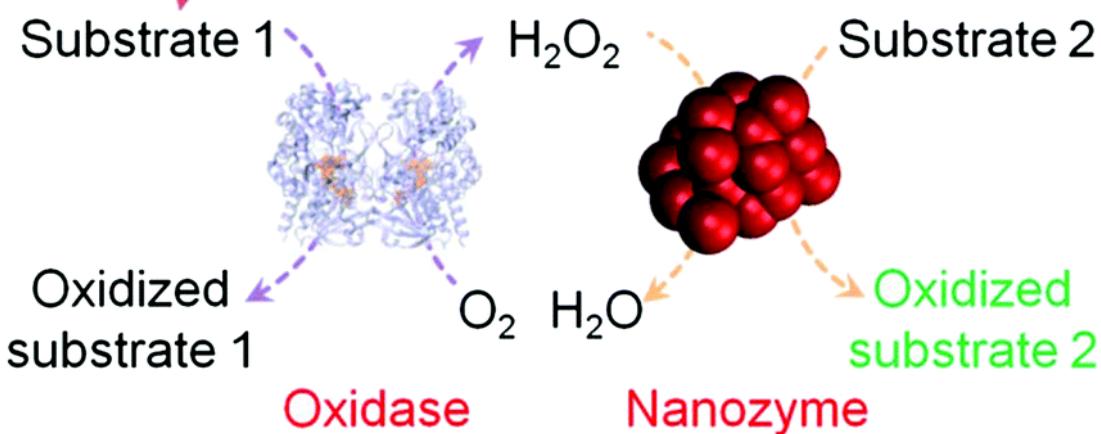**Figure 5.** (**a**) Nanozyme as peroxidase mimic for colorimetric sensing of H_2O_2, and glucose when combined with glucose oxidase. (**b**) The sensing format in (**a**) could be extended to other targets (substrate 1 here) when combined with a suitable oxidase. (**c**) The target of interest as substrate 0 could be determined if it could be converted into an oxidase substrate. Numerous transduction signals can be adopted for sensing (such as colorimetric, fluorometric, chemiluminescent, and surface enhanced Raman spectroscopy (SERS) signals when the corresponding substrates are used; and electrochemical signals when a nanozyme is immobilized on an electrode). Adapted with permission from [17]. Copyright (2013) Royal Society of Chemistry.

Sometimes a nanozyme may fulfill a tandem role, as obtained by Li et al., of "non-naked" AuNP coated with protein (bovine serum albumin). Although the "naked" Au NPs have peroxidase-like activity and GOx-like activity, the optimal pH ranges of the two activities are different. Fortunately, synthesized "non-naked" Au NPs exhibit dual enzymatic activity at the same pH, benefiting the establishment of one-pot enzyme-free glucose detection.

The on/off colorimetric sensors have been also designed, for example, based on the reversible surface passivation of noble metal nanozymes with single-stranded DNA [142] (ss-DNA) or an aptamer [143]. Self-regulated colorimetric sensors use the nanozyme activity of nanoceria to detect acetylcholinesterase, nerve agents, drugs, and bioactive ions, by in situ modulating the oxidase-like activity of nanoceria through proton-producing (or proton-consuming) enzymatic reactions [144]. Several other sensitive colorimetric sensors based on functional nanozymes have been reported, among others for the detection of cocaine [145], immunochromatographic analysis of the *Ebola virus* [146], and *Escherichia coli* [147]. In addition, a sensor array based on combined analysis of analytes' influence on Pt Ru and IrNPs' peroxidase-like activities has been designed to discriminate between biothiols, proteins, and cancer cells [148].

In terms of sensitivity, one of the most spectacular improvements brought by nanozymes concerns their application in the popular enzyme-linked immunosorbent assay (ELISA). ELISA is the most widely used technique for the detection and quantification of peptides and antigens. The enzyme-conjugated primary antibody (direct ELISA) or the secondary antibody (indirect or sandwich ELISA) in the ELISA test specifically recognizes the antigen. The most commonly used enzyme reporter in the ELISA test is HRP. It catalyzes the oxidation of TMB in the presence of H_2O_2 to produce a colorimetric signal, and the intensity of the signal is proportional to the concentration of the recognized antigen. However, HRP has a lot of limitations that are typical of proteins. It is not resistant to many preservatives such as sodium azide. It is also subject to proteolytic degradation. Its enzymatic activity is limited to a narrow range of pH and temperature [10]. In addition, the sensitivity of a conventional

ELISA is limited [149]. To overcome these limitations, numerous nanozymes have been developed, considered direct substitutes for HRP [150]. For instance, Xu and Cheng [151], to avoid the occurrence of false positives and false negatives caused by conventional ELISA, have recently developed a nanozyme-linked immunosorbent assay based on metal-organic frameworks (MOFs) for sensitive detection of aflatoxin B1. As a result, the limit of detection (LOD) of the MOFLISA method was 0.009 ng/mL with a linear working range from 0.01 to 20 ng/mL, thus having a 20-fold improved LOD value compared with the conventional test.

In a fluorescent sensor, nanozyme usually converts a non-fluorescent substrate into a fluorescent-active substrate by catalyzing a hydrolysis or oxidation reaction [152–154], including application in fluorescent ELISA tests [155,156]. For example, Perez et al. demonstrated that the ability of poly (acrylic acid)-coated nanoceria to mimic oxidase depends on the pH of the solution [156]. In the pH range $4-7$, HRP/H_2O_2 oxidized ampliflu to nonfluorescent resazurin. By contrast, at pH 6–8 nanoceria oxidized ampliflu to the intermediate oxidation fluorescent product resorufin, while at or below pH 5.0, nanoceria also yielded the terminal oxidized nonfluorescent product resazurin. Thus, the ability of nanoceria to oxidize ampliflu to a stable fluorescent product in the pH range $6-8$ was used to develop a sensitive cell-based ELISA at neutral pH without the use of H_2O_2. In recent years, the ratiometric fluorescence sensors have gained popularity due to their ability to autocalibrate to correct the signal, allowing for more reliable detection [157,158]. The work of Mao et al. [159] describes a solution slightly different from these classic examples but due to its specific design allowing cellular imaging. The authors have reported an example of using nanozeolitic imidazolate framework (ZIFs), ZIF-90, self-assembled from Zn^{2+} and imidazole-2-carboxyaldehyde, to target subcellular mitochondria and image dynamics of mitochondrial ATP in live cells by fluoroscopy. Rhodamine B (RhB) loading into ZIF-90 suppressed the emission of RhB, while the competitive coordination between ATP and the metal node of ZIF-90 dissembled ZIFs, resulting in the release of RhB for fluorimetric ATP sensing. This allowed cellular imaging of the mitochondrial ATP and fluctuations in ATP levels in the processes of cell glycolysis and apoptosis.

It should not be forgotten that metal-based nanoparticles, apart from their redox activities, very often consist of an excellent contrast agent in magnetic resonance imaging (MRI). Of particular interest are multimodal MOF-based platforms, such as those described by Yang et al. [128]. An intelligent theranostic nanoplatform based on nanovalve operated metal-organic framework (MOF) core-shell hybrids, incorporating tumorous microenvironment-triggered drug release, MRI, and effective chemotherapy in one pot was reported. This complex structure was based on the Fe_3O_4 core, covered by the UiO-66 an archetypal Zr-based MOF with a very high surface area. Due to its high thermal stability, tunability, and functionality, UiO-66 has gained scientific popularity over the last decade [160]. Thus, the mentioned multimodal core/shell NPs were further loaded with 5-fluorouracil (5FU) and equipped with the so-called stalk components binding pillarene-based nanovalves via host–guest binding. This arrangement allowed the multistimuli responsive drug release. In acidic extracellular microenvironments of cancer cells, the host–guest interaction between a nanovalve and a stalk could be broken, causing the turn-on of the nanovalve and subsequent release of cytostatic 5FU loaded in the as-prepared core–shell nanoplatform. Consequently, the release rate increased with the decrease in pH, at pH 5.0, achieving approximately two times faster rate than in pH 7.0. Furthermore, abnormal ion content caused by pathological changes was also shown to trigger dissociation of the nanovalve and release the drug load. This renders the obtained nanoplatforms useful in the treatment of medical conditions characterized by disrupted ion levels, such as the increased Zn^{2+} concentration in the central nervous system and Ca^{2+} dyshomeostasis in related bone diseases. The host–guest interaction was also shown to be weakened as temperature increased, giving prerequisites for photothermal therapy (PTT) [128].

A promising direction in biosensing is connected to modification of the metal-based NPs allowing their selective affinity towards important macromolecular biomarkers, such as nucleic acids [161–163] and peptides [164]. Over the past few decades, electrochemical

biosensors have been successfully used to detect a wide variety of molecular and cellular biomarkers. Most importantly, the electrochemical detection system is susceptible to miniaturization and offers advantages such as simplicity, cost-effectiveness, and high sensitivity and specificity [165]. Tunable electrochemical biosensors based on analogous Zr-MOFs were developed for protein detection, the performances of which rely on the pore sizes and surroundings of the MOFs that show diverse binding behaviors to aptamers and then the targeted proteins [166]. The optimized Zr-MOF-based sensor was shown to be highly selective to lysozyme in a wide concentration range and a low detection limit of 3.6 pg mL^{-1}, with good repeatability, stability, and applicability in real samples. The selectivity of the Zr-MOF-based sensor was explored toward a series of interference proteins. However, this study has not yet provided any cellular-based evidence for the possibility of the test to be used in vivo, and there soon emerged new instances, such as presented in the work of Chen and co-workers, who designed a sandwich-type Zr-MOFs biosensor with amino-functionalization for the detection of human breast cancer MCF-7 cells (human breast cancer cell line with estrogen, progesterone, and glucocorticoid receptors) [167] and developed them as platforms to anchor phosphate group-modified HER2-targeted aptamer (PO$_4$-Apt) to sensitively detect MCF-7 cancer cells. The UiO-66-2NH$_2$-based aptasensor exhibited highly significant biosensing to detect MCF-7 cells and showed an extremely low detection limit of 31 cell mL^{-1}. The electrochemical impedance spectroscopy (EIS) and cyclic voltammetry (CV) techniques were used as the detection method. As HER-2 is overexpressed in many, especially breast, cancer cells, the choice of the aptamer was highly justified. However, it is worth emphasizing that in the conducted research it is extremely important to prove the significance of the principle of operation of such a sensing method, while the issue of selecting appropriate aptamers is an open issue for modification in accordance with the diagnostic requirements. From the medical point of view, the prospect of imaging cancerous lesions is of particular importance. However, still, there is room for extensive research in this field, so that the research could be translated into methods that can be carried out on living tissue. A nonobvious but extremely promising solution to this issue was presented in the paper of Wang and coworkers [168]. This group reported a high-sensitivity strategy to selectively detect a lung cancer biomarker of patients' exhalation, aldehydes that possess small Raman cross-section via using gold particles coated with ZIF-8 GSPs@ZIF-8 as a SERS substrate. They used core-shell 3D MOF-based biosensor called GSPs@ZIF-8, composed of Au NPs as core and ZIF-8 as shell, with the pore size allowing adsorption of small aromatic compounds. After the Raman-active 4-ATP molecules were grafted onto the ZIF-8 surface, 4-ethylbenzaldehyde reacted with the amino group on 4-ATP and allowed sensitive aldehyde detection at the ppb level. The porous structure of MOF shell allowed better surface-substrate interaction, overcoming long-standing limitations that gaseous molecule difficultly absorb on solid substrates. By nucleophilic addition reaction with the pregrafted Raman-active molecule of 4-ATP, the gaseous aldehydes were selectively captured and could be detected at ppb level. The GSPs@ZIF-8 exhibited additional Raman enhancements due to not only the precise arrangement of nanoparticles but also the altering penetration depth of electromagnetic field that enhanced the Raman signal of analytes. A capability to selectively trace gaseous cancer biomarkers at ppb levels in mixed exhalation gases gives promising prospects for noninvasive recognition of lung malignancies.

Another biomarker testing the level of homeostasis is the methylation of DNA, which is a well-known way of regulating gene expression [169]. In recent years, nanozymes have been used for the colorimetric detection of DNA methylation as a potential epigenetic biomarker. For instance, Shiddiky et al. [75] developed a unique method to detect DNA methylation using the peroxidase-like activity of mesoporous iron oxides. The test successfully detected up to a 10% difference in global DNA methylation levels in synthetic samples and cell lines with good reproducibility and specificity (% RSD = <5%, for n = 3).

7. Nanozymes in the Fighting of Neurodegenerative Diseases

The examples described above show that many nanozymes have an inherent activity similar to that of antioxidant enzymes. On this basis, they can be used for cytoprotection, relieving inflammation; thus, they promise possible applications in the treatment of oxidative stress-related medical conditions, including alleviating neurodegenerative diseases.

Parkinson's disease (PD) is the second most common neurodegenerative disorder characterized by misfolded accumulation of α-synuclein (α-syn) [170]. New evidence suggests that oxidative stress is an inevitable pathogenesis factor contributing to the prion-like spread of protein damage [171,172]. For example, paraquat can induce oxidative stress in vivo and in vitro, significantly leading to increased spread of α-syn [171,173,174]. Pathological α-syn has been shown to increase ROS by facilitating the spread of α-syn and causing severe neurodegeneration and behavioral deficits in vivo [175]. At the same time, inhibitors of the NOS-related pathway can significantly prevent α-syn-induced pathogenesis [175], indicating that reducing the level of oxidative stress may be an effective means of counteracting the pathological spread of α-syn in PD. Therefore, experiments on metal-based nanozymes having antioxidative action [176], consisting of platinum and copper (called bimetallic PtCu nanoalloys), showed that the nanozymes could be applied in the treatment for PD due to their antioxidative potential. It was shown that the antioxidative action of nanozymes could prevent the spread of misfolded alpha-synuclein by breaking the positive feedback loop between the accumulation of misfolded alpha-synuclein and the formation of free radicals (Figure 6).
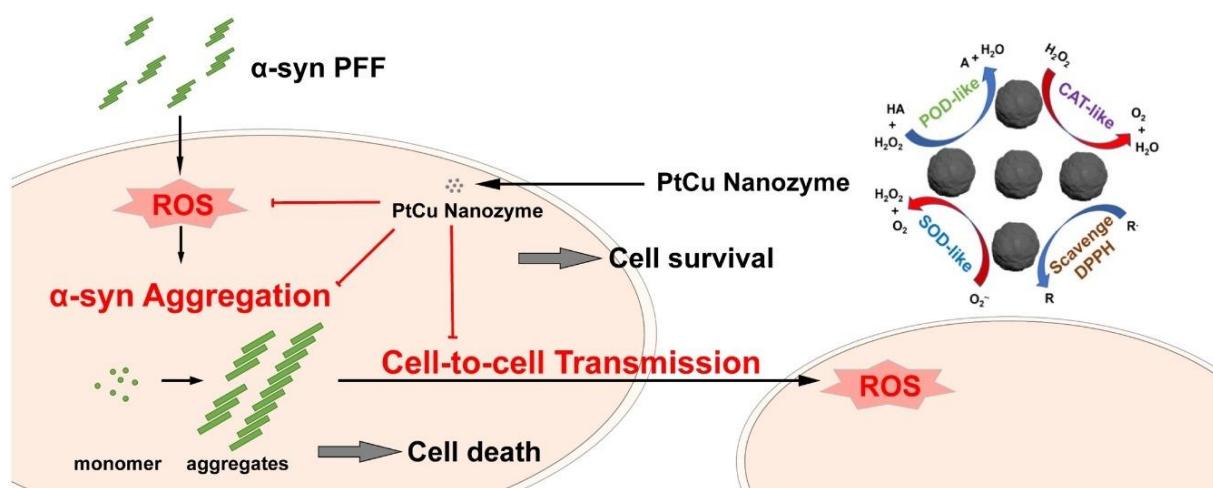

Figure 6. The mechanism action of PtCu nanozyme in the treatment of PD. Reprinted from [176], with the permission of Elsevier.

Platinum and copper were used because of their strong antioxidant properties. The antioxidant capacity of an alloy largely depends on its composition. When injected into the brain, PtCu nanoalloys acted as CAT and SOD. It was found that nanozyme reduced disease symptoms caused by misfolded alpha-synuclein, inhibited neurotoxicity, and reduced the number of free radicals in mice. Nanozyme also prevented alpha-synuclein from moving from cell to cell and from the substantia nigra to the dorsal striatum, two midbrain areas responsible for movement and cognition [176]. Kuang et al. designed phenylalanine-modified CuxO nanoclusters showing potential for the treatment of PD [177]. The generated CuxO nanoclusters behaved like SOD, CAT, and GPx mimics. To further explore the potential therapeutic efficacy of these nanozymes, a mouse model of Parkinson's disease was constructed. Cu$_x$O nanoclusters were shown to modify the levels of Allograft inflammatory factor 1 (AIF-1, Iba1), whose expression is upregulated in microglia following nerve injury central nervous system ischemia, and several other brain diseases [178]. Iba1 levels were lowered in the PD mouse model after treatment with CuxO compared to the

untreated PD mice. PD mice treated with Cu_xO nanoclusters also showed significantly better spatial learning, memory, escape latency, and swim speed during the training process, indicating that Cu_xO induced cognitive regeneration.

Another example of a disease whose pathogenesis is associated with the overproduction of ROS is Alzheimer's disease (AD). Cellular changes show that oxidative stress precedes the appearance of the hallmark pathologies of the disease [179]. AD, one of the most common types of dementia, affects approximately 10% of the elderly (age 65 and over) [180,181]. Accumulation of amyloid protein (Aβ) plaques and neurofibrillary tangles in the brain are the two major pathological markers of AD [182]. Aβ accumulation induced by protein misfolding has been recognized as a hallmark of neurodegenerative disease. Moreover, Aβ-induced mitochondrial dysfunction is also considered a possible AD caused through abnormal ROS expression [183].

Since ROS-induced mitochondrial dysfunction occurs earlier than Aβ plaque formation in the brain, protecting the mitochondria from oxidative damage would be useful in the prevention and early treatment of AD. Recently, Hyeon et al. designed CeO_2 nanoparticle modified with triphenylphosphonyl (TPP) as a new platform for the treatment of AD [184]. The resulting nanocomposite favored being localized to the mitochondria, markedly inhibiting Aβ-induced mitochondrial ROS and inhibiting neuronal death in the 5XFAD AD transgenic mouse model. In a mouse model, TPP-modified CeO_2 nanoparticles attenuated Aβ-Induced neuronal cell damage. This can be used as a new mitochondrial therapy for neuroinflammation, which is of great importance in the treatment of Alzheimer's disease and other neurodegenerative diseases.

Qu et al. [185] designed ceria/polyoxometalate hybrid nanomaterials (CeONP@POMs) nanoparticles. As mimics of proteolytic enzymes. These nanozymes were shown to effectively inhibit Aβ aggregation as well as reduce intracellular ROS levels. CeONP@POM was found to promote the proliferation of PC12 pheochromocytoma of the rat adrenal medulla cells, while effectively inhibiting the Aβ-induced activation of BV2 microglial cells. An earlier study found that POMs, especially characterized with Wells–Dawson structure, inhibited the aggregation of Aβ by binding to the His13 to Lys16 (HHQK) cationic region [186].

Fan et al. [187] studied the antioxidant effects in vitro and in vivo of the Fe_3O_4 nanoparticles. Two cell lines were used in their work in vitro tests, including PC12, rat adrenal medullary phaeochromocytoma from the fetal nerve crest. NPs were shown to locate in cytosol. Fe_3O_4 NPs with CAT-like properties can efficiently remove intracellular excess ROS in this neutral environment, protecting cells from oxidative damage and H_2O_2-induced apoptosis. The neuroprotective properties of Fe_3O_4 nanoparticles were tested in vitro on PC12 cells. PC12 cells originate from the neural crest that has a mixture of neuroblastic cells and eosinophilic cells and can differentiate into neuron-like cells by nerve growth factor (NGF) stimulation. 1-methyl-4-phenylpyridinium ion (MPP^+) induces oxidative stress and apoptosis in differentiated PC12 cells, which is often used as a model for neuroprotective assays relevant to PD. Cellular studies showed that NP Fe_3O_4 can be effective in ameliorating cell death induced by 1-methyl-4-phenylpyridinium (MPP+) as well as reducing the levels of α-synuclein activation protein and caspase-3. The authors investigated the function of NPs also in AD. They applied a classic in vivo model based on ectopic expression of Aβ in *Drosophila* [188]. For the fly AD model, neuronal-specific expression of Aβ peptide was achieved by crossing the *elav*-Gal4 and UAS-Aβ lines, allowing tissue-specific expression of Aβ throughout the nervous system. When fed with food containing Fe_3O_4 NP, AD-model fruit flies showed increased climbing ability and longer lifespan as compared to untreated ones. The Drosophila AD model further verified the excellent antioxidant properties of NP Fe_3O_4 in delaying animal aging and ameliorating ROS-induced neurodegeneration.

It is widely known that high concentrations of metal ions (such as Cu^{2+} and Zn^{2+}) play an important role in the accumulation of Aβ deposition and its neurotoxicity [189–191]. Therefore, in addition to oxidative damage, metal ion abnormalities can also be used as targets in AD therapy [26]. Having this in mind, Qu et al. [125] used the discussed

above multimodal G-CeO$_2$NPs nanoparticles to prevent Aβ aggregation. Thanks to the cooperative H$_2$O$_2$-induced Cu chelator release and the anti-ROS enzymatic activity of CeO$_2$ NPs, a synergistic therapeutic effect was observed in PC12 neuronal cells. Moreover, Aβ plaque inhibition effect via copper chelation was confirmed in the noncellular buffered systems at low pH, upon the release of CQ from the NPs.

8. Metal Nanozymes in Cancer Treatment

Cancer is one of the leading causes of death worldwide. In the last two decades, the development of nanotechnology has facilitated researchers' ability to design new nanoparticles for sensitive, rapid, and specific methods to detect and quantify cancer cells at an early stage and kill the existing tumor cells. A nanozyme can kill cancer cells in two ways. The first is direct killing by increasing ROS in vivo through the oxidase and peroxidase activities of nanozymes [192]. The second is indirect killing, which is related to the CAT or SOD activity of nanozymes by relieving the hypoxia of a tumor microenvironment (TME), aided by light, sound, or chemotherapy.

It is good to remember that ROS, also called oxygen free radicals, are a side product of cellular metabolism, generated primarily by mitochondrial activity, and other sources such as xenobiotics [193], cytostatics [194], and UV-radiation [195]. In excess, ROS contribute to membrane damage by lipid peroxide formation and are part of the signaling sequence leading to apoptosis [196]. However, if not regulated properly, e.g., antioxidants, excess ROS result in oxidative stress. Consequently, this leads to damage of cellular macromolecules and inhibits cellular functions, leading to certain pathologies, including cancer [197].

The important technological advantages of nanoparticles used as drug carriers are their high stability and high carrier capacity. The ability to adjust the composition of nanoparticles to the properties of the drug makes them feasible for the incorporation of both hydrophilic and hydrophobic substances. This is of paramount importance for drug delivery because lipophilicity is a major determining factor in a compound's absorption, distribution in the body, penetration across vital membranes and biological barriers, metabolism, and excretion [198]. The surface of the NP is a target for functionalization. By modifying the NPs surface with hydrophilic moieties, one can improve NPs' stability in the biological fluids. Charged functional groups provide adequate zeta potential and prevent their aggregation and precipitation. Due to the possibility to functionalize NPs with targeting molecules, it is possible to increase the drug concentration at desired sites of action and reduce systemic levels of the drug in healthy tissues. In addition, functionalizing of fluorescent or radioactive NPs with targeting molecules allows the imaging of lesions using PET (Positron emission tomography) [199], SPECT (Single-photon emission computed tomography) [200], MRI [199,201], and spectroscopic [202] methods.

In the therapy and visualization of cancer, NPs have another very important feature: in contrast to small molecules that do not discriminate tumor and normal tissue [203], high-molecular-weight substances preferably accumulate in cancer. This is related to the specific properties of tumorous tissue: poorly aligned defective endothelial cells with wide fenestration, innervation with the wider lumen, impaired angiotensin II receptors' lack of effective lymphatic drainage [204]. At the same time, normal tissue is not permeable to big particles and quickly purified due to lymphatic clearance, the tumor tissue tends to accumulate macromolecules, especially lipids [203,205–207]. This phenomenon has been characterized and termed the tumor-selective enhanced permeability and retention (EPR) effect. The enhancement of vascular permeability plays a critically important role in tumor growth to facilitate an adequate supply of nutrients and possibly oxygen to meet the great demands of rapidly growing tumors. Here, the vascular permeability is concerned with the macromolecular size of the drugs with which selective tumor targeting is highly enhanced. Therefore the EPR idea is now regarded as a gold standard in designing new ant-cancer agents [206].

Herein, we describe two main categories of nanozymes according to material types: metal-based nanozymes (e.g., gold, silver, palladium, platinum, and cobalt) [208] and

metal oxides or metal sulfide nanozymes (e.g., cerium dioxide, ferric oxide, vanadium pentaoxide, and iron sulfide), which are applied for cancer treatment [6].

One of the best-described metals-based nanozymes are ultrasmall gold nanoparticles (AuNPs), which show oxidase, peroxidase, and catalase mimicking activities. They have been reported to show improved therapeutic effects when coupled with drug molecules [209,210]. This is because the AuNPs have a large surface area which provides high packing capacity for drug loading and improves the hydrophilicity and stability of drugs. Furthermore, their surface can be modified by targeting ligands to enhance the tumor-selective accumulation compared to free drugs. Nanozymes can passively target neoplastic lesions with leaky neovessels by the EPR effect. The additional advantage is the skill to control the release of loaded drugs in response to internal or external stimuli [211]. AuNPs were also reported to be effectively employed in cancer treatment by applying photodynamic therapy (PDT) and PTT [212]. For example, Li et al. constructed indocyanine green (ICG)-loaded ultrasmall gold nanoclusters (Au NCs-ICG) to modulate tumor hypoxia and augment cancer PDT and RT, respectively. In in vivo studies (4T1 tumor-bearing mouse models), the authors observed a high tumor accumulation of Au NC-ICG nanozymes visualized by near-infrared fluorescence, photoacoustic, and computed tomography imaging. They proved the potential of obtained nanozymes for the monitoring and guidance of PDT and RT.

Additionally, they pointed out that the Au NCs-ICG nanozymes effectively decomposed intratumoral H_2O_2 into O_2 for overcoming hypoxia [213]. Another example of metal-based nanozymes is copper hexacyanoferrate (Cu-HCF), with active single-site copper exhibits cascade enzymatic activity within TME, describe by Wanget et al. Their work demonstrated that Cu-HCF could amplify the killing efficacy of singlet oxygen species and suppress tumor growth in vivo [214].

Furthermore, Zhu et al. [215] constructed a PEGylated manganese-based SAE (Mn/PSAE) by coordinating single-atom manganese to nitrogen atoms in hollow zeolitic imidazolate frameworks. Mn/PSAE catalyzes the conversion of cellular H_2O_2 to COH, promotes the decomposition of H_2O_2 to O_2, and continuously catalyzes the conversion of O_2 to cytotoxic CO_2 via oxidase-like activity. The catalytic activity of Mn/PSAE is more pronounced in the weak acidic tumor environment; therefore, these cascade reactions enable the sufficient generation of ROS and effectively kill tumor cells.

Another aspect of tumor treatment is the diagnosis of tumor tissue which is crucial in cancer detection. Metal-based nanozymes built from iron are one of the earliest inorganic nanomaterials with available catalytic behaviors [216]. Some representative examples are ferromagnetic nanoparticles which may provide critical benefits for tumor treatment, including Fenton-augmented ROS stress and hypoxia amelioration [217].

Fan et al. found that magnetic ferritin nanozymes (M-HFn) can be used to target and visualize tumor tissues without any targeted ligands or contrast agents [218]. Ferritin is an iron storage protein that plays a key role in iron homeostasis and the antioxidation of cells [219]. Iron oxide nanozymes (CS-IONzyme) are encapsulated in a recombinant human heavy chain ferritin (HFn) shell, which binds to tumor cells that overexpress transferrin receptor 1 (TfR1). CS-IONzymes catalyzes the oxidation of peroxidase substrates in the presence of hydrogen peroxide to produce a chromogenic reaction for the observation of tumor tissues. They confirm that this diagnostic method detects tumor tissue with 98% sensitivity and 95% specificity. In addition, the ferritin nanozyme diagnostic technique is simple, rapid, and economical. This method simplifies the conventional immunohistochemical experiment for tumor detection and shortens the testing time from 4 to 1 h.

Gao et al. [14] reported that magnetite nanoparticles (Fe_3O_4) possess an intrinsic enzyme mimetic activity similar to that found in natural peroxidases and developed two immunoassays using the intrinsic dual functionality of the Fe_3O_4 MNPs as a peroxidase and magnetic separator.

Metal-based and metal-organic-based nanozymes are not the only ones applied for cancer diagnosis. Wang et al. underline that early cancer diagnosis is the key to improving patient survival rate [220] and point out that metal-organic frameworks (MOFs) consist

of infinite crystalline lattices with metal clusters and organic linkers may provide opportunities for detection of cancer cells which has remained unknown. They reported the successful use of Fe-MIL-101 MOF with intrinsic peroxidase-like to detect cancer cells by conjugating folic acid onto Fe-MIL-101 without any surface modification. Furthermore, the authors found that the Fe-MIL-101-FA bound selectively to the target cells (human cervical carcinoma cells (Hela), colon adenocarcinoma cells (HT-29), and human mouth epidermal carcinoma cells (KB)) through the interaction between FA and folate receptor. Correspondingly, Chen et al. used MOF as an exemplary model of oxygen catalyzer because of their rich catalytic site and sensitizing effect due to the presence of radiosensitizer (high-Z element Hf) in their structural array [221] (Figure 7). The authors designed a folic acid-modified enzyme-like hafnium-based manganoporphyrin metal-organic framework nanoparticles (MnTCPP-Hf-FA MOF NPs) to overcome hypoxia-induced radioresistance and prevent a postoperative recurrence. The MOF NPs they proposed increased radiotherapy's therapeutic efficiency and significantly decreased the risk of local tumor recurrence inside a solid tumor with an inadequate oxygen supply. In vivo experiments revealed that the MnTCPP-Hf-FA MOF NPs could effectively inhibit melanoma growth and prevent tumor postoperative recurrence with only one X-ray irradiation after intravenous injection.
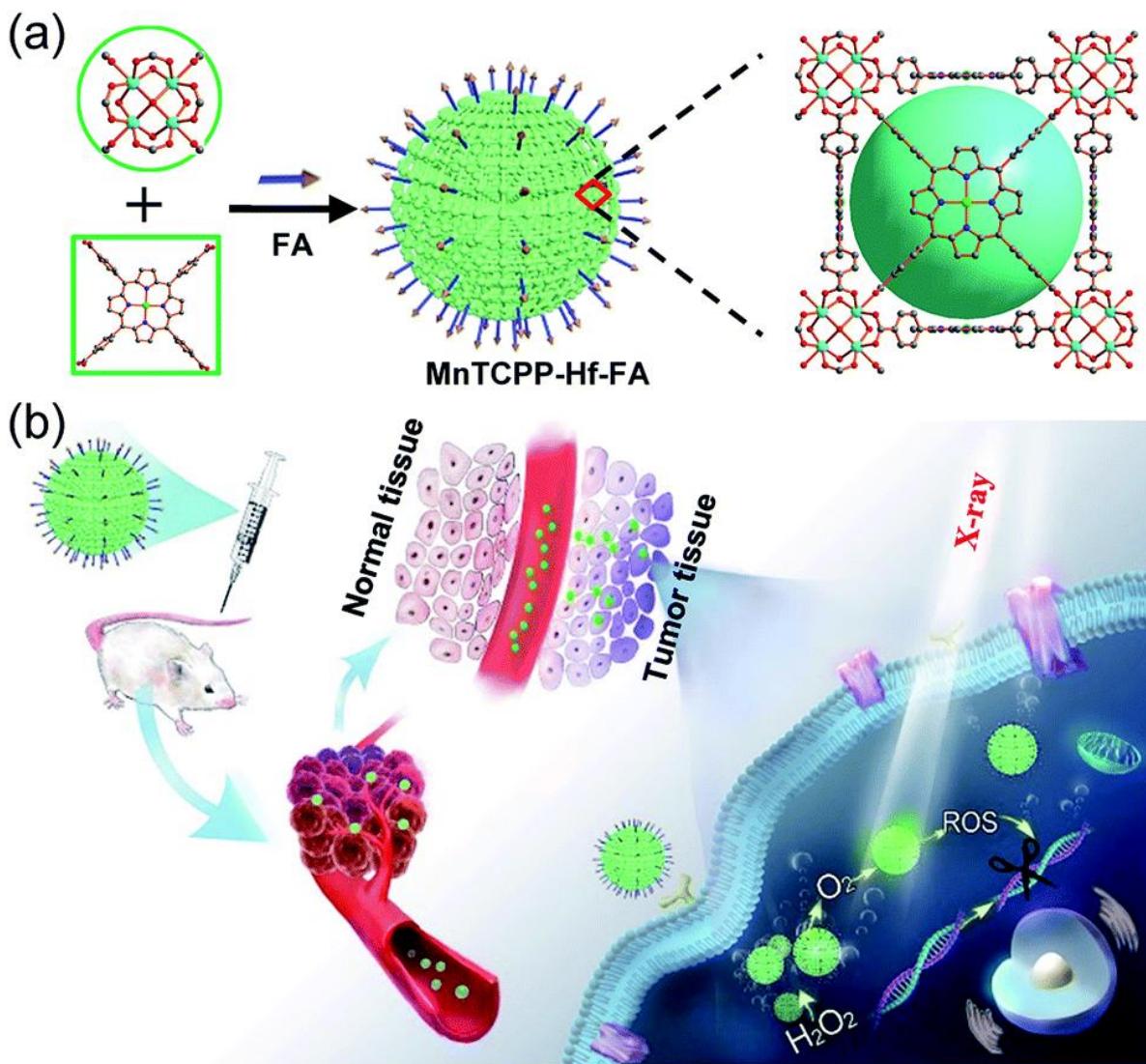

Figure 7. Schematic illustrations of the process for synthesizing nanosensitizer (**a**) and the representation of systemic and intracellular pathways and the action of nanosensitizer (**b**). Reproduced from Reference [221] with permission from the Royal Society of Chemistry.

The presented study revealed that MOF NPs could be used not only for cancer diagnosis but also for cancer therapy, especially when radiosensitizers are at MOF NPs. The additional value of combining X-ray irradiation with MOF-NP joined with radiosensitizer and prospects is a versatile approach to solving hypoxic tumors' critical radioresistance issue [222].

Zhang, Liu et al. [223] constructed a nanozyme with dual enzyme-like activities (PtFe@Fe$_3$O$_4$) for highly efficient tumor catalytic therapy in response to the TME, which is generally known to feature unique characteristics such as the mildly acidic nature, hypoxia, and overproduced hydrogen peroxide (H$_2$O$_2$). Serving as an H$_2$O$_2$-responsive nanozyme, PtFe@Fe$_3$O$_4$ exhibited both intrinsic POD-like and CAT-like activities under acidic conditions. On the other hand, due to the reduced H$_2$O$_2$ concentration in TME, the effect of single-nanozyme-based catalytic therapy is not competent enough compared with combination therapy. The authors have shown that it is possible to achieve efficient deep pancreatic cancer therapy by combining photothermal effects. The catalytic activities of PtFe@Fe$_3$O$_4$ and their therapeutic effect were significantly enhanced under the irradiation of the near-infrared (NIR) laser. At the same time, under light irradiation, nanocatalysts could promote ROS production by direct electron transfer and photoenhanced Fenton reaction [223], (Figure 8). Furthermore, they presented that metal/metal oxide nanomaterials with excellent dual enzyme-like activities can provide a new perspective for the design of nanomedicines and achieve the balanced combination of tumor catalytic therapy and PTT.
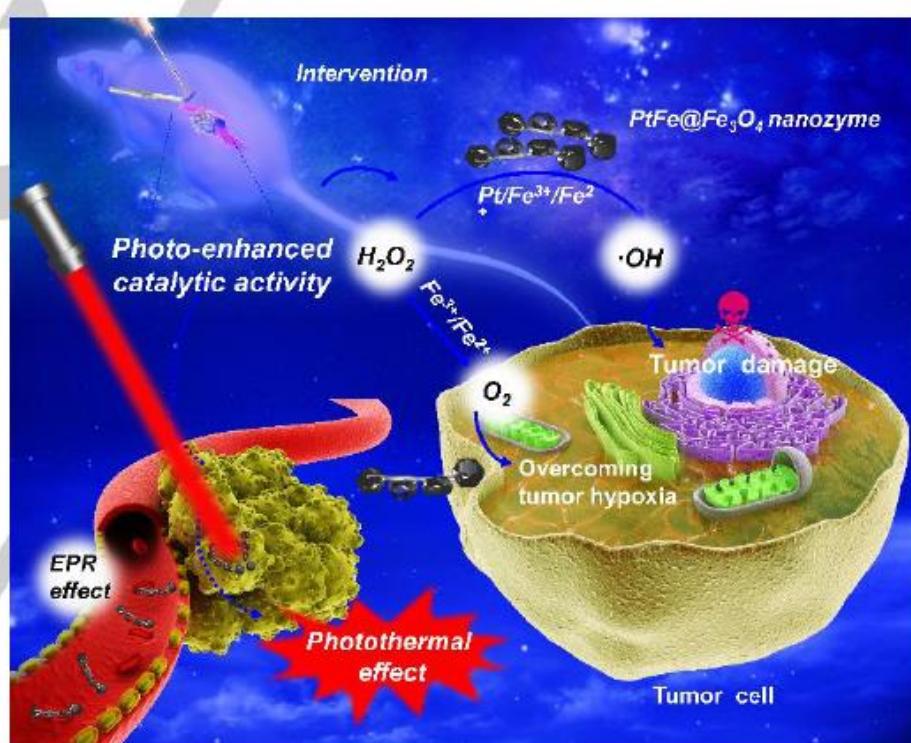

Figure 8. Schematic illustration of the photo-enhanced tumor catalytic therapy for PtFe@Fe$_3$O$_4$ nanozyme. Reproduced from Reference [223] with permission from John Wiley and Sons.

Petty et al. have focused on metal-oxidase nanozymes WO$_3$/Pt nanoparticles, an NADPH oxidase biomimetic that uses NADPH to synthesize ROS. They prepared nanoparticles that can be excited by visible light using the photodeposition method. WO$_3$ absorbed a visible light, and an electron was promoted from the valence band to the conduction band and accumulated at Pt sites. Next, it catalyzed the multielectron reduction of O$_2$ to hydroxyl radicals. At the same time, in the semiconductor, a valence band hole appeared and migrated to the NPs surface, where it abstracted an electron from the environment

(e.g., TME). The reaction at both the photocathode and photoanode led to target tumor cell damage. The authors developed WO_3/Pt nanoparticles tailored for implementation and use in PDT. They have found that the chemical reactions of WO_3/Pt nanoparticles mimic those of the NADPH oxidase and suggest that WO_3/Pt nanoparticles can augment or replace this functional attribute of immune effector cells and, in consequence, to killing tumor cells. Furthermore, they suggested that these nanoparticles could be targeted to other sites or employed in other indications by using different ligands. The WO_3/Pt nanoparticles developed by Petty et al. have numerous therapeutic benefits such as producing large amounts of hydroxyl radicals, lowering cellular anti-oxidant defenses by utilizing NADPH while simultaneously producing hydroxyl radicals, minimal toxicity, remaining effective at low pH, and being resistant to photobleaching [224–226].

However, due to light's limited tissue penetration depth, PDT is commonly used to treat relatively small, superficial tumors [227]. Moreover, the drawback of PDT clinical application is serious skin phototoxicity after systemic administration of photosensitizers. As an alternative to PDT, sonodynamic therapy (SDT) developed uses highly penetrating acoustic waves to activate a class of sound-responsive materials called sonosensitizers (organic sonosensitizers and inorganic sonosensitizers). Organic sonosensitizers are mostly porphyrin derivatives and other fat-soluble small molecules. However, they have some limitations concerning water solubility, poor stability during ultrasound (US), and fast body clearance, leading to low enrichment in tumor sites.

By contrast, inorganic sonosensitizers have stable chemical properties, long blood circulation time, and can effectively reduce phototoxicity. They can also operate as carriers for delivering organic sonosensitizers, effectively overcoming their inherent shortcomings. Possible mechanisms of SDT could be summed up as a generation of ROS, mechanical effects, and thermal effects [228,229].

The most recognized mechanism of SDT is the ROS, including singlet oxygen ($^1O_2$), hydroxyl radicals ($^{\bullet}OH$), superoxide anion ($O_2^{\bullet}-$), or hydrogen peroxide (H_2O_2) after absorbing the energy from the ultrasound. As an example, Cheng et al. presented an ultrasmall oxygen-deficient bimetallic oxide MnWOX nanoparticle for multimodal imaging-guided enhanced SDT against cancer which, as PEGylated MnWOX nanoparticles, could be used for efficient ultrasound (US)-triggered cancer therapy [227]. Similar observations related to generating singlet oxygen and hydroxyl radicals for enhanced SDT efficiency were made by Han et al. [230], who applied for the experiments titanium oxide TiO_2 NPs NPs. However, Cheng et al. found that the generation of $^1O_2$ by MnWOX-PEG was much higher under the same US irradiation conditions than TiO_2 and PpIX nanoparticles.

Mechanical effects of SDT mostly include the cavitation and sonoporation effect. Cavitation is a complex mechanism closely related to gas oscillation and generates ROS by inducing water thermal dissociation. During exposure to the US, gas bubbles rapidly collapse, and then the cavitation of inertial induces the release of energy, producing high temperature and pressures, leading to cell necrosis or producing strong shock waves, resulting in the mechanical damage for cell destruction. The sonoporation effect refers to the formation of pores in the cell membrane under US irradiation. These formed pores allow for the transfer of molecules and NPs into cells. In that way, the sonoporation effect could increase the uptake and accumulation of drug molecules, genes, or NPs.

The last mechanism is the thermal effect trigger by increasing tissue temperature due to the absorption of US energy to destroy tumor cells.

To increase the therapeutic responses to SDT, ultrafine titanium monoxide nanorods (TiO_{1+x} NRs) were used by Chang et al., with great improvement of sonosensitization and Fenton-like catalytic activity [231] (Figure 9). In addition, the authors modified conventional TiO_2 nanoparticles with the $PEG-TiO_{1+x}$ NRs resulted in a much more efficient US-induced generation of ROS. On the other hand, $PEG-TiO_{1+x}$ NRs also exhibit horseradish-peroxidase-like nanozyme activity and can produce hydroxyl radicals ($^{\bullet}OH$) from endogenous H_2O_2 in the tumor. This cancer treatment strategy, consisting of the conversion of hydrogen peroxide (H_2O_2) into a hydroxyl radical (OH), is gaining popularity

in recent times and has been called chemodynamic therapy (CDT). The hydroxyl radical is the most harmful ROS produced in the Fenton-like reaction, and its high overproduction induces apoptosis and cell necrosis.
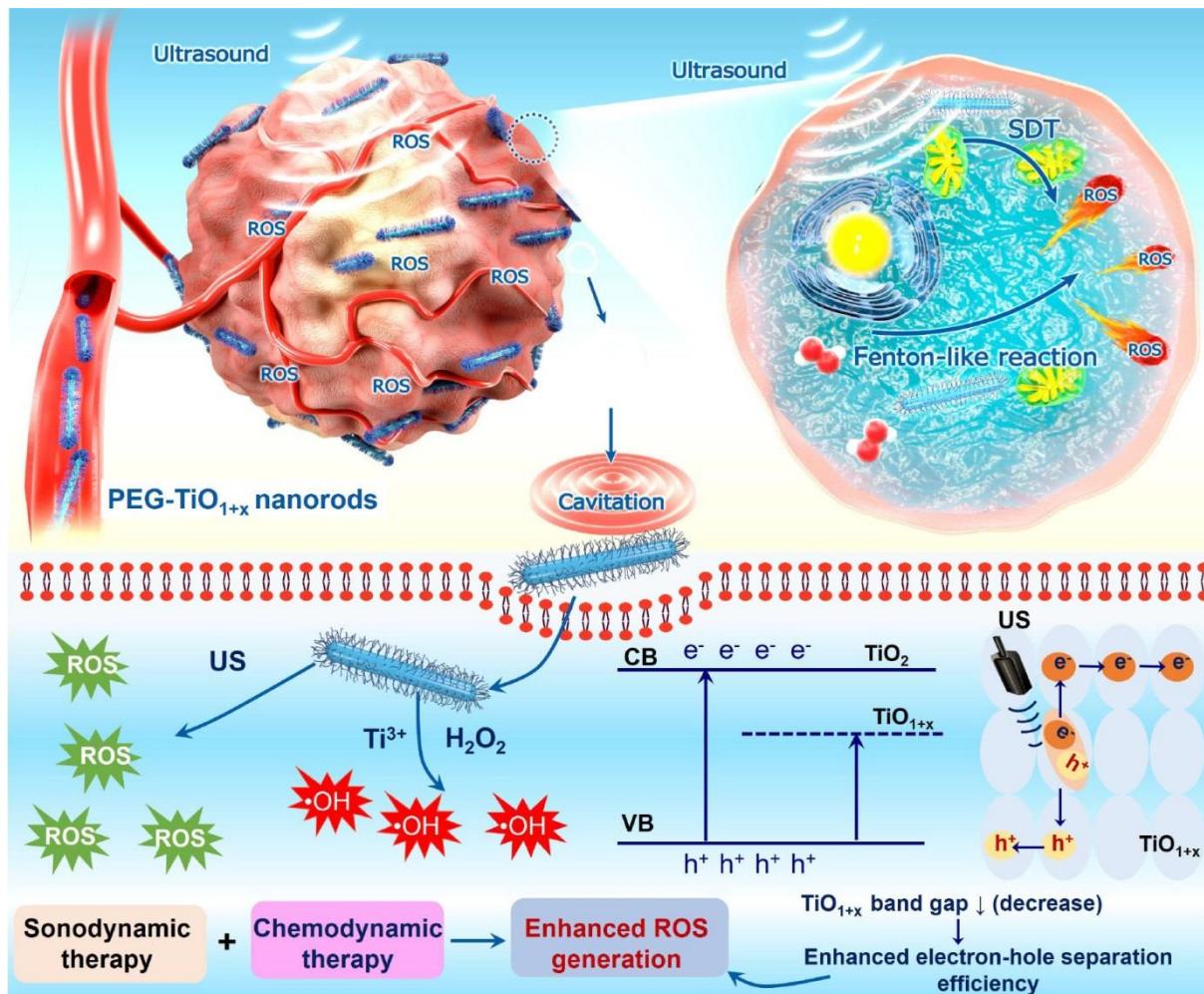

Figure 9. Schematic diagram of ultrafine TiO_{1+x} NRs used as a novel sonosensitizer for SDT/CDT of cancer. Reprinted from [231], with the permission of the American Chemical Society.

Ahamed et al. [232] tackled the toxicity of CuO NPs, which is the limitation for CuO NPs implementation in cancer therapy [233,234]. At the in vitro level, the authors demonstrated the cytotoxicity in a dose-dependent manner, oxidative stress, and apoptosis response of CuO NPs on human hepatocellular carcinoma HepG2 [232]. Their study showed that tumor suppressor gene p53 and apoptotic gene caspase-3 were upregulated due to exposure to CuO NPs. Similar in vitro studies aimed at apoptosis induction were performed by Mkandavire et al. [235]. The authors targeted mitochondria with AuNP conjugated with turbo green fluorescent protein (mitoTGFP) harboring an amino-terminal mitochondrial localization signal and investigated its apoptosis effects on the human breast cancer cell line Jimt-1. Fluorescence and transmission electron microscopy revealed that Au nanoparticle conjugates targeted the mitochondria, causing partial rupture of the outer mitochondrial membrane and cell death.

Wang et al. [236] published information about metal-oxidase-based nanozymes with peroxidase-like activity triggering a novel cell death through an ATP-citrate lyase (ACLY)-dependent rat sarcoma viral oncogene (RAS) signaling mechanism and termed it as nanoptosis (a term proposed by authors). They examined 11 representative nanomaterials

(Cu(OH)$_2$, V$_2$O$_5$, Ag, Fe$_2$O$_3$, ZnO, SiO$_2$, ZnO, TiO$_2$, and Fe$_3$O$_4$ characterized by different dimensions) at the human HepG2 hepatoma cells treatment study.

Their study revealed that HepG2 cells treated with Fe$_3$O$_4$ nanozymes exhibited the characteristic morphologic features of swelling and vacuolation of the mitochondria, disrupting the endoplasmic reticulum and chromatin condensation and margination, and nucleolus disintegration. Furthermore, nanozymes with significant peroxidase activity (such as Cu(OH)$_2$, V$_2$O$_5$, or Ag NPs) activated cell death exhibiting common morphological features and nanozymes with little peroxidase activity (such as Fe$_2$O$_3$, SiO$_2$, TiO$_2$, or ZnO) induced only limited cell death of HepG2. This observation based on transition electron microscopy showed that Fe$_3$O$_4$ nanozyme induced unique cell lethality distinct from the currently well-defined apoptosis, necrosis, autophagy, pyroptosis (inflammation-triggered programmed cell death), and ferroptosis (iron-triggered programmed cell death).

The authors checked the variations of protein profiles and gene expression in Fe$_3$O$_4$ nanozyme-treated HepG2 cells and found that Kirsten rat sarcoma viral oncogene (KRAS) and ACLY played the central roles in Fe$_3$O$_4$ nanozyme-induced cell death. Moreover, they join the fact that Fe$_3$O$_4$ nanozyme-induced cell lethality was regulated by ACLY-dependent RAS signaling because ACLY is a cytosolic enzyme required for RAS farnesylation.

The short review describing the translation of metal and metal oxide nanozymes in cancer treatment showed that regardless, cancer remains a disease with limited treatment approaches, researchers are developing more and more complex nanosomes to overcome these barriers. The cancer treatment can be spiked by combining nanozymes such as modified MOF with radiosensitizers or metal/metal oxide nanozymes with dual enzyme-like activity and irradiation or even molecules in newly discovered pathways. The created new class of nanozymes are candidates for enhancing the efficiency and safety of cancer diagnosis and therapy. However, more efforts should be taken into pharmacological safety, toxicological safety, and the illumination of EPR and protein corona (PC) mechanisms in the human body. Looking forward, the new complex nanozymes will be tailored to target not only cancer cells but also the TME environment, including the immune system.

9. Nanozymes Combating Pathogens

Bacterial infections continue to be a growing global health problem affecting millions of people every year [237,238], and the most commonly used treatment regimens are limited to antibiotics, which increases multidrug resistance. The antimicrobial activity of nanozymes also offers potential for the development of new antimicrobial agents. Many reports on such an action can be found in the latest literature, and examples of application trials are discussed below. The antimicrobial mechanism of nanozymes depends mainly on the activity of peroxidase and oxidase catalyzing the decomposition of H$_2$O$_2$ to •OH in order to regulate ROS [239–242]. Through redox activity, nanozymes generate highly toxic ROS, including free radicals, hydrogen peroxide, superoxide anion, and singlet oxygen, which can destroy the integrity of cell membranes or damage bacterial DNA (Figure 10). Nanozymes also catalyze the degradation of a wide variety of molecules, including polysaccharides, lipids, proteins, and extracellular DNA in the bacterial biofilm matrix. Again, the changes of the nanoenzyme architecture, metal oxidation states, and physicochemical parameters determine the enzyme action in a decisive manner. For example, Fan and Gao [243] designed two kinds of copper/carbon nanozymes, with copper states tuned from Cu^0 to Cu^{2+}. Cu or CuO was deposited on hollow carbon spheres. The authors demonstrated that the nanozymes exhibited peroxidase-, catalase-, or superoxide dismutase-like activities dependent on the copper state. Interestingly, results indicated that the different enzymatic activity modes resulted in different antibacterial modes of action against bacteria. For the CuO nanozymes, the released Cu^{2+} ions caused membrane damage, lipid peroxidation, and DNA degradation of Gram-negative bacteria, whereas the Cu^0-based NP induced the generation of ROS via peroxidase-like catalytic reactions, determining their effect against both Gram-positive and Gram-negative bacteria [243].
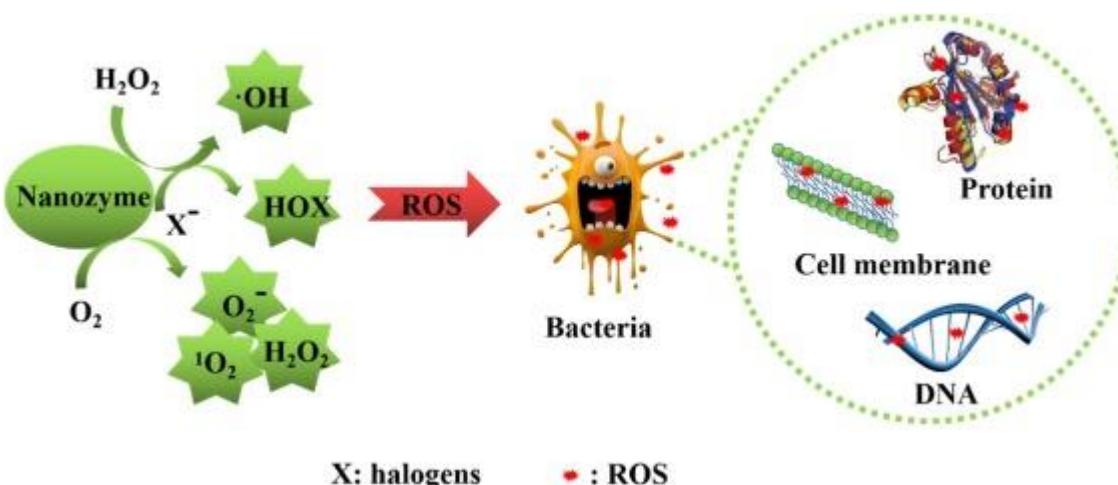
Figure 10. Schematic of the damage of ROS produced by nanozyme to bacteria. Reprinted from [244], with the permission of Elsevier.

In terms of nanoparticle architecture, promising effects gave nanozyme defect modulation, analogous to defect engineering, applied in electronics industrial catalysis and photocatalysis [245]. In the cited study, Wang, Qu et al. Developed a procedure for obtaining defect-rich adhesive nanozymes which, due to their special surface properties, tend to trap bacteria and have effective antibacterial properties (Figure 11). The defect-rich, adhesive nanozyme was constructed by using MoS_2 nanozymes as nanobuilding blocks and copper nanowires (Cu NWs) as a support, while resulting in a rough surface for bacteria trapping and more active defect-rich edge sites which improved peroxidase-mimicking activity. These nanozymes showed increased antibacterial activity against both drug-resistant Gram-negative *E. coli* and Gram-positive *Staphylococcus aureus*. Moreover, their use in vitro and in vivo has been demonstrated, with a strong antibacterial effect and good biocompatibility. Possessed strong near-infrared (NIR) absorbance and outstanding photothermal effects with a rapid elevating temperature under 808 nm light irradiation, which improved their therapeutic potential. Due to their excellent bacterial binding capacity and efficient catalytic activity, defect-rich adhesive nanozymes pave the way for the development of alternative antibiotics.

Similarly, Ywen, Wang et al. reported that Cu_2MoS_4 nanoplates showed NIR-II light enhanced catalytic activity similar to oxidase and peroxidase, which caused an 8 log reduction in *E. coli* titer and a 6 log reduction in *S. aureus* titer after only 10 min in an in vitro system. Moreover, Cu_2MoS_4 showed excellent therapeutic efficacy against *S. aureus* infection in vivo with negligible toxicity to red blood cells and mice. The recently reported study on defect-rich MoS_2 on reduced graphene oxide heterostructure also displayed a capacity for bacterial capture, with ROS-induced damage enhanced by local topological interactions [246].

Under natural, clinical, and industrial circumstances, bacteria tend to attach themselves to surfaces and organize into multicellular communities known as biofilms [247]. Nanozymes have proven effective in many applications related to the reduction of bacterial biofilm formation. One of these promising applications addresses the common problem of biofilm formation on the surface of the teeth and the epithelium of the oral cavity, resulting in tooth decay. Dental biofilm (plaque) is very difficult to remove or treat, but antibacterial drugs can kill the microbes found in the plaque biofilm. Gao et al. discovered that catalytic Fe_3O_4-based nanoparticles (CAT-NP) could be used to control plaque [248]. Peroxidase-mimicking ability of CAT-NP is responsible for this effect, causing the degradation of the extracellular matrix and killing tooth-decay bacteria. Similarly, Gao et al. [249] extracted various natural organic sulfides from garlic and transformed them into nano-iron sulfides with high antibacterial activity. Compared to natural organic sulfides, nano-iron sulfide

showed a broad spectrum of highly efficient bactericidal activity. Iron nanosulfides kill bacteria by releasing hydrogen polysulfide. In addition, iron nanosulfide is a nanozyme having peroxidase and catalase activity that can catalyze the decomposition of hydrogen peroxide. These enzyme-like catalytic activities can further accelerate the release of hydrogen polysulfide, thus enhancing the bactericidal effect. FeS NPs can not only kill various Gram-negative bacteria but also significantly inhibit the action of Gram-positive bacteria such as oral *Streptococcus mutants*, *S. aureus*, and their drug-resistant strains (MRSA and MDR). In addition, they can also effectively accelerate the healing of infected wounds.
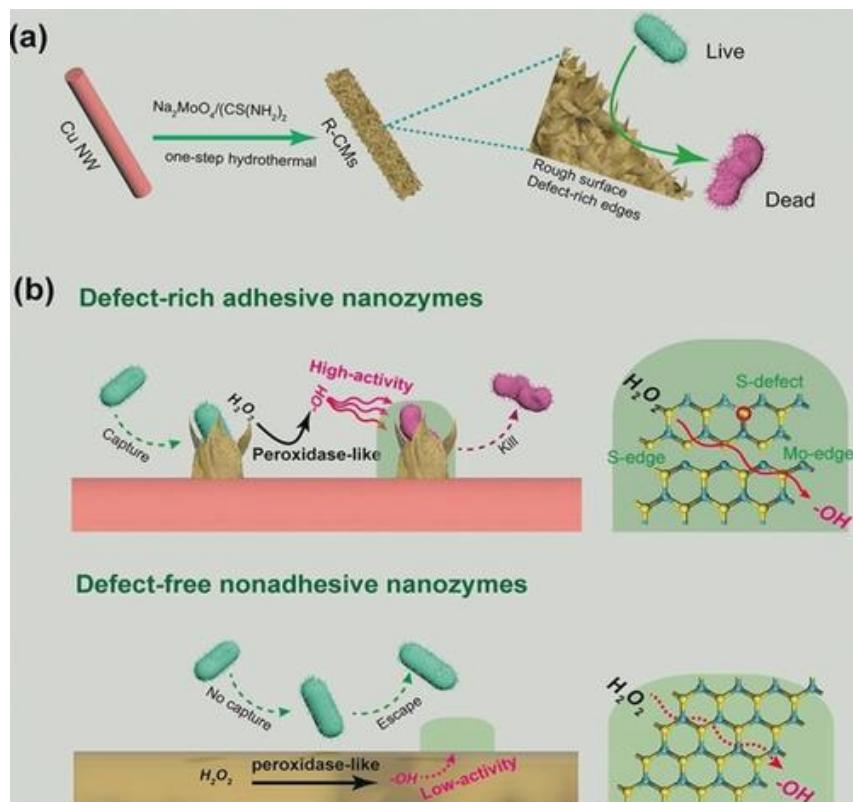

Figure 11. (**a**) One-step formation of defect-rich, adhesive nanozymes and (**b**) their use for improved bacterial capture and elimination. Reprinted from [245], with the permission of Wiley-VCH GmbH, Weinheim.

Many Au-based NPs have been shown to possess antibacterial properties [250–255], their design covering topological modifications, natural ligand applications, and size manipulations. An interesting example of multimodal gold-based nanosystem was reported very recently by Ren, Qu et al. [256], who demonstrated hybrid nanozymes in defense against bacterial infections. Integration of AuNPs with ultrathin graphite carbon nitride (g-C3N4) enhanced peroxidase catalytic activity in catalyzing the decomposition of H_2O_2 to $^{\bullet}$OH radicals. This system was bactericidal against *S. aureus* and *E. coli*, caused biofilm degradation, and prevented the formation of new biofilms in vitro. These nanoparticles were used to create a dressing that accelerated the treatment of bacterial infections and promoted wound healing in a mouse model.

However, a monomodal antimicrobial agent is often insufficient to effectively eliminate biofilms; therefore, Qu et al. [257] proposed MOF/Ce-based nanozymes with dual-enzyme-mimicking activity. The cerium (IV) complexes display DNase-like activity and are capable of hydrolyzing eDNA in biofilms, while the Au-doped MIL-88B(Fe) with peroxidase-like activity can kill bacteria exposed in dispersed biofilms in the presence of H_2O_2. Therefore the MOF-Au-Ce complexes were prepared, displaying a combination of these enzymatic activities. Studies showed that this type of bimodal artificial enzyme could penetrate

biofilms and intensely inhibit their formation. Consequently, in vivo use of MOF-Au-Ce in the treatment of *S. aureus*-induced subcutaneous abscess in mice enhanced wound healing and proved bacteriostatic [257]. The cerium oxide nanoparticle (nanoceria) was shown to possess high peroxidase activity [257,258]. Provided that high peroxidase activity is more conducive to promoting the production of ROS, the CeO_2-H_2O_2 system might be regarded generally a good solution for bacterial disinfection. However, as shown and discussed by Bing et al. [259], CeO_2 nanoparticles show multiple enzyme-like activities depending on their shapes and sizes [26,260]. Beside the high peroxidase activity, CeO_2 also have high SOD and antioxidant activities and depending on the conditions could as well be used as a ROS scavengers. In the system investigated by Bing et al. [259], the peroxidase activity of CeO_2 did not contribute to the antibacterial effect; instead, the ROS scavenging capacity of CeO_2 could protect the bacteria from being killed by H_2O_2.

Recently, the highly photoluminescent glucosamine-derived nitrogen and zinc-doped carbon dots (N, Zn-CDs) were developed as a fluorescence sensor for the detection of Fe^{3+} ions. At the same time, the bactericidal properties of the synthesized nanodots against gram-negative (*Escherichia*) and gram-positive (*S. aureus*) pathogens were investigated. It turned out that these nanodots showed good bactericidal activity against both pathogens under light conditions, and *E. coli*, also in the dark. According to the authors, the small size of the nanodots facilitated their entry into the bacteria, causing the enzymatic imbalance enhanced by the light energy and, as a result, the accumulation of ROS due to stress. The mechanism of action in dark conditions was explained by the release of Zn^{2+} ions and their interaction with the cytoplasmic content of the bacterial cell, followed by the formation of ROS [261].

Nanozymes can be effective agents enhancing infection-fighting during wound healing. A group of researchers from the Xiamen University [262] constructed a nanoplatform based on Pd@Pt- nanoparticles decorated with a synthetic sonosensitizer, meso-tetra(4-carboxyphenyl)porphine (T790). The nanoplatform was used for catalysis-enhanced SDT to treat myositis infected by methicyllin-resistant *S. aureus*. Due to the covalent bond, the sonosensitizer showed good stability and did not release from nanoparticles. Pd@Pt-T790 accumulated effectively in a deeply embedded bacterial infection by using the above-discussed EPR effect, which was a good prerequisite for SDT. T790 anchored on Pd@Pt NPs could significantly block the CAT-like activity of NPs, whereas, upon US irradiation, the nanozyme activity was effectively recovered to catalyze the decomposition of endogenous H_2O_2 into O_2. At the same time, the nanosystem was shown as an attractive medium for fluorescence imaging, PA, and CT in mice. MRI and PA imaging of oxyhemoglobin saturation were used to monitor the treatment process in real-time, revealing a complete eradication of bacterial myositis in mice [262].

It should also be noted that an important issue when designing nanozyme systems is the carrier which can be e.g., a hydrogel composition [263]. An interesting approach was presented by Qu, Ren et al. [264]. When neutrophils encounter an invasive pathogenic microorganism in the human immune system, they typically form branch-like pseudopodia to surround and trap the bacteria for phagocytosis [265]. In the mentioned work [264], a construct was used containing iron-based NM-88 MOF as active centers, as a highly efficient peroxidase mimic, and hierarchical nanocavities produced by the growth of covalent organic structures (COF) as binding pockets to create an adapted microenvironment of pores around active sites to enrich and activate substrate molecules, to perform enhanced bacterial inhibition. The pseudopodia-like surface of the COF allowed the system to efficiently trap bacteria to enhance further the therapeutic efficacy of the MOF-based nanozyme [263].

Nanozymes are also regarded as potential antiviral agents. The classical iron oxide (Fe_3O_4) nanoparticles are well-known double-enzyme-mimics, showing peroxidase and catalase activities [266]. These nanoparticles are currently used for bioseparation, biosensing, bioimaging, drug delivery, and hyperthermia therapy, primarily because of their unique magnetic properties [266]. Recently, Gao et al. used Fe_3O_4 NPs to catalyze the

inactivation of the influenza virus by targeting their lipid envelope [267] (Figure 12). In Gao's work, the Fe_3O_4 NPs (IONs), characterized by lipid peroxidation activity, progressively initiated the breakdown of the viral lipid envelope to destroy adjacent proteins (e.g., haemagglutinin, neuraminidase, and matrix protein 1) and cause concomitant structural damage. Thus, IONs impair the various structures and functions of the virus, resulting in unsuccessful infection of the host cells, ultimately inducing inactivation of influenza A viruses. In mice (BALB/c) infected withH5N1 virus, bodyweight reduction by over 20% during the 14 day infection period was abolished upon treatment with 4 mg/mL IONzymes.
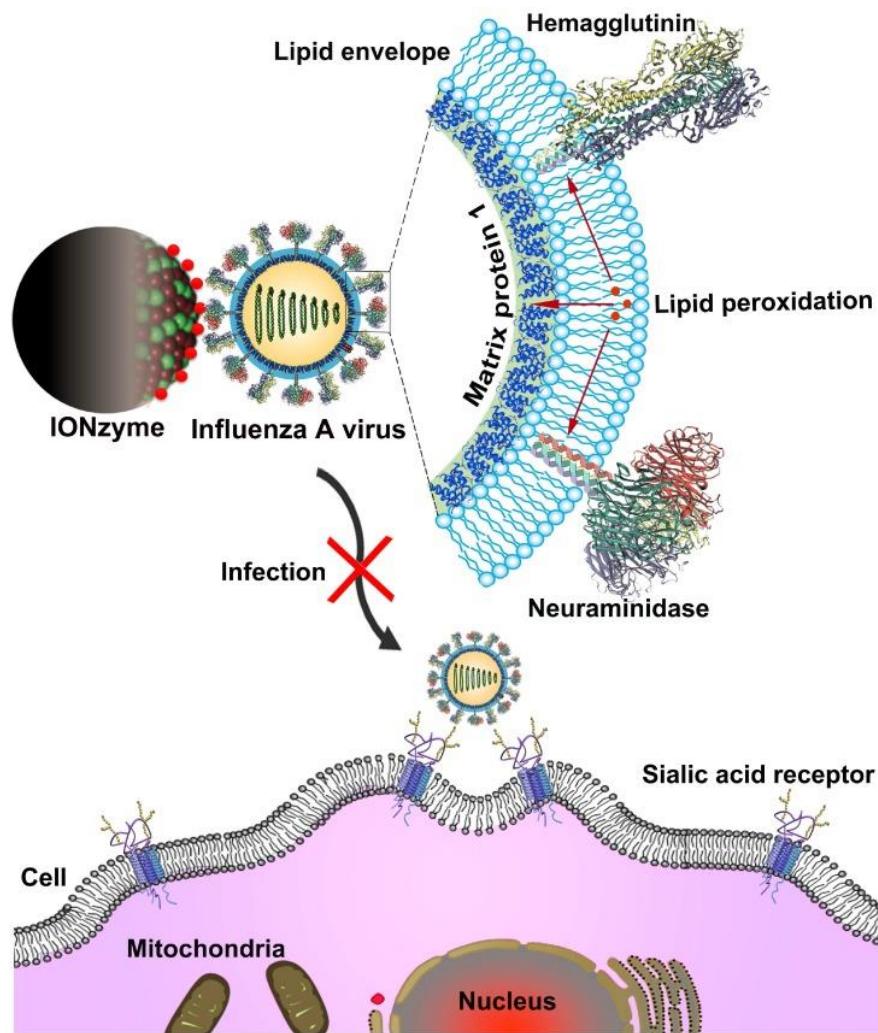

Figure 12. Schematic of viral liperoxidation by IONzymes for virus inactivation. IONzymes directly contact influenza A virus particles and collapse viral lipid envelope via enhancing the level of lipid peroxidation, which further produces free radicals to destroy the neighboring proteins, including hemagglutinin, neuraminidase, and matrix protein 1 and then impair various viral structures and functions, resulting in a failed infection into host cells. Reprinted from [267], with the permission of https://www.thno.org/ (accessed on 6 September 2021).

IONs can be also used to develop new catalytic mucosal vaccine adjuvants by exploiting its POD-like activity in acidic lysosomes to direct DC maturation.

Mucosal vaccination to protect against influenza enhanced by a catalytic ION-based immune adjuvant has recently been elaborated by Gao et al. [268], who designed a new mucosal vaccine based on the combination of chitosan (CS) functionalized iron oxide nanozyme and H1N1 whole inactivated virus (WIV). First, CS-IONzyme was synthesized

by a solvothermic method in which CS in the reaction system acted as both a ligand and a surface functionalization factor. CS was shown to cause a positive surface charge of IONzyme increasing potential antigen delivery. In a mouse model, CS-IONzyme was shown to have good biosafety. When mice were immunized intranasally with CS-IONzyme and H1N1 WIV complexes, the amount of the CS-IONzyme-H1N1 WIV complex was about 30-fold increased on the nasal mucosa compared to the H1N1 WIV only formulation after 15 min of incubation. The complex adhered stably to the mucosa surface. Furthermore, in in vivo study, CS-IONzyme facilitated H1N1 WIV to enhance CCL20-driven submucosal dendritic cell (DC) recruitment and transepithelial dendrite (TED) formation for viral uptake via the toll-like receptor (TLR) 2/4-dependent pathway. Moreover, IONzyme catalyzed a ROS-dependent DC maturation, which further enhanced the migration of H1N1 WIV-loaded DCs into the draining lymph nodes for antigen presentation. In result, CS-IONzyme-based nasal vaccine triggered an 8.9-fold increase in IgA-mucosal adaptive immunity in mice, providing a 100% protection against influenza, while only a 30% protection by H1N1 WIV alone (Figure 13).
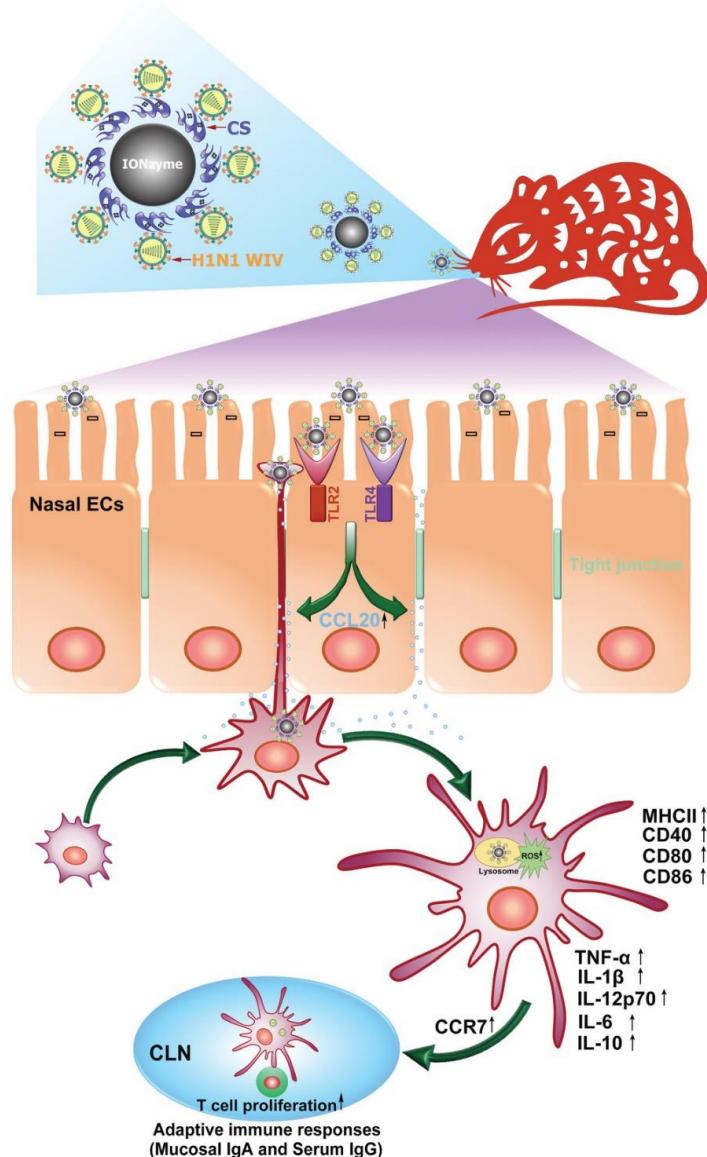

Figure 13. Schematic of proposed mechanism for enhancing antigen-specific immune response by the CS-IONzyme-based influenza vaccine. CS-IONzyme first enhances the adhesion levels of H1N1

WIV to nasal mucosa after intranasal immunization of CS-IONzyme-based influenza vaccine in mice. Next, CS-IONzyme strongly stimulates nasal epithelial cells (ECs) to secrete chemokine CCL20 via TLR 2/4 pathway, which recruits more DCs into the submucosal regions to form TEDs for H1N1 WIV uptake. After viral capture, DCs gradually reach the phenotypic and functional maturation and then quickly migrate into draining cervical lymph nodes (CLNs) for antigen presentation. Finally, the antigen-specific immune response is initiated. Reprinted from [268] with the permission of Wiley under the Creative Commons license (CC BY 4.0).

Currently, the antiviral effect of many metallic nanoparticles is known [269,270]. The knowledge on this subject has expanded recently due to numerous studies conducted in connection with the COVID-19 pandemic [271–273]. For example, the mitochondrial proteins of the virus can be degraded by the multivalent silver nanozymes [274]. Silver ions bind to the RNA virus genome to activate antiviral mitochondrial proteins [270]. Gold nanozymes have the ability to mimic the virus-binding receptor, leading to virus deformation [275]. Zinc oxide nanozymes are also able to reduce viral infection by enhancing T cell and antibody responses [276,277]. Overall, nanozymes seem to be an effective alternative for detecting and targeting viruses, including coronaviruses; however, the catalytic mechanisms are poorly understood and require research in nanotechnology, computational engineering, machine learning, artificial intelligence, and computer science.

Nanozymes also offer hope to overcome diseases caused by parasites, although this field of science is only emerging. Among the few reports on this subject, of special interest is the work Yan and Fan [278], who constructed a ferritin nanozyme (Fenozyme) composed of recombinant human ferritin (HFn) protein shells that specifically target blood–brain barrier endothelial cells (BBB ECs) and the inner Fe_3O_4 nanozyme core that exhibits ROS-scavenging CAT-like activity. When administered to mice with experimental cerebral malaria, Fenozyme significantly increased the survival rate, protecting BBB ECs from ROS damage and reducing parasitemia by polarizing macrophages to the M1 phenotype. The Fenozyme colocalized with CD31, an adhesion molecule normally found on BBB endothelial cells. Moreover, Fenozyme binding to endothelial cells was largely blocked by an anti-HFn receptor antibody. The accumulation of Fenozyme in the brains of mice occurred in a time-dependent manner. Fluorescence imaging showed that Fenozyme could specifically bind to macro- and micro-vasculature in the brain. In summary, the HFn envelope bound the HFn receptor and directed the fenozyme to BBB endothelial cells in the mouse brain. Fenozyme localized inside the endosomes, presumably through HFn receptor-mediated endocytosis to function as a catalase in the endothelial cells. While 50 µM of H_2O_2 killed approximately 50% of the model endothelial cells, the addition of Fenozyme almost fully protected the cells from the damage induced by H_2O_2 at the concentration of 0.1 mg/mL. In addition, co-administration of Fenozyme and antimalarial artemether alleviated encephalopathy and memory impairment in mice that survived the experimental cerebral malaria [278]. These results demonstrated the importance of ROS-induced stress in parasite-caused inflammation and indicated that the nanozymes could be used as an adjuvant in parasitic diseases.

10. Conclusions

In recent decades, the range of available metallic catalytic systems has been significantly increased due to the introduction of organometallic catalysts that better differentiate the substrates allowed for further transformations. While the classic man-made constructs typically recognize and preorganize substrates in the immediate vicinity of the bond being formed or broken, the active sites of enzymes represent a complex mosaic of amino acids that recognize substrates based on their more distant characteristics and thus operate with correspondingly increased selectivity. The presently acquired possibilities of nanotechnology to construct complex "artificial active sites" allows controlling the position of incoming substrates with precision more and more comparable to real enzymes. The resulting nanozymes offer durability characteristics of nanomaterials and the flexibility of supramolecular systems. Nevertheless, presently, nanozyme design still struggles with the

requirements for large-scale application due to the compromise between catalytic activity and substrate selectivity in combination with the complicated structure and chemistry required that is still beyond our reach. Still, a high number of herein presented papers document the constant trials of modern scientists, where a variety of tactics used include modifications of ligands allowing the change in the surface characteristics of nanozymes, lipophilic/hydrophilic properties, acceleration of electron transfer, and improving the affinity and selectivity between nanozymes and substrates.

When designing new artificial enzymes based on nanomaterials, careful consideration should be given to the overall relationship between structure and activity. The optimization of nanozymes should be based on the imitation of natural catalytic structures and take into account the degree of oxidation of metal centers and their geometry, ligand surroundings, surface strain, and hydrophilicity. Recently, a series of bioinspired nanozymes have been synthesized by simulating the structural characteristics and action patterns of the core compounds in natural enzymes, such as cofactors and active centers [279].

Most nanozymes only catalyze redox reactions but lack catalytic activities such as synthesis and hydrolysis, narrowing the range of possible applications of nanozymes in industry and medicine. Currently, most bioinspired nanozymes focus on increasing catalytic activity, and relatively little attention has been paid to improving their substrate selectivity. This may be due to the aforementioned shortcomings in the current technology, which do not allow for the precise development of fine nanozyme structures. A field of nanoscience that is still awaiting development is the enantioselectivity of nanozymes. In turn, the multicatalytic activity of nanozymes, which now makes them less specific and less useful, may prove beneficial in the future, provided that good strategies are found to fine-tune their catalytic activity. Taking inspiration from biology, it is worth noting that the binding sites and catalytic sites of some natural enzymes are not in the same position. This observation may provide a clue in the design of future nanozymes. Strategies for separating binding sites and nanozyme catalytic sites may be adopted to optimize both substrate selectivity and catalytic activity.

An interesting thesis was put forward in the recent publication by Yan, Fan, and Zhang [280]. The authors point our attention to the fact, that nanoscopic materials might have been adapted early in the evolution of organisms, being the first step in the development of the perfect and complex structures of contemporary natural enzymes. Some biomineralized nanomaterials found in organisms, such as magnetosomes [280] and iron core in ferritin [281,282], have been reported to have peroxidase-like activities. Thus, nanozymes could have appeared earlier than organic natural enzymes in biology and are likely to play a role in the process of biological evolution.

Until now, rationally designed, biologically inspired, highly active nanozymes have become a hot topic in ongoing nanozyme research. With the help of these unique constructs, we will be able to develop useful new strategies to control the homeostasis of cells, tissues, and organisms.

Author Contributions: Conceptualization, H.L. formal analysis, H.L., U.K. and K.W.; investigation, H.L. and U.K.; resources, H.L., U.K. and K.W.; data curation, H.L., U.K. and K.W.; writing—original draft preparation, H.L. and U.K.; writing—review and editing, H.L., U.K. and K.W.; visualization, H.L., U.K. and K.W.; supervision, H.L.; project administration, H.L.; funding acquisition, H.L. All authors have read and agreed to the published version of the manuscript.

Institutional Review Board Statement: Not applicable.

Informed Consent Statement: Not applicable.

Data Availability Statement: Not applicable.

Conflicts of Interest: The authors declare no conflict of interest. The funders had no role in the design of the study; in the collection, analyses, or interpretation of data; in the writing of the manuscript, or in the decision to publish the results.

References

1. Korschelt, K.; Tahir, M.N.; Tremel, W. A Step into the Future: Applications of Nanoparticle Enzyme Mimics. *Chemistry* **2018**, *24*, 9703–9713. [CrossRef]
2. Kuah, E.; Toh, S.; Yee, J.; Ma, Q.; Gao, Z. Enzyme Mimics: Advances and Applications. *Chem. Eur. J.* **2016**, *22*, 8404–8430. [CrossRef]
3. Wiester, M.J.; Ulmann, P.A.; Mirkin, C.A. Enzyme Mimics Based upon Supramolecular Coordination Chemistry. *Angew. Chem. Int. Ed. Engl.* **2011**, *50*, 114–137. [CrossRef]
4. Wei, H.; Wang, E. Nanomaterials with Enzyme-like Characteristics (Nanozymes): Next-Generation Artificial Enzymes. *Chem. Soc. Rev.* **2013**, *42*, 6060–6093. [CrossRef]
5. Zhang, R.; Yan, X.; Fan, K. Nanozymes Inspired by Natural Enzymes. *Acc. Mater. Res.* **2021**, *2*, 534–547. [CrossRef]
6. Gomaa, E.Z. Nanozymes: A Promising Horizon for Medical and Environmental Applications. *J. Clust. Sci.* **2021**. [CrossRef]
7. Ansari, S.A.; Husain, Q. Potential Applications of Enzymes Immobilized on/in Nano Materials: A Review. *Biotechnol. Adv.* **2012**, *30*, 512–523. [CrossRef] [PubMed]
8. Bora, T.; Dutta, J. Applications of Nanotechnology in Wastewater Treatment—A Review. *J. Nanosci. Nanotechnol.* **2014**, *14*, 613–626. [CrossRef] [PubMed]
9. Qi, Z.; Wang, L.; You, Q.; Chen, Y. PA-Tb-Cu MOF as Luminescent Nanoenzyme for Catalytic Assay of Hydrogen Peroxide. *Biosens. Bioelectron.* **2017**, *96*, 227–232. [CrossRef] [PubMed]
10. Jiang, D.; Ni, D.; Rosenkrans, Z.T.; Huang, P.; Yan, X.; Cai, W. Nanozyme: New Horizons for Responsive Biomedical Applications. *Chem. Soc. Rev.* **2019**, *48*, 3683–3704. [CrossRef] [PubMed]
11. Yang, T.; Zelikin, A.N.; Chandrawati, R. Enzyme Mimics for the Catalytic Generation of Nitric Oxide from Endogenous Prodrugs. *Small* **2020**, *16*, e1907635. [CrossRef] [PubMed]
12. Breslow, R.; Overman, L.E. "Artificial Enzyme" Combining a Metal Catalytic Group and a Hydrophobic Binding Cavity. *J. Am. Chem. Soc.* **1970**, *92*, 1075–1077. [CrossRef]
13. Manea, F.; Houillon, F.B.; Pasquato, L.; Scrimin, P. Nanozymes: Gold-Nanoparticle-Based Transphosphorylation Catalysts. *Angew. Chem. Int. Ed.* **2004**, *43*, 6165–6169. [CrossRef]
14. Gao, L.; Zhuang, J.; Nie, L.; Zhang, J.; Zhang, Y.; Gu, N.; Wang, T.; Feng, J.; Yang, D.; Perrett, S.; et al. Intrinsic Peroxidase-like Activity of Ferromagnetic Nanoparticles. *Nat. Nanotechnol.* **2007**, *2*, 577–583. [CrossRef]
15. Nath, I.; Chakraborty, J.; Verpoort, F. Metal Organic Frameworks Mimicking Natural Enzymes: A Structural and Functional Analogy. *Chem. Soc. Rev.* **2016**, *45*, 4127–4170. [CrossRef]
16. Sun, H.; Zhou, Y.; Ren, J.; Qu, X. Carbon Nanozymes: Enzymatic Properties, Catalytic Mechanism, and Applications. *Angew. Chem. Int. Ed.* **2018**, *57*, 9224–9237. [CrossRef]
17. Wu, J.; Wang, X.; Wang, Q.; Lou, Z.; Li, S.; Zhu, Y.; Qin, L.; Wei, H. Nanomaterials with Enzyme-like Characteristics (Nanozymes): Next-Generation Artificial Enzymes (II). *Chem. Soc. Rev.* **2019**, *48*, 1004–1076. [CrossRef]
18. Chen, Z.; Wang, Z.; Ren, J.; Qu, X. Enzyme Mimicry for Combating Bacteria and Biofilms. *Acc. Chem. Res.* **2018**, *51*, 789–799. [CrossRef]
19. Stasyuk, N.; Smutok, O.; Demkiv, O.; Prokopiv, T.; Gayda, G.; Nisnevitch, M.; Gonchar, M. Synthesis, Catalytic Properties and Application in Biosensorics of Nanozymes and Electronanocatalysts: A Review. *Sensors* **2020**, *20*, 4509. [CrossRef] [PubMed]
20. Yang, H.; Yang, R.; Zhang, P.; Qin, Y.; Chen, T.; Ye, F. A Bimetallic (Co/2Fe) Metal-Organic Framework with Oxidase and Peroxidase Mimicking Activity for Colorimetric Detection of Hydrogen Peroxide. *Microchim. Acta* **2017**, *184*, 4629–4635. [CrossRef]
21. Sun, J.; Li, C.; Qi, Y.; Guo, S.; Liang, X. Optimizing Colorimetric Assay Based on V_2O_5 Nanozymes for Sensitive Detection of H_2O_2 and Glucose. *Sensors* **2016**, *16*, 584. [CrossRef]
22. Fan, L.; Lou, D.; Wu, H.; Zhang, X.; Zhu, Y.; Gu, N.; Zhang, Y. A Novel AuNP-Based Glucose Oxidase Mimic with Enhanced Activity and Selectivity Constructed by Molecular Imprinting and O_2-Containing Nanoemulsion Embedding. *Adv. Mater. Interfaces* **2018**, *5*, 1801070. [CrossRef]
23. Khade, B.S.; Gawali, P.G.; Waghmare, M.M.; Dongre, P. Adsorption of α-Amylase and Starch on Porous Zinc Oxide Nanosheet: Biophysical Study. *Food Biophys.* **2021**, *16*, 280–291. [CrossRef]
24. Liu, W.; Ruan, M.-L.; Liu, L.; Ji, X.; Ma, Y.; Yuan, P.; Tang, G.; Lin, H.; Dai, J.; Xue, W. Self-Activated *in Vivo* Therapeutic Cascade of Erythrocyte Membrane-Cloaked Iron-Mineralized Enzymes. *Theranostics* **2020**, *10*, 2201–2214. [CrossRef] [PubMed]
25. Chen, Q.; Liu, Y.; Liu, J.; Liu, J. Liposome-Boosted Peroxidase-Mimicking Nanozymes Breaking the PH Limit. *Chemistry* **2020**, *26*, 16659–16665. [CrossRef] [PubMed]
26. Huang, Y.; Ren, J.; Qu, X. Nanozymes: Classification, Catalytic Mechanisms, Activity Regulation, and Applications. *Chem. Rev.* **2019**, *119*, 4357–4412. [CrossRef] [PubMed]
27. Dong, S.; Dong, Y.; Jia, T.; Liu, S.; Liu, J.; Yang, D.; He, F.; Gai, S.; Yang, P.; Lin, J. GSH-Depleted Nanozymes with Hyperthermia-Enhanced Dual Enzyme-Mimic Activities for Tumor Nanocatalytic Therapy. *Adv. Mater.* **2020**, *32*, e2002439. [CrossRef]

28. Gonzalez-Vicente, A.; Garvin, J. Effects of Reactive Oxygen Species on Tubular Transport along the Nephron. *Antioxidants* **2017**, *6*, 23. [CrossRef]

29. D'Autréaux, B.; Toledano, M.B. ROS as Signalling Molecules: Mechanisms That Generate Specificity in ROS Homeostasis. *Nat. Rev. Mol. Cell Biol.* **2007**, *8*, 813–824. [CrossRef]

30. Yu, L.; Liu, Z.; Qiu, L.; Hao, L.; Guo, J. Ipatasertib Sensitizes Colon Cancer Cells to TRAIL-Induced Apoptosis through ROS-Mediated Caspase Activation. *Biochem. Biophys. Res. Commun.* **2019**, *519*, 812–818. [CrossRef]

31. Kaminskyy, V.O.; Piskunova, T.; Zborovskaya, I.B.; Tchevkina, E.M.; Zhivotovsky, B. Suppression of Basal Autophagy Reduces Lung Cancer Cell Proliferation and Enhances Caspase-Dependent and -Independent Apoptosis by Stimulating ROS Formation. *Autophagy* **2012**, *8*, 1032–1044. [CrossRef]

32. Mu, W.; Cheng, X.; Zhang, X.; Liu, Y.; Lv, Q.; Liu, G.; Zhang, J.; Li, X. Hinokiflavone Induces Apoptosis via Activating Mitochondrial ROS/JNK/Caspase Pathway and Inhibiting NF-KB Activity in Hepatocellular Carcinoma. *J. Cell Mol. Med.* **2020**, *24*, 8151–8165. [CrossRef] [PubMed]

33. Li, X.; Fang, F.; Gao, Y.; Tang, G.; Xu, W.; Wang, Y.; Kong, R.; Tuyihong, A.; Wang, Z. ROS Induced by KillerRed Targeting Mitochondria (MtKR) Enhances Apoptosis Caused by Radiation via Cyt c/Caspase-3 Pathway. *Oxid. Med. Cell Longev.* **2019**, *2019*, 4528616. [CrossRef]

34. Sun, S.; Zhang, C.; Gao, J.; Qin, Q.; Zhang, Y.; Zhu, H.; Yang, X.; Yang, D.; Yan, H. Benzoquinone Induces ROS-Dependent Mitochondria-Mediated Apoptosis in HL-60 Cells. *Toxicol. Ind. Health* **2018**, *34*, 270–281. [CrossRef] [PubMed]

35. Liguori, I.; Russo, G.; Curcio, F.; Bulli, G.; Aran, L.; Della-Morte, D.; Gargiulo, G.; Testa, G.; Cacciatore, F.; Bonaduce, D. Oxidative Stress, Aging, and Diseases. *Clin. Interv. Aging* **2018**, *13*, 757. [CrossRef]

36. Muller, J.; Huaux, F.; Fonseca, A.; Nagy, J.B.; Moreau, N.; Delos, M.; Raymundo-Piñero, E.; Béguin, F.; Kirsch-Volders, M.; Fenoglio, I. Structural Defects Play a Major Role in the Acute Lung Toxicity of Multiwall Carbon Nanotubes: Toxicological Aspects. *Chem. Res. Toxicol.* **2008**, *21*, 1698–1705. [CrossRef]

37. Brzoska, K.; Szczygiel, M.; Drzał, A.; Sniegocka, M.; Michalczyk-Wetula, D.; Biela, E.; Elas, M.; Kapka-Skrzypczak, L.; Lewandowska-Siwkiewicz, H.; Urbańska, K. Transient Vasodilation in Mouse 4T1 Tumors after Intragastric and Intravenous Administration of Gold Nanoparticles. *Int. J. Mol. Sci.* **2021**, *22*, 2361. [CrossRef]

38. Tschopp, J. Mitochondria: Sovereign of Inflammation? *Eur. J. Immunol.* **2011**, *41*, 1196–1202. [CrossRef]

39. Karataş, Ö.F.; Sezgin, E.; Aydın, Ö.; Çulha, M. Interaction of Gold Nanoparticles with Mitochondria. *Colloids Surf. B Biointerfaces* **2009**, *71*, 315–318. [CrossRef] [PubMed]

40. Wu, Y.-N.; Yang, L.-X.; Shi, X.-Y.; Li, I.-C.; Biazik, J.M.; Ratinac, K.R.; Chen, D.-H.; Thordarson, P.; Shieh, D.-B.; Braet, F. The Selective Growth Inhibition of Oral Cancer by Iron Core-Gold Shell Nanoparticles through Mitochondria-Mediated Autophagy. *Biomaterials* **2011**, *32*, 4565–4573. [CrossRef] [PubMed]

41. Wilhelmi, V.; Fischer, U.; Weighardt, H.; Schulze-Osthoff, K.; Nickel, C.; Stahlmecke, B.; Kuhlbusch, T.A.; Scherbart, A.M.; Esser, C.; Schins, R.P. Zinc Oxide Nanoparticles Induce Necrosis and Apoptosis in Macrophages in a P47phox-and Nrf2-Independent Manner. *PLoS ONE* **2013**, *8*, e65704. [CrossRef] [PubMed]

42. Abrikossova, N.; Skoglund, C.; Ahrén, M.; Bengtsson, T.; Uvdal, K. Effects of Gadolinium Oxide Nanoparticles on the Oxidative Burst from Human Neutrophil Granulocytes. *Nanotechnology* **2012**, *23*, 275101. [CrossRef] [PubMed]

43. Sun, B.; Wang, X.; Ji, Z.; Wang, M.; Liao, Y.-P.; Chang, C.H.; Li, R.; Zhang, H.; Nel, A.E.; Xia, T. NADPH Oxidase-Dependent NLRP3 Inflammasome Activation and Its Important Role in Lung Fibrosis by Multiwalled Carbon Nanotubes. *Small* **2015**, *11*, 2087–2097. [CrossRef] [PubMed]

44. Murphy, F.A.; Schinwald, A.; Poland, C.A.; Donaldson, K. The Mechanism of Pleural Inflammation by Long Carbon Nanotubes: Interaction of Long Fibres with Macrophages Stimulates Them to Amplify pro-Inflammatory Responses in Mesothelial Cells. *Part. Fibre Toxicol.* **2012**, *9*, 8. [CrossRef]

45. Culcasi, M.; Benameur, L.; Mercier, A.; Lucchesi, C.; Rahmouni, H.; Asteian, A.; Casano, G.; Botta, A.; Kovacic, H.; Pietri, S. EPR Spin Trapping Evaluation of ROS Production in Human Fibroblasts Exposed to Cerium Oxide Nanoparticles: Evidence for NADPH Oxidase and Mitochondrial Stimulation. *Chem.-Biol. Interact.* **2012**, *199*, 161–176. [CrossRef]

46. Damasco, J.A.; Ravi, S.; Perez, J.D.; Hagaman, D.E.; Melancon, M.P. Understanding Nanoparticle Toxicity to Direct a Safe-by-Design Approach in Cancer Nanomedicine. *Nanomaterials* **2020**, *10*, 2186. [CrossRef]

47. Manke, A.; Wang, L.; Rojanasakul, Y. Mechanisms of Nanoparticle-Induced Oxidative Stress and Toxicity. *Biomed. Res. Int* **2013**, *2013*, 942916. [CrossRef]

48. Zhou, Y.-T.; He, W.; Wamer, W.G.; Hu, X.; Wu, X.; Lo, Y.M.; Yin, J.-J. Enzyme-Mimetic Effects of Gold@ Platinum Nanorods on the Antioxidant Activity of Ascorbic Acid. *Nanoscale* **2013**, *5*, 1583–1591. [CrossRef]

49. Palierse, E.; Hélary, C.; Krafft, J.-M.; Génois, I.; Masse, S.; Laurent, G.; Alvarez Echazu, M.I.; Selmane, M.; Casale, S.; Valentin, L.; et al. Baicalein-Modified Hydroxyapatite Nanoparticles and Coatings with Antibacterial and Antioxidant Properties. *Mater. Sci. Eng. C Mater. Biol. Appl.* **2021**, *118*, 111537. [CrossRef]

50. Khorrami, S.; Zarrabi, A.; Khaleghi, M.; Danaei, M.; Mozafari, M.R. Selective Cytotoxicity of Green Synthesized Silver Nanoparticles against the MCF-7 Tumor Cell Line and Their Enhanced Antioxidant and Antimicrobial Properties. *Int. J. Nanomed.* **2018**, *13*, 8013–8024. [CrossRef]

51. Mohd Zaffarin, A.S.; Ng, S.-F.; Ng, M.H.; Hassan, H.; Alias, E. Pharmacology and Pharmacokinetics of Vitamin E: Nanoformulations to Enhance Bioavailability. *Int. J. Nanomed.* **2020**, *15*, 9961–9974. [CrossRef]

52. Lewandowska, H.; Kalinowska, M. New Polyphenol-Containing LDL Nano-Preparations in Oxidative Stress and DNA Damage: A Potential Route for Cell-Targeted PP Delivery. *Materials* **2020**, *13*, 5106. [CrossRef] [PubMed]

53. Flieger, J.; Flieger, W.; Baj, J.; Maciejewski, R. Antioxidants: Classification, Natural Sources, Activity/Capacity Measurements, and Usefulness for the Synthesis of Nanoparticles. *Materials* **2021**, *14*, 4135. [CrossRef] [PubMed]

54. Bajić, V.; Spremo-Potparević, B.; Živković, L.; Čabarkapa, A.; Kotur-Stevuljević, J.; Isenović, E.; Sredojević, D.; Vukoje, I.; Lazić, V.; Ahrenkiel, S.P.; et al. Surface-Modified TiO₂ Nanoparticles with Ascorbic Acid: Antioxidant Properties and Efficiency against DNA Damage In Vitro. *Colloids Surf. B Biointerfaces* **2017**, *155*, 323–331. [CrossRef]

55. Elemike, E.E.; Fayemi, O.E.; Ekennia, A.C.; Onwudiwe, D.C.; Ebenso, E.E. Silver Nanoparticles Mediated by Costus Afer Leaf Extract: Synthesis, Antibacterial, Antioxidant and Electrochemical Properties. *Molecules* **2017**, *22*, 701. [CrossRef]

56. Grace, A.N.; Pandian, K. Organically Dispersible Gold and Platinum Nanoparticles Using Aromatic Amines as Phase Transfer and Reducing Agent and Their Applications in Electro-Oxidation of Glucose. *Colloids Surf. A Physicochem. Eng. Asp.* **2007**, *302*, 113–120. [CrossRef]

57. Gozdziewska, M.; Cichowicz, G.; Markowska, K.; Zawada, K.; Megiel, E. Nitroxide-Coated Silver Nanoparticles: Synthesis, Surface Physicochemistry and Antibacterial Activity. *RSC Adv.* **2015**, *5*, 58403–58415. [CrossRef]

58. Sadi, G.; Sadi, Ö. Antioxidants and Regulation of Antioxidant Enzymes by Cellular Redox Status. *Turk. J. Sci. Rev.* **2010**, *3*, 95–107.

59. Hikosaka, K.; Kim, J.; Kajita, M.; Kanayama, A.; Miyamoto, Y. Platinum Nanoparticles Have an Activity Similar to Mitochondrial NADH:Ubiquinone Oxidoreductase. *Colloids Surf. B Biointerfaces* **2008**, *66*, 195–200. [CrossRef]

60. Baldim, V.; Yadav, N.; Bia, N.; Graillot, A.; Loubat, C.; Singh, S.; Karakoti, A.S.; Berret, J.-F. Polymer-Coated Cerium Oxide Nanoparticles as Oxidoreductase-like Catalysts. *ACS Appl. Mater. Interfaces* **2020**, *12*, 42056–42066. [CrossRef]

61. Alula, M.T.; Madingwane, M.L. Colorimetric Quantification of Chromium (VI) Ions Based on Oxidoreductase-like Activity of Fe₃O₄. *Sens. Actuators B Chem.* **2020**, *324*, 128726. [CrossRef]

62. Bonomi, R.; Cazzolaro, A.; Sansone, A.; Scrimin, P.; Prins, L.J. Detection of Enzyme Activity through Catalytic Signal Amplification with Functionalized Gold Nanoparticles. *Angew. Chem. Int. Ed.* **2011**, *50*, 2307–2312. [CrossRef]

63. Pasquato, L.; Rancan, F.; Scrimin, P.; Mancin, F.; Frigeri, C. N-Methylimidazole-Functionalized Gold Nanoparticles as Catalysts for Cleavage of a Carboxylic Acid Ester. *Chem. Commun.* **2000**, 2253–2254. [CrossRef]

64. Pengo, P.; Polizzi, S.; Pasquato, L.; Scrimin, P. Carboxylate−Imidazole Cooperativity in Dipeptide-Functionalized Gold Nanoparticles with Esterase-like Activity. *J. Am. Chem. Soc.* **2005**, *127*, 1616–1617. [CrossRef]

65. Singh, S. Nanomaterials Exhibiting Enzyme-Like Properties (Nanozymes): Current Advances and Future Perspectives. *Front. Chem.* **2019**, *7*, 46. [CrossRef] [PubMed]

66. Prousek, J. Fenton Chemistry in Biology and Medicine. *Pure Appl. Chem.* **2007**, *79*, 2325–2338. [CrossRef]

67. Yu, C.-J.; Lin, C.-Y.; Liu, C.-H.; Cheng, T.-L.; Tseng, W.-L. Synthesis of Poly(Diallyldimethylammonium Chloride)-Coated Fe₃O₄ Nanoparticles for Colorimetric Sensing of Glucose and Selective Extraction of Thiol. *Biosens. Bioelectron.* **2010**, *26*, 913–917. [CrossRef] [PubMed]

68. Kim, M.I.; Shim, J.; Li, T.; Lee, J.; Park, H.G. Fabrication of Nanoporous Nanocomposites Entrapping Fe₃O₄ Magnetic Nanoparticles and Oxidases for Colorimetric Biosensing. *Chem. Eur. J.* **2011**, *17*, 10700–10707. [CrossRef] [PubMed]

69. Dong, Y.; Zhang, H.; Rahman, Z.U.; Su, L.; Chen, X.; Hu, J.; Chen, X. Graphene Oxide–Fe₃O₄ Magnetic Nanocomposites with Peroxidase-like Activity for Colorimetric Detection of Glucose. *Nanoscale* **2012**, *4*, 3969. [CrossRef]

70. Huang, F.; Wang, J.; Chen, W.; Wan, Y.; Wang, X.; Cai, N.; Liu, J.; Yu, F. Synergistic Peroxidase-like Activity of CeO₂-Coated Hollow Fe₃O₄ Nanocomposites as an Enzymatic Mimic for Low Detection Limit of Glucose. *J. Taiwan Inst. Chem. Eng.* **2018**, *83*, 40–49. [CrossRef]

71. Cheng, H.; Zhang, L.; He, J.; Guo, W.; Zhou, Z.; Zhang, X.; Nie, S.; Wei, H. Integrated Nanozymes with Nanoscale Proximity for in Vivo Neurochemical Monitoring in Living Brains. *Anal. Chem.* **2016**, *88*, 5489–5497. [CrossRef] [PubMed]

72. Tian, J.; Liu, S.; Luo, Y.; Sun, X. Fe(III)-Based Coordination Polymernanoparticles: Peroxidase-like Catalytic Activity and Their Application to Hydrogen Peroxide and Glucose Detection. *Catal. Sci. Technol.* **2012**, *2*, 432–436. [CrossRef]

73. Liu, Y.L.; Zhao, X.J.; Yang, X.X.; Li, Y.F. A Nanosized Metal–Organic Framework of Fe-MIL-88NH2 as a Novel Peroxidase Mimic Used for Colorimetric Detection of Glucose. *Analyst* **2013**, *138*, 4526. [CrossRef] [PubMed]

74. Rahal, A.; Kumar, A.; Singh, V.; Yadav, B.; Tiwari, R.; Chakraborty, S.; Dhama, K. Oxidative Stress, Prooxidants, and Antioxidants: The Interplay. *BioMed Res. Int.* **2014**, *2014*, 1–19. [CrossRef] [PubMed]

75. Mahmudunnabi, R.G.; Farhana, F.Z.; Kashaninejad, N.; Firoz, S.H.; Shim, Y.-B.; Shiddiky, M.J. Nanozyme-Based Electrochemical Biosensors for Disease Biomarker Detection. *Analyst* **2020**, *145*, 4398–4420. [CrossRef] [PubMed]

76. Moons, J.; de Azambuja, F.; Mihailovic, J.; Kozma, K.; Smiljanic, K.; Amiri, M.; Cirkovic Velickovic, T.; Nyman, M.; Parac-Vogt, T.N. Discrete Hf18 Metal-oxo Cluster as a Heterogeneous Nanozyme for Site-Specific Proteolysis. *Angew. Chem.* **2020**, *132*, 9179–9186. [CrossRef]

77. Hille, R.; Hall, J.; Basu, P. The Mononuclear Molybdenum Enzymes. *Chem. Rev.* **2014**, *114*, 3963–4038. [CrossRef]

78. Lin, T.; Zhong, L.; Guo, L.; Fu, F.; Chen, G. Seeing Diabetes: Visual Detection of Glucose Based on the Intrinsic Peroxidase-like Activity of MoS₂ Nanosheets. *Nanoscale* **2014**, *6*, 11856–11862. [CrossRef]

79. Li, S.; Liu, X.; Chai, H.; Huang, Y. Recent Advances in the Construction and Analytical Applications of Metal-Organic Frameworks-Based Nanozymes. *TrAC Trends Anal. Chem.* **2018**, *105*, 391–403. [CrossRef]

80. Wu, X.; Chen, T.; Wang, J.; Yang, G. Few-Layered MoSe$_2$ Nanosheets as an Efficient Peroxidase Nanozyme for Highly Sensitive Colorimetric Detection of H$_2$O$_2$ and Xanthine. *J. Mater. Chem. B* **2018**, *6*, 105–111. [CrossRef]

81. Huang, L.; Li, Z.; Guo, L. Colorimetric Assay of Acetylcholinesterase Inhibitor Tacrine Based on MoO$_2$ Nanoparticles as Peroxidase Mimetics. *Spectrochim. Acta Part. A Mol. Biomol. Spectrosc.* **2020**, *224*, 117412. [CrossRef]

82. Yang, Z.-D.; Chang, Z.-W.; Zhang, Q.; Huang, K.; Zhang, X.-B. Decorating Carbon Nanofibers with Mo$_2$C Nanoparticles towards Hierarchically Porous and Highly Catalytic Cathode for High-Performance Li-O$_2$ Batteries. *Sci. Bull.* **2018**, *63*, 433–440. [CrossRef]

83. Li, J.; Tang, C.; Liang, T.; Tang, C.; Lv, X.; Tang, K.; Li, C.M. Porous Molybdenum Carbide Nanostructured Catalyst toward Highly Sensitive Biomimetic Sensing of H$_2$O$_2$. *Electroanalysis* **2020**, *32*, 1243–1250. [CrossRef]

84. Sun, Z.; Zhao, Q.; Zhang, G.; Li, Y.; Zhang, G.; Zhang, F.; Fan, X. Exfoliated MoS$_2$ Supported Au–Pd Bimetallic Nanoparticles with Core–Shell Structures and Superior Peroxidase-like Activities. *RSC Adv.* **2015**, *5*, 10352–10357. [CrossRef]

85. Zhu, W.; Li, M.; Chen, S.; Wang, C.; Lu, X. Interfacial Engineering Regulating the Peroxidase-like Property of Ternary Composite Nanofibers and Their Sensing Applications. *Appl. Surf. Sci.* **2019**, *491*, 138–146. [CrossRef]

86. Liu, C.; Zhang, M.; Geng, H.; Zhang, P.; Zheng, Z.; Zhou, Y.; He, W. NIR Enhanced Peroxidase-like Activity of Au@CeO$_2$ Hybrid Nanozyme by Plasmon-Induced Hot Electrons and Photothermal Effect for Bacteria Killing. *Appl. Catal. B Environ.* **2021**, *295*, 120317. [CrossRef]

87. Murugan, C.; Murugan, N.; Sundramoorthy, A.K.; Sundaramurthy, A. Nanoceria Decorated Flower-like Molybdenum Sulphide Nanoflakes: An Efficient Nanozyme for Tumour Selective ROS Generation and Photo Thermal Therapy. *Chem. Commun.* **2019**, *55*, 8017–8020. [CrossRef]

88. Ragg, R.; Natalio, F.; Tahir, M.N.; Janssen, H.; Kashyap, A.; Strand, D.; Strand, S.; Tremel, W. Molybdenum Trioxide Nanoparticles with Intrinsic Sulfite Oxidase Activity. *ACS Nano* **2014**, *8*, 5182–5189. [CrossRef]

89. Chen, T.; Zou, H.; Wu, X.; Liu, C.; Situ, B.; Zheng, L.; Yang, G. Nanozymatic Antioxidant System Based on MoS$_2$ Nanosheets. *ACS Appl. Mater. Interfaces* **2018**, *10*, 12453–12462. [CrossRef]

90. Li, L.; Liu, L.; Hu, Z.; Lu, Y.; Liu, Q.; Jin, S.; Zhang, Q.; Zhao, S.; Chou, S. Understanding High-Rate K$^+$-Solvent Co-Intercalation in Natural Graphite for Potassium-Ion Batteries. *Angew. Chem. Int. Ed.* **2020**, *59*, 12917–12924. [CrossRef]

91. Zhang, X.-D.; Zhang, J.; Wang, J.; Yang, J.; Chen, J.; Shen, X.; Deng, J.; Deng, D.; Long, W.; Sun, Y.-M.; et al. Highly Catalytic Nanodots with Renal Clearance for Radiation Protection. *ACS Nano* **2016**, *10*, 4511–4519. [CrossRef] [PubMed]

92. Wang, X.; Cao, W.; Qin, L.; Lin, T.; Chen, W.; Lin, S.; Yao, J.; Zhao, X.; Zhou, M.; Hang, C. Boosting the Peroxidase-like Activity of Nanostructured Nickel by Inducing Its 3+ Oxidation State in LaNiO$_2$ Perovskite and Its Application for Biomedical Assays. *Theranostics* **2017**, *7*, 2277. [CrossRef] [PubMed]

93. Heckert, E.G.; Karakoti, A.S.; Seal, S.; Self, W.T. The Role of Cerium Redox State in the SOD Mimetic Activity of Nanoceria. *Biomaterials* **2008**, *29*, 2705–2709. [CrossRef]

94. Pirmohamed, T.; Dowding, J.M.; Singh, S.; Wasserman, B.; Heckert, E.; Karakoti, A.S.; King, J.E.; Seal, S.; Self, W.T. Nanoceria Exhibit Redox State-Dependent Catalase Mimetic Activity. *Chem. Commun.* **2010**, *46*, 2736–2738. [CrossRef]

95. Zhang, X.-Q.; Gong, S.-W.; Zhang, Y.; Yang, T.; Wang, C.-Y.; Gu, N. Prussian Blue Modified Iron Oxide Magnetic Nanoparticles and Their High Peroxidase-like Activity. *J. Mater. Chem.* **2010**, *20*, 5110–5116. [CrossRef]

96. Zhao, J.; de Serrano, V.; Dumarieh, R.; Thompson, M.; Ghiladi, R.A.; Franzen, S. The Role of the Distal Histidine in H$_2$O$_2$ Activation and Heme Protection in Both Peroxidase and Globin Functions. *J. Phys. Chem. B* **2012**, *116*, 12065–12077. [CrossRef]

97. Fan, K.; Wang, H.; Xi, J.; Liu, Q.; Meng, X.; Duan, D.; Gao, L.; Yan, X. Optimization of Fe$_3$O$_4$ Nanozyme Activity via Single Amino Acid Modification Mimicking an Enzyme Active Site. *Chem. Commun.* **2017**, *53*, 424–427. [CrossRef] [PubMed]

98. Sono, M.; Roach, M.P.; Coulter, E.D.; Dawson, J.H. Heme-Containing Oxygenases. *Chem. Rev.* **1996**, *96*, 2841–2888. [CrossRef]

99. Johnson, D.C.; Dean, D.R.; Smith, A.D.; Johnson, M.K. Structure, Function, and Formation of Biological Iron-Sulfur Clusters. *Annu. Rev. Biochem.* **2005**, *74*, 247–281. [CrossRef] [PubMed]

100. Rouault, T.A.; Klausner, R.D. Iron-Sulfur Clusters as Biosensors of Oxidants and Iron. *Trends Biochem. Sci.* **1996**, *21*, 174–177. [CrossRef]

101. Zhang, W.; Hu, S.; Yin, J.-J.; He, W.; Lu, W.; Ma, M.; Gu, N.; Zhang, Y. Prussian Blue Nanoparticles as Multienzyme Mimetics and Reactive Oxygen Species Scavengers. *J. Am. Chem. Soc.* **2016**, *138*, 5860–5865. [CrossRef]

102. Hosseini, M.; Mozafari, M. Cerium Oxide Nanoparticles: Recent Advances in Tissue Engineering. *Materials* **2020**, *13*, 3072. [CrossRef]

103. Gorecki, M.; Beck, Y.; Hartman, J.R.; Fischer, M.; Weiss, L.; Tochner, Z.; Slavin, S.; Nimrod, A. Recombinant Human Superoxide Dismutases: Production and Potential Therapeutic Uses. *Free Radic. Res. Commun.* **1991**, *12*, 401–410. [CrossRef]

104. Yao, J.; Cheng, Y.; Zhou, M.; Zhao, S.; Lin, S.; Wang, X.; Wu, J.; Li, S.; Wei, H. ROS Scavenging Mn$_3$O$_4$ Nanozymes for In Vivo Anti-Inflammation. *Chem. Sci.* **2018**, *9*, 2927–2933. [CrossRef]

105. Liu, C.-P.; Wu, T.-H.; Lin, Y.-L.; Liu, C.-Y.; Wang, S.; Lin, S.-Y. Tailoring Enzyme-Like Activities of Gold Nanoclusters by Polymeric Tertiary Amines for Protecting Neurons Against Oxidative Stress. *Small* **2016**, *12*, 4127–4135. [CrossRef]

106. He, S.B.; Yang, L.; Lin, M.T.; Balasubramanian, P.; Peng, H.P.; Kuang, Y.; Deng, H.H.; Chen, W. Platinum group element-based nanozymes for biomedical applications: An overview. *Biomed. Mater.* **2020**, *16*, 3, 032001. [CrossRef]

107. Gatto, F.; Moglianetti, M.; Pompa, P.; Bardi, G. Platinum Nanoparticles Decrease Reactive Oxygen Species and Modulate Gene Expression without Alteration of Immune Responses in THP-1 Monocytes. *Nanomaterials* **2018**, *8*, 392. [CrossRef] [PubMed]

108. Pedone, D.; Moglianetti, M.; De Luca, E.; Bardi, G.; Pompa, P.P. Platinum Nanoparticles in Nanobiomedicine. *Chem. Soc. Rev.* **2017**, *46*, 4951–4975. [CrossRef] [PubMed]

109. Lee, Y.-P.; Kim, S.-H.; Bang, J.-W.; Lee, H.-S.; Kwak, S.-S.; Kwon, S.-Y. Enhanced Tolerance to Oxidative Stress in Transgenic Tobacco Plants Expressing Three Antioxidant Enzymes in Chloroplasts. *Plant. Cell Rep.* **2007**, *26*, 591–598. [CrossRef]

110. Lubos, E.; Loscalzo, J.; Handy, D.E. Glutathione Peroxidase-1 in Health and Disease: From Molecular Mechanisms to Therapeutic Opportunities. *Antioxid. Redox Signal.* **2011**, *15*, 1957–1997. [CrossRef] [PubMed]

111. Day, B.J. Catalase and Glutathione Peroxidase Mimics. *Biochem. Pharmacol.* **2009**, *77*, 285–296. [CrossRef] [PubMed]

112. Zhou, W.; Li, H.; Xia, B.; Ji, W.; Ji, S.; Zhang, W.; Huang, W.; Huo, F.; Xu, H. Selenium-Functionalized Metal-Organic Frameworks as Enzyme Mimics. *Nano Res.* **2018**, *11*, 5761–5768. [CrossRef]

113. Hou, C.; Luo, Q.; Liu, J.; Miao, L.; Zhang, C.; Gao, Y.; Zhang, X.; Xu, J.; Dong, Z.; Liu, J. Construction of GPx Active Centers on Natural Protein Nanodisk/Nanotube: A New Way to Develop Artificial Nanoenzyme. *ACS Nano* **2012**, *6*, 8692–8701. [CrossRef] [PubMed]

114. Sun, H.; Miao, L.; Li, J.; Fu, S.; An, G.; Si, C.; Dong, Z.; Luo, Q.; Yu, S.; Xu, J.; et al. Self-Assembly of Cricoid Proteins Induced by "Soft Nanoparticles": An Approach To Design Multienzyme-Cooperative Antioxidative Systems. *ACS Nano* **2015**, *9*, 5461–5469. [CrossRef]

115. Vernekar, A.A.; Sinha, D.; Srivastava, S.; Paramasivam, P.U.; D'Silva, P.; Mugesh, G. An Antioxidant Nanozyme That Uncovers the Cytoprotective Potential of Vanadia Nanowires. *Nat. Commun.* **2014**, *5*, 5301. [CrossRef]

116. Singh, N.; Savanur, M.A.; Srivastava, S.; D'Silva, P.; Mugesh, G. A Redox Modulatory Mn_3O_4 Nanozyme with Multi-Enzyme Activity Provides Efficient Cytoprotection to Human Cells in a Parkinson's Disease Model. *Angew. Chem. Int. Ed.* **2017**, *56*, 14267–14271. [CrossRef]

117. Peng, Y.; Wang, C.; Li, J. Structure–Activity Relationship of VOx/CeO_2 Nanorod for NO Removal with Ammonia. *Appl. Catal. B Environ.* **2014**, *144*, 538–546. [CrossRef]

118. Singh, N.; NaveenKumar, S.K.; Geethika, M.; Mugesh, G. A Cerium Vanadate Nanozyme with Specific Superoxide Dismutase Activity Regulates Mitochondrial Function and ATP Synthesis in Neuronal Cells. *Angew. Chem. Int. Ed.* **2021**, *60*, 3121–3130. [CrossRef]

119. Huang, Y.; Liu, Z.; Liu, C.; Ju, E.; Zhang, Y.; Ren, J.; Qu, X. Self-Assembly of Multi-Nanozymes to Mimic an Intracellular Antioxidant Defense System. *Angew. Chem. Int. Ed.* **2016**, *55*, 6646–6650. [CrossRef]

120. Sui, L.; Wang, J.; Xiao, Z.; Yang, Y.; Yang, Z.; Ai, K. ROS-Scavenging Nanomaterials to Treat Periodontitis. *Front. Chem.* **2020**, *8*, 595530. [CrossRef]

121. Padwal, P.; Bandyopadhyaya, R.; Mehra, S. Polyacrylic Acid-Coated Iron Oxide Nanoparticles for Targeting Drug Resistance in Mycobacteria. *Langmuir* **2014**, *30*, 15266–15276. [CrossRef]

122. Moglianetti, M.; De Luca, E.; Pedone, D.; Marotta, R.; Catelani, T.; Sartori, B.; Amenitsch, H.; Retta, S.F.; Pompa, P.P. Platinum Nanozymes Recover Cellular ROS Homeostasis in an Oxidative Stress-Mediated Disease Model. *Nanoscale* **2016**, *8*, 3739–3752. [CrossRef] [PubMed]

123. Moglianetti, M.; Pedone, D.; Udayan, G.; Retta, S.F.; Debellis, D.; Marotta, R.; Turco, A.; Rella, S.; Malitesta, C.; Bonacucina, G.; et al. Intracellular Antioxidant Activity of Biocompatible Citrate-Capped Palladium Nanozymes. *Nanomaterials* **2020**, *10*, 99. [CrossRef]

124. Fan, J.; Yin, J.-J.; Ning, B.; Wu, X.; Hu, Y.; Ferrari, M.; Anderson, G.J.; Wei, J.; Zhao, Y.; Nie, G. Direct Evidence for Catalase and Peroxidase Activities of Ferritin–Platinum Nanoparticles. *Biomaterials* **2011**, *32*, 1611–1618. [CrossRef] [PubMed]

125. Li, M.; Shi, P.; Xu, C.; Ren, J.; Qu, X. Cerium Oxide Caged Metal Chelator: Anti-Aggregation and Anti-Oxidation Integrated H_2O_2-Responsive Controlled Drug Release for Potential Alzheimer's Disease Treatment. *Chem. Sci.* **2013**, *4*, 2536–2542. [CrossRef]

126. Zhao, Y.; Trewyn, B.G.; Slowing, I.I.; Lin, V.S.-Y. Mesoporous Silica Nanoparticle-Based Double Drug Delivery System for Glucose-Responsive Controlled Release of Insulin and Cyclic AMP. *J. Am. Chem. Soc.* **2009**, *131*, 8398–8400. [CrossRef] [PubMed]

127. Geng, J.; Li, M.; Wu, L.; Chen, C.; Qu, X. Mesoporous Silica Nanoparticle-based H_2O_2 Responsive Controlled-release System Used for Alzheimer's Disease Treatment. *Adv. Healthc. Mater.* **2012**, *1*, 332–336. [CrossRef] [PubMed]

128. Wu, M.; Gao, J.; Wang, F.; Yang, J.; Song, N.; Jin, X.; Mi, P.; Tian, J.; Luo, J.; Liang, F. Multistimuli Responsive Core–Shell Nanoplatform Constructed from Fe_3O_4@ MOF Equipped with Pillar [6] Arene Nanovalves. *Small* **2018**, *14*, 1704440. [CrossRef]

129. Estelrich, J.; Busquets, M.A. Prussian Blue: A Nanozyme with Versatile Catalytic Properties. *Int. J. Mol. Sci.* **2021**, *22*, 5993. [CrossRef]

130. Huang, Y.; Jiang, J.; Wang, Y.; Chen, J.; Xi, J. Nanozymes as Enzyme Inhibitors. *Int. J. Nanomed.* **2021**, *16*, 1143–1155. [CrossRef]

131. Liu, B.; Liu, J. Surface Modification of Nanozymes. *Nano Res.* **2017**, *10*, 1125–1148. [CrossRef]

132. You, C.-C.; De, M.; Han, G.; Rotello, V.M. Tunable Inhibition and Denaturation of α-Chymotrypsin with Amino Acid-Functionalized Gold Nanoparticles. *J. Am. Chem. Soc.* **2005**, *127*, 12873–12881. [CrossRef] [PubMed]

133. Sellergren, B. Shaping Enzyme Inhibitors. *Nat. Chem.* **2010**, *2*, 7–8. [CrossRef] [PubMed]

134. You, C.-C.; Agasti, S.S.; De, M.; Knapp, M.J.; Rotello, V.M. Modulation of the Catalytic Behavior of α-Chymotrypsin at Monolayer-Protected Nanoparticle Surfaces. *J. Am. Chem. Soc.* **2006**, *128*, 14612–14618. [CrossRef]

135. Cha, S.-H.; Hong, J.; McGuffie, M.; Yeom, B.; VanEpps, J.S.; Kotov, N.A. Shape-Dependent Biomimetic Inhibition of Enzyme by Nanoparticles and Their Antibacterial Activity. *ACS Nano* **2015**, *9*, 9097–9105. [CrossRef] [PubMed]

136. Ali, S.R.; Pandit, S.; De, M. 2D-MoS$_2$ -Based β-Lactamase Inhibitor for Combination Therapy against Drug-Resistant Bacteria. *ACS Appl. Biol. Mater.* **2018**, *1*, 967–974. [CrossRef]

137. Taubes, G. The Bacteria Fight Back. *Science* **2008**, *321*, 356–361. [CrossRef]

138. Karunakaran, S.; Pandit, S.; De, M. Functionalized Two-Dimensional MoS$_2$ with Tunable Charges for Selective Enzyme Inhibition. *ACS Omega* **2018**, *3*, 17532–17539. [CrossRef]

139. Wu, J.; Li, S.; Wei, H. Multifunctional Nanozymes: Enzyme-like Catalytic Activity Combined with Magnetism and Surface Plasmon Resonance. *Nanoscale Horiz.* **2018**, *3*, 367–382. [CrossRef]

140. Liu, Q.; Zhang, A.; Wang, R.; Zhang, Q.; Cui, D. A Review on Metal-and Metal Oxide-Based Nanozymes: Properties, Mechanisms, and Applications. *Nanomicro Lett.* **2021**, *13*, 154. [CrossRef]

141. Chen, W.; Chen, J.; Feng, Y.-B.; Hong, L.; Chen, Q.-Y.; Wu, L.-F.; Lin, X.-H.; Xia, X.-H. Peroxidase-like Activity of Water-Soluble Cupric Oxide Nanoparticles and Its Analytical Application for Detection of Hydrogen Peroxide and Glucose. *Analyst* **2012**, *137*, 1706–1712. [CrossRef] [PubMed]

142. Li, Z.-M.; Zhong, X.-L.; Wen, S.-H.; Zhang, L.; Liang, R.-P.; Qiu, J.-D. Colorimetric Detection of Methyltransferase Activity Based on the Enhancement of CoOOH Nanozyme Activity by SsDNA. *Sens. Actuators B Chem.* **2019**, *281*, 1073–1079. [CrossRef]

143. Sharma, T.K.; Ramanathan, R.; Weerathunge, P.; Mohammadtaheri, M.; Daima, H.K.; Shukla, R.; Bansal, V. Aptamer-Mediated 'Turn-off/Turn-on'Nanozyme Activity of Gold Nanoparticles for Kanamycin Detection. *Chem. Commun.* **2014**, *50*, 15856–15859. [CrossRef]

144. Cheng, H.; Lin, S.; Muhammad, F.; Lin, Y.-W.; Wei, H. Rationally Modulate the Oxidase-like Activity of Nanoceria for Self-Regulated Bioassays. *ACS Sens.* **2016**, *1*, 1336–1343. [CrossRef]

145. Zhu, Z.; Guan, Z.; Jia, S.; Lei, Z.; Lin, S.; Zhang, H.; Ma, Y.; Tian, Z.; Yang, C.J. Au@ Pt Nanoparticle Encapsulated Target-responsive Hydrogel with Volumetric Bar-chart Chip Readout for Quantitative Point-of-care Testing. *Angew. Chem. Int. Ed.* **2014**, *53*, 12503–12507.

146. Duan, D.; Fan, K.; Zhang, D.; Tan, S.; Liang, M.; Liu, Y.; Zhang, J.; Zhang, P.; Liu, W.; Qiu, X. Nanozyme-Strip for Rapid Local Diagnosis of Ebola. *Biosens. Bioelectron.* **2015**, *74*, 134–141. [CrossRef] [PubMed]

147. Han, J.; Zhang, L.; Hu, L.; Xing, K.; Lu, X.; Huang, Y.; Zhang, J.; Lai, W.; Chen, T. Nanozyme-Based Lateral Flow Assay for the Sensitive Detection of *Escherichia coli* O157: H7 in Milk. *J. Dairy Sci.* **2018**, *101*, 5770–5779. [CrossRef] [PubMed]

148. Wang, X.; Qin, L.; Zhou, M.; Lou, Z.; Wei, H. Nanozyme Sensor Arrays for Detecting Versatile Analytes from Small Molecules to Proteins and Cells. *Anal. Chem.* **2018**, *90*, 11696–11702. [CrossRef]

149. Li, C.; Yang, Y.; Wu, D.; Li, T.; Yin, Y.; Li, G. Improvement of Enzyme-Linked Immunosorbent Assay for the Multicolor Detection of Biomarkers. *Chem. Sci.* **2016**, *7*, 3011–3016. [CrossRef]

150. Liang, M.; Yan, X. Nanozymes: From New Concepts, Mechanisms, and Standards to Applications. *Acc. Chem. Res.* **2019**, *52*, 2190–2200. [CrossRef]

151. Xu, Z.; Long, L.; Chen, Y.; Chen, M.-L.; Cheng, Y.-H. A Nanozyme-Linked Immunosorbent Assay Based on Metal–Organic Frameworks (MOFs) for Sensitive Detection of Aflatoxin B1. *Food Chem.* **2021**, *338*, 128039. [CrossRef]

152. Jin, T.; Li, Y.; Jing, W.; Li, Y.; Fan, L.; Li, X. Cobalt-Based Metal Organic Frameworks: A Highly Active Oxidase-Mimicking Nanozyme for Fluorescence "Turn-on" Assays of Biothiol. *Chem. Commun.* **2020**, *56*, 659–662. [CrossRef]

153. Miao, L.; Jiao, L.; Tang, Q.; Li, H.; Zhang, L.; Wei, Q. A Nanozyme-Linked Immunosorbent Assay for Dual-Modal Colorimetric and Ratiometric Fluorescent Detection of Cardiac Troponin I. *Sens. Actuators B Chem.* **2019**, *288*, 60–64. [CrossRef]

154. Lin, T.; Qin, Y.; Huang, Y.; Yang, R.; Hou, L.; Ye, F.; Zhao, S. A Label-Free Fluorescence Assay for Hydrogen Peroxide and Glucose Based on the Bifunctional MIL-53 (Fe) Nanozyme. *Chem. Commun.* **2018**, *54*, 1762–1765. [CrossRef] [PubMed]

155. Jiao, L.; Zhang, L.; Du, W.; Li, H.; Yang, D.; Zhu, C. Hierarchical Manganese Dioxide Nanoflowers Enable Accurate Ratiometric Fluorescence Enzyme-Linked Immunosorbent Assay. *Nanoscale* **2018**, *10*, 21893–21897. [CrossRef] [PubMed]

156. Asati, A.; Kaittanis, C.; Santra, S.; Perez, J.M. PH-Tunable Oxidase-like Activity of Cerium Oxide Nanoparticles Achieving Sensitive Fluorigenic Detection of Cancer Biomarkers at Neutral PH. *Anal. Chem.* **2011**, *83*, 2547–2553. [CrossRef] [PubMed]

157. Deng, W.; Peng, Y.; Yang, H.; Tan, Y.; Ma, M.; Xie, Q.; Chen, S. Ruthenium Ion-Complexed Carbon Nitride Nanosheets with Peroxidase-like Activity as a Ratiometric Fluorescence Probe for the Detection of Hydrogen Peroxide and Glucose. *ACS Appl. Mater. Interfaces* **2019**, *11*, 29072–29077. [CrossRef] [PubMed]

158. Lee, M.H.; Kim, J.S.; Sessler, J.L. Small Molecule-Based Ratiometric Fluorescence Probes for Cations, Anions, and Biomolecules. *Chem. Soc. Rev.* **2015**, *44*, 4185. [CrossRef]

159. Deng, J.; Wang, K.; Wang, M.; Yu, P.; Mao, L. Mitochondria Targeted Nanoscale Zeolitic Imidazole Framework-90 for ATP Imaging in Live Cells. *J. Am. Chem. Soc.* **2017**, *139*, 5877–5882. [CrossRef]

160. Winarta, J.; Shan, B.; Mcintyre, S.M.; Ye, L.; Wang, C.; Liu, J.; Mu, B. A Decade of UiO-66 Research: A Historic Review of Dynamic Structure, Synthesis Mechanisms, and Characterization Techniques of an Archetypal Metal–Organic Framework. *Cryst. Growth Des.* **2020**, *20*, 1347–1362. [CrossRef]

161. Koo, K.M.; Carrascosa, L.G.; Shiddiky, M.J.A.; Trau, M. Poly(A) Extensions of MiRNAs for Amplification-Free Electrochemical Detection on Screen-Printed Gold Electrodes. *Anal. Chem.* **2016**, *88*, 2000–2005. [CrossRef] [PubMed]

162. Masud, M.K.; Umer, M.; Hossain, M.S.A.; Yamauchi, Y.; Nguyen, N.-T.; Shiddiky, M.J.A. Nanoarchitecture Frameworks for Electrochemical MiRNA Detection. *Trends Biochem. Sci.* **2019**, *44*, 433–452. [CrossRef] [PubMed]

163. Kanjanawarut, R.; Su, X. Colorimetric Detection of DNA Using Unmodified Metallic Nanoparticles and Peptide Nucleic Acid Probes. *Anal. Chem.* **2009**, *81*, 6122–6129. [CrossRef] [PubMed]

164. Li, Y.; Lim, E.; Fields, T.; Wu, H.; Xu, Y.; Wang, Y.A.; Mao, H. Improving Sensitivity and Specificity of Amyloid-β Peptides and Tau Protein Detection with Antibiofouling Magnetic Nanoparticles for Liquid Biopsy of Alzheimer's Disease. *ACS Biomater. Sci. Eng.* **2019**, *5*, 3595–3605. [CrossRef]

165. Blair, E.O.; Corrigan, D.K. A Review of Microfabricated Electrochemical Biosensors for DNA Detection. *Biosens. Bioelectron.* **2019**, *134*, 57–67. [CrossRef] [PubMed]

166. Liu, C.-S.; Zhang, Z.-H.; Chen, M.; Zhao, H.; Duan, F.-H.; Chen, D.-M.; Wang, M.-H.; Zhang, S.; Du, M. Pore Modulation of Zirconium–Organic Frameworks for High-Efficiency Detection of Trace Proteins. *Chem. Commun.* **2017**, *53*, 3941–3944. [CrossRef] [PubMed]

167. Li, Y.; Hu, M.; Huang, X.; Wang, M.; He, L.; Song, Y.; Jia, Q.; Zhou, N.; Zhang, Z.; Du, M. Multicomponent Zirconium-Based Metal-Organic Frameworks for Impedimetric Aptasensing of Living Cancer Cells. *Sens. Actuators B Chem.* **2020**, *306*, 127608. [CrossRef]

168. Qiao, X.; Su, B.; Liu, C.; Song, Q.; Luo, D.; Mo, G.; Wang, T. Selective Surface Enhanced Raman Scattering for Quantitative Detection of Lung Cancer Biomarkers in Superparticle@ MOF Structure. *Adv. Mater.* **2018**, *30*, 1702275. [CrossRef]

169. Ansari, I.; Raddatz, G.; Gutekunst, J.; Ridnik, M.; Cohen, D.; Abu-Remaileh, M.; Tuganbaev, T.; Shapiro, H.; Pikarsky, E.; Elinav, E.; et al. The Microbiota Programs DNA Methylation to Control Intestinal Homeostasis and Inflammation. *Nat. Microbiol.* **2020**, *5*, 610–619. [CrossRef]

170. Alecu, I.; Bennett, S.A.L. Dysregulated Lipid Metabolism and Its Role in α-Synucleinopathy in Parkinson's Disease. *Front. Neurosci.* **2019**, *13*, 328. [CrossRef]

171. Musgrove, R.E.; Helwig, M.; Bae, E.-J.; Aboutalebi, H.; Lee, S.-J.; Ulusoy, A.; Di Monte, D.A. Oxidative Stress in Vagal Neurons Promotes Parkinsonian Pathology and Intercellular α-Synuclein Transfer. *J. Clin. Investig.* **2019**, *129*, 3738–3753. [CrossRef]

172. Scudamore, O.; Ciossek, T. Increased Oxidative Stress Exacerbates α-Synuclein Aggregation In Vivo. *J. Neuropathol. Exp. Neurol.* **2018**, *77*, 443–453. [CrossRef]

173. Luk, K.C. Oxidative Stress and α-Synuclein Conspire in Vulnerable Neurons to Promote Parkinson's Disease Progression. *J. Clin. Investig.* **2019**, *129*, 3530–3531. [CrossRef]

174. McCormack, A.L.; Thiruchelvam, M.; Manning-Bog, A.B.; Thiffault, C.; Langston, J.W.; Cory-Slechta, D.A.; Di Monte, D.A. Environmental Risk Factors and Parkinson's Disease: Selective Degeneration of Nigral Dopaminergic Neurons Caused by the Herbicide Paraquat. *Neurobiol. Dis.* **2002**, *10*, 119–127. [CrossRef] [PubMed]

175. Kam, T.-I.; Mao, X.; Park, H.; Chou, S.-C.; Karuppagounder, S.S.; Umanah, G.E.; Yun, S.P.; Brahmachari, S.; Panicker, N.; Chen, R.; et al. Poly(ADP-Ribose) Drives Pathologic α-Synuclein Neurodegeneration in Parkinson's Disease. *Science* **2018**, *362*, eaat8407. [CrossRef] [PubMed]

176. Liu, Y.-Q.; Mao, Y.; Xu, E.; Jia, H.; Zhang, S.; Dawson, V.L.; Dawson, T.M.; Li, Y.-M.; Zheng, Z.; He, W.; et al. Nanozyme Scavenging ROS for Prevention of Pathologic α-Synuclein Transmission in Parkinson's Disease. *Nano Today* **2021**, *36*, 101027. [CrossRef]

177. Hao, C.; Qu, A.; Xu, L.; Sun, M.; Zhang, H.; Xu, C.; Kuang, H. Chiral Molecule-Mediated Porous Cu$_x$O Nanoparticle Clusters with Antioxidation Activity for Ameliorating Parkinson's Disease. *J. Am. Chem. Soc.* **2019**, *141*, 1091–1099. [CrossRef] [PubMed]

178. Ma, M.; Liu, Z.; Gao, N.; Pi, Z.; Du, X.; Ren, J.; Qu, X. Self-Protecting Biomimetic Nanozyme for Selective and Synergistic Clearance of Peripheral Amyloid-β in an Alzheimer's Disease Model. *J. Am. Chem. Soc.* **2020**, *142*, 21702–21711. [CrossRef]

179. Perry, G.; Cash, A.D.; Smith, M.A. Alzheimer Disease and Oxidative Stress. *J. Biomed. Biotechnol.* **2002**, *2*, 120–123. [CrossRef] [PubMed]

180. Patnode, C.D.; Perdue, L.A.; Rossom, R.C.; Rushkin, M.C.; Redmond, N.; Thomas, R.G.; Lin, J.S. *Screening for Cognitive Impairment in Older Adults: An Evidence Update for the U.S. Preventive Services Task Force*; U.S. Preventive Services Task Force Evidence Syntheses, Formerly Systematic Evidence Reviews; Agency for Healthcare Research and Quality (US): Rockville, MD, USA, 2020.

181. *Swedish Council on Health Technology Assessment Dementia—Caring, Ethics, Ethnical and Economical Aspects: A Systematic Review*; SBU Systematic Reviews; Swedish Council on Health Technology Assessment (SBU): Stockholm, Sweden, 2008; ISBN 978-91-85413-23-2.

182. Tomita, T. Aberrant Proteolytic Processing and Therapeutic Strategies in Alzheimer Disease. *Adv. Biol. Regul.* **2017**, *64*, 33–38. [CrossRef]

183. Shin, S.J.; Jeon, S.G.; Kim, J.; Jeong, Y.; Kim, S.; Park, Y.H.; Lee, S.-K.; Park, H.H.; Hong, S.B.; Oh, S.; et al. Red Ginseng Attenuates Aβ-Induced Mitochondrial Dysfunction and Aβ-Mediated Pathology in an Animal Model of Alzheimer's Disease. *Int. J. Mol. Sci.* **2019**, *20*, 3030. [CrossRef] [PubMed]

184. Kwon, H.J.; Cha, M.-Y.; Kim, D.; Kim, D.K.; Soh, M.; Shin, K.; Hyeon, T.; Mook-Jung, I. Mitochondria-Targeting Ceria Nanoparticles as Antioxidants for Alzheimer's Disease. *ACS Nano* **2016**, *10*, 2860–2870. [CrossRef] [PubMed]

185. Guan, Y.; Li, M.; Dong, K.; Gao, N.; Ren, J.; Zheng, Y.; Qu, X. Ceria/POMs Hybrid Nanoparticles as a Mimicking Metallopeptidase for Treatment of Neurotoxicity of Amyloid-β Peptide. *Biomaterials* **2016**, *98*, 92–102. [CrossRef] [PubMed]

186. Gao, N.; Sun, H.; Dong, K.; Ren, J.; Duan, T.; Xu, C.; Qu, X. Transition-Metal-Substituted Polyoxometalate Derivatives as Functional Anti-Amyloid Agents for Alzheimer's Disease. *Nat. Commun.* **2014**, *5*, 1–9. [CrossRef] [PubMed]

187. Zhang, Y.; Wang, Z.; Li, X.; Wang, L.; Yin, M.; Wang, L.; Chen, N.; Fan, C.; Song, H. Dietary Iron Oxide Nanoparticles Delay Aging and Ameliorate Neurodegeneration in Drosophila. *Adv. Mater.* **2016**, *28*, 1387–1393. [CrossRef] [PubMed]

188. Moloney, A.; Sattelle, D.B.; Lomas, D.A.; Crowther, D.C. Alzheimer's Disease: Insights from Drosophila Melanogaster Models. *Trends Biochem. Sci.* **2010**, *35*, 228–235. [CrossRef]

189. Ha, C.; Ryu, J.; Park, C.B. Metal Ions Differentially Influence the Aggregation and Deposition of Alzheimer's β-Amyloid on a Solid Template. *Biochemistry* **2007**, *46*, 6118–6125. [CrossRef]

190. Ejaz, H.W.; Wang, W.; Lang, M. Copper Toxicity Links to Pathogenesis of Alzheimer's Disease and Therapeutics Approaches. *Int. J. Mol. Sci.* **2020**, *21*, 7660. [CrossRef]

191. Kenche, V.B.; Barnham, K.J. Alzheimer's Disease & Metals: Therapeutic Opportunities. *Br. J. Pharmacol.* **2011**, *163*, 211–219.

192. Dickinson, B.C.; Chang, C.J. Chemistry and Biology of Reactive Oxygen Species in Signaling or Stress Responses. *Nat. Chem. Biol.* **2011**, *7*, 504–511. [CrossRef]

193. Klotz, L.-O.; Steinbrenner, H. Cellular Adaptation to Xenobiotics: Interplay between Xenosensors, Reactive Oxygen Species and FOXO Transcription Factors. *Redox Biol.* **2017**, *13*, 646–654. [CrossRef]

194. Forrester, S.J.; Kikuchi, D.S.; Hernandes, M.S.; Xu, Q.; Griendling, K.K. Reactive Oxygen Species in Metabolic and Inflammatory Signaling. *Circ. Res.* **2018**, *122*, 877–902. [CrossRef]

195. de Jager, T.L.; Cockrell, A.E.; Du Plessis, S.S. Ultraviolet Light Induced Generation of Reactive Oxygen Species. In *Ultraviolet Light in Human Health, Diseases and Environment*; Advances in Experimental Medicine and Biology; Ahmad, S.I., Ed.; Springer International Publishing: Cham, Switzerland, 2017; Volume 996, pp. 15–23, ISBN 978-3-319-56016-8.

196. Opie, L.H. Cardiac Metabolism in Health and Disease. In *Cellular and Molecular Pathobiology of Cardiovascular Disease*; Elsevier: Amsterdam, The Netherlands, 2014; pp. 23–36, ISBN 978-0-12-405206-2.

197. Alili, L.; Sack, M.; von Montfort, C.; Giri, S.; Das, S.; Carroll, K.S.; Zanger, K.; Seal, S.; Brenneisen, P. Downregulation of Tumor Growth and Invasion by Redox-Active Nanoparticles. *Antioxid. Redox Signal.* **2013**, *19*, 765–778. [CrossRef]

198. Arnott, J.A.; Planey, S.L. The Influence of Lipophilicity in Drug Discovery and Design. *Expert Opin. Drug Discov.* **2012**, *7*, 863–875. [CrossRef]

199. Forte, E.; Fiorenza, D.; Torino, E.; Costagliola di Polidoro, A.; Cavaliere, C.; Netti, P.A.; Salvatore, M.; Aiello, M. Radiolabeled PET/MRI Nanoparticles for Tumor Imaging. *J. Clin. Med.* **2020**, *9*, 89. [CrossRef]

200. Kochebina, O.; Halty, A.; Taleb, J.; Kryza, D.; Janier, M.; Sadr, A.B.; Baudier, T.; Rit, S.; Sarrut, D. In Vivo Gadolinium Nanoparticle Quantification with SPECT/CT. *EJNMMI Phys.* **2019**, *6*, 9. [CrossRef]

201. Mao, X.; Xu, J.; Cui, H. Functional Nanoparticles for Magnetic Resonance Imaging. *Wiley Interdiscip. Rev. Nanomed. Nanobiotechnol.* **2016**, *8*, 814–841. [CrossRef] [PubMed]

202. Piergies, N.; Oćwieja, M.; Paluszkiewicz, C.; Kwiatek, W.M. Spectroscopic Insights into the Effect of PH, Temperature, and Stabilizer on Erlotinib Adsorption Behavior onto Ag Nanosurface. *Spectrochim. Acta A Mol. Biomol. Spectrosc.* **2019**, 117737. [CrossRef] [PubMed]

203. Maeda, H. The Enhanced Permeability and Retention (EPR) Effect in Tumor Vasculature: The Key Role of Tumor-Selective Macromolecular Drug Targeting. *Adv. Enzym. Regul.* **2001**, *41*, 189–207. [CrossRef]

204. Yang, C.; Liu, H.Z.; Fu, Z.X.; Lu, W.D. Oxaliplatin Long-Circulating Liposomes Improved Therapeutic Index of Colorectal Carcinoma. *BMC Biotechnol.* **2011**, *11*, 21. [CrossRef] [PubMed]

205. Maeda, H.; Matsumura, Y. Tumoritropic and Lymphotropic Principles of Macromolecular Drugs. *Crit. Rev. Ther. Drug Carr. Syst.* **1988**, *6*, 193–210.

206. Maeda, H. SMANCS and Polymer-Conjugated Macromolecular Drugs: Advantages in Cancer Chemotherapy. *Adv. Drug Deliv. Rev.* **2001**, *46*, 169–185. [CrossRef]

207. Maeda, H.; Seymour, L.W.; Miyamoto, Y. Conjugates of Anticancer Agents and Polymers: Advantages of Macromolecular Therapeutics In Vivo. *Bioconj. Chem.* **1992**, *3*, 351–362. [CrossRef]

208. Wang, X.; Guo, W.; Hu, Y.; Wu, J.; Wei, H. Nanozymes: Next Wave of Artificial Enzymes. In *SpringerBriefs in Molecular Science*; Springer: Berlin/Heidelberg, Germany, 2016; ISBN 978-3-662-53066-5.

209. Fan, M.; Han, Y.; Gao, S.; Yan, H.; Cao, L.; Li, Z.; Liang, X.-J.; Zhang, J. Ultrasmall Gold Nanoparticles in Cancer Diagnosis and Therapy. *Theranostics* **2020**, *10*, 4944–4957. [CrossRef]

210. He, J.; Liu, S.; Zhang, Y.; Chu, X.; Lin, Z.; Zhao, Z.; Qiu, S.; Guo, Y.; Ding, H.; Pan, Y.; et al. The Application of and Strategy for Gold Nanoparticles in Cancer Immunotherapy. *Front. Pharmacol.* **2021**, *12*, 687399. [CrossRef]

211. Wang, S.; Lu, G. Applications of Gold Nanoparticles in Cancer Imaging and Treatment. In *Noble and Precious Metals—Properties, Nanoscale Effects and Applications*; Seehra, M.S., Bristow, A.D., Eds.; InTech: London, UK, 2018; ISBN 978-1-78923-292-9.

212. García Calavia, P.; Bruce, G.; Pérez-García, L.; Russell, D.A. Photosensitiser-Gold Nanoparticle Conjugates for Photodynamic Therapy of Cancer. *Photochem. Photobiol. Sci.* **2018**, *17*, 1534–1552. [CrossRef]

213. Dan, Q.; Hu, D.; Ge, Y.; Zhang, S.; Li, S.; Gao, D.; Luo, W.; Ma, T.; Liu, X.; Zheng, H.; et al. Ultrasmall Theranostic Nanozymes to Modulate Tumor Hypoxia for Augmenting Photodynamic Therapy and Radiotherapy. *Biomater. Sci.* **2020**, *8*, 973–987. [CrossRef] [PubMed]

214. Wang, D.; Wu, H.; Wang, C.; Gu, L.; Chen, H.; Jana, D.; Feng, L.; Liu, J.; Wang, X.; Xu, P.; et al. Self-Assembled Single-Site Nanozyme for Tumor-Specific Amplified Cascade Enzymatic Therapy. *Angew. Chem. Int. Ed.* **2021**, *60*, 3001–3007. [CrossRef]

215. Guo, Z.; Li, C.; Gao, M.; Han, X.; Zhang, Y.; Zhang, W.; Li, W. Inside Cover: Mn−O Covalency Governs the Intrinsic Activity of Co-Mn Spinel Oxides for Boosted Peroxymonosulfate Activation (Angew. Chem. Int. Ed. 1/2021). *Angew. Chem. Int. Ed.* **2021**, *60*, 2. [CrossRef]

216. Cramer, F.; Kampe, W. Inclusion Compounds. XVII.[1] Catalysis of Decarboxylation by Cyclodextrins. A Model Reaction for the Mechanism of Enzymes. *J. Am. Chem. Soc.* **1965**, *87*, 1115–1120. [CrossRef] [PubMed]

217. Sutrisno, L.; Hu, Y.; Hou, Y.; Cai, K.; Li, M.; Luo, Z. Progress of Iron-Based Nanozymes for Antitumor Therapy. *Front. Chem.* **2020**, *8*, 680. [CrossRef] [PubMed]

218. Fan, K.; Cao, C.; Pan, Y.; Lu, D.; Yang, D.; Feng, J.; Song, L.; Liang, M.; Yan, X. Magnetoferritin Nanoparticles for Targeting and Visualizing Tumour Tissues. *Nat. Nanotechnol.* **2012**, *7*, 459–464. [CrossRef] [PubMed]

219. He, J.; Fan, K.; Yan, X. Ferritin Drug Carrier (FDC) for Tumor Targeting Therapy. *J. Control. Release* **2019**, *311–312*, 288–300. [CrossRef]

220. Chen, D.; Li, B.; Jiang, L.; Duan, D.; Li, Y.; Wang, J.; He, J.; Zeng, Y. Highly Efficient Colorimetric Detection of Cancer Cells Utilizing Fe-MIL-101 with Intrinsic Peroxidase-like Catalytic Activity over a Broad PH Range. *RSC Adv.* **2015**, *5*, 97910–97917. [CrossRef]

221. Chen, Y.; Zhong, H.; Wang, J.; Wan, X.; Li, Y.; Pan, W.; Li, N.; Tang, B. Catalase-like Metal–Organic Framework Nanoparticles to Enhance Radiotherapy in Hypoxic Cancer and Prevent Cancer Recurrence. *Chem. Sci.* **2019**, *10*, 5773–5778. [CrossRef] [PubMed]

222. Munjal, T.; Dutta, S. Biocompatible Nanoreactors of Catalase and Nanozymes for Anticancer Therapeutics. *Nano Select* **2021**. nano.202100040. [CrossRef]

223. Li, S.; Shang, L.; Xu, B.; Wang, S.; Gu, K.; Wu, Q.; Sun, Y.; Zhang, Q.; Yang, H.; Zhang, F.; et al. A Nanozyme with Photo-Enhanced Dual Enzyme-Like Activities for Deep Pancreatic Cancer Therapy. *Angew. Chem. Int. Ed.* **2019**, *58*, 12624–12631. [CrossRef]

224. Petty, H.R. Could Nanoparticles That Mimic the NADPH Oxidase Be Used to Kill Tumor Cells? *Nanomedicine* **2016**, *11*, 1631–1634. [CrossRef]

225. Clark, A.J.; Petty, H.R. WO$_3$/Pt Nanoparticles Promote Light-Induced Lipid Peroxidation and Lysosomal Instability within Tumor Cells. *Nanotechnology* **2016**, *27*, 075103. [CrossRef]

226. Clark, A.J.; Coury, E.L.; Meilhac, A.M.; Petty, H.R. WO$_3$/Pt Nanoparticles Are NADPH Oxidase Biomimetics That Mimic Effector Cells In Vitro and In Vivo. *Nanotechnology* **2016**, *27*, 065101. [CrossRef] [PubMed]

227. Gong, F.; Cheng, L.; Yang, N.; Betzer, O.; Feng, L.; Zhou, Q.; Li, Y.; Chen, R.; Popovtzer, R.; Liu, Z. Ultrasmall Oxygen-Deficient Bimetallic Oxide MnWO$_X$ Nanoparticles for Depletion of Endogenous GSH and Enhanced Sonodynamic Cancer Therapy. *Adv. Mater.* **2019**, *31*, 1900730. [CrossRef] [PubMed]

228. Zhao, P.; Deng, Y.; Xiang, G.; Liu, Y. Nanoparticle-Assisted Sonosensitizers and Their Biomedical Applications. *IJN* **2021**, *16*, 4615–4630. [CrossRef] [PubMed]

229. Lin, X.; Song, J.; Chen, X.; Yang, H. Ultrasound-Activated Sensitizers and Applications. *Angew. Chem. Int. Ed.* **2020**, *59*, 14212–14233. [CrossRef] [PubMed]

230. Han, X.; Huang, J.; Jing, X.; Yang, D.; Lin, H.; Wang, Z.; Li, P.; Chen, Y. Oxygen-Deficient Black Titania for Synergistic/Enhanced Sonodynamic and Photoinduced Cancer Therapy at Near Infrared-II Biowindow. *ACS Nano* **2018**, *12*, 4545–4555. [CrossRef] [PubMed]

231. Wang, X.; Zhong, X.; Bai, L.; Xu, J.; Gong, F.; Dong, Z.; Yang, Z.; Zeng, Z.; Liu, Z.; Cheng, L. Ultrafine Titanium Monoxide (TiO$_{1+x}$) Nanorods for Enhanced Sonodynamic Therapy. *J. Am. Chem. Soc.* **2020**, *142*, 6527–6537. [CrossRef] [PubMed]

232. Siddiqui, M.A.; Alhadlaq, H.A.; Ahmad, J.; Al-Khedhairy, A.A.; Musarrat, J.; Ahamed, M. Copper Oxide Nanoparticles Induced Mitochondria Mediated Apoptosis in Human Hepatocarcinoma Cells. *PLoS ONE* **2013**, *8*, e69534. [CrossRef] [PubMed]

233. Xu, J.; Li, Z.; Xu, P.; Xiao, L.; Yang, Z. Nanosized Copper Oxide Induces Apoptosis through Oxidative Stress in Podocytes. *Arch. Toxicol.* **2013**, *87*, 1067–1073. [CrossRef]

234. Perreault, F.; Melegari, S.P.; da Costa, C.H.; Rossetto, A.L.D.O.F.; Popovic, R.; Matias, W.G. Genotoxic Effects of Copper Oxide Nanoparticles in Neuro 2A Cell Cultures. *Sci. Total Environ.* **2012**, *441*, 117–124. [CrossRef]

235. Mkandawire, M.M.; Lakatos, M.; Springer, A.; Clemens, A.; Appelhans, D.; Krause-Buchholz, U.; Pompe, W.; Rödel, G.; Mkandawire, M. Induction of Apoptosis in Human Cancer Cells by Targeting Mitochondria with Gold Nanoparticles. *Nanoscale* **2015**, *7*, 10634–10640. [CrossRef]

236. Wang, P.; Liu, S.; Hu, M.; Zhang, H.; Duan, D.; He, J.; Hong, J.; Lv, R.; Choi, H.S.; Yan, X. Peroxidase-Like Nanozymes Induce a Novel Form of Cell Death and Inhibit Tumor Growth In Vivo. *Adv. Funct. Mater.* **2020**, *30*, 2000647. [CrossRef]

237. Chen, S.; Quan, Y.; Yu, Y.-L.; Wang, J.-H. Graphene Quantum Dot/Silver Nanoparticle Hybrids with Oxidase Activities for Antibacterial Application. *ACS Biomater. Sci. Eng.* **2017**, *3*, 313–321. [CrossRef] [PubMed]

238. Wang, Z.; Dong, K.; Liu, Z.; Zhang, Y.; Chen, Z.; Sun, H.; Ren, J.; Qu, X. Corrigendum to "Activation of Biologically Relevant Levels of Reactive Oxygen Species by Au/g-C$_3$N$_4$ Hybrid Nanozyme for Bacteria Killing and Wound Disinfection" [Biomaterials, 113(2017)145–157]. *Biomaterials* **2020**, *233*, 119754. [CrossRef] [PubMed]

239. Zhang, Y.; Jin, Y.; Cui, H.; Yan, X.; Fan, K. Nanozyme-Based Catalytic Theranostics. *RSC Adv.* **2020**, *10*, 10–20. [CrossRef]

240. Ji, H.; Dong, K.; Yan, Z.; Ding, C.; Chen, Z.; Ren, J.; Qu, X. Bacterial Hyaluronidase Self-Triggered Prodrug Release for Chemo-Photothermal Synergistic Treatment of Bacterial Infection. *Small* **2016**, *12*, 6200–6206. [CrossRef]

241. Herget, K.; Hubach, P.; Pusch, S.; Deglmann, P.; Götz, H.; Gorelik, T.E.; Gural'skiy, I.A.; Pfitzner, F.; Link, T.; Schenk, S.; et al. Haloperoxidase Mimicry by CeO$_{2-x}$ Nanorods Combats Biofouling. *Adv. Mater.* **2017**, *29*, 1603823. [CrossRef]

242. Gao, L.; Giglio, K.M.; Nelson, J.L.; Sondermann, H.; Travis, A.J. Ferromagnetic Nanoparticles with Peroxidase-like Activity Enhance the Cleavage of Biological Macromolecules for Biofilm Elimination. *Nanoscale* **2014**, *6*, 2588–2593. [CrossRef]

243. Xi, J.; Wei, G.; An, L.; Xu, Z.; Xu, Z.; Fan, L.; Gao, L. Copper/Carbon Hybrid Nanozyme: Tuning Catalytic Activity by the Copper State for Antibacterial Therapy. *Nano Lett.* **2019**, *19*, 7645–7654. [CrossRef]

244. Li, Y.; Zhu, W.; Li, J.; Chu, H. Research Progress in Nanozyme-Based Composite Materials for Fighting against Bacteria and Biofilms. *Colloids Surf. B Biointerfaces* **2020**, *198*, 111465. [CrossRef]

245. Cao, F.; Zhang, L.; Wang, H.; You, Y.; Wang, Y.; Gao, N.; Ren, J.; Qu, X. Defect-Rich Adhesive Nanozymes as Efficient Antibiotics for Enhanced Bacterial Inhibition. *Angew. Chem. Int. Ed.* **2019**, *58*, 16236–16242. [CrossRef]

246. Wang, L.; Gao, F.; Wang, A.; Chen, X.; Li, H.; Zhang, X.; Zheng, H.; Ji, R.; Li, B.; Yu, X. Defect-Rich Adhesive Molybdenum Disulfide/RGO Vertical Heterostructures with Enhanced Nanozyme Activity for Smart Bacterial Killing Application. *Adv. Mater.* **2020**, *32*, 2005423. [CrossRef]

247. Chen, Z.; Ji, H.; Liu, C.; Bing, W.; Wang, Z.; Qu, X. A Multinuclear Metal Complex Based DNase-Mimetic Artificial Enzyme: Matrix Cleavage for Combating Bacterial Biofilms. *Angew. Chem. Int. Ed.* **2016**, *55*, 10732–10736. [CrossRef] [PubMed]

248. Gao, L.; Liu, Y.; Kim, D.; Li, Y.; Hwang, G.; Naha, P.C.; Cormode, D.P.; Koo, H. Nanocatalysts Promote Streptococcus Mutans Biofilm Matrix Degradation and Enhance Bacterial Killing to Suppress Dental Caries In Vivo. *Biomaterials* **2016**, *101*, 272–284. [CrossRef] [PubMed]

249. Xu, Z.; Qiu, Z.; Liu, Q.; Huang, Y.; Li, D.; Shen, X.; Fan, K.; Xi, J.; Gu, Y.; Tang, Y.; et al. Converting Organosulfur Compounds to Inorganic Polysulfides against Resistant Bacterial Infections. *Nat. Commun.* **2018**, *9*, 3713. [CrossRef] [PubMed]

250. Zhao, X.; Jia, Y.; Li, J.; Dong, R.; Zhang, J.; Ma, C.; Wang, H.; Rui, Y.; Jiang, X. Indole Derivative-Capped Gold Nanoparticles as an Effective Bactericide in Vivo. *ACS Appl. Mater. Interfaces* **2018**, *10*, 29398–29406. [CrossRef]

251. Cai, S.; Jia, X.; Han, Q.; Yan, X.; Yang, R.; Wang, C. Porous Pt/Ag Nanoparticles with Excellent Multifunctional Enzyme Mimic Activities and Antibacterial Effects. *Nano Res.* **2017**, *10*, 2056–2069. [CrossRef]

252. Mo, S.; Chen, X.; Chen, M.; He, C.; Lu, Y.; Zheng, N. Two-Dimensional Antibacterial Pd@ Ag Nanosheets with a Synergetic Effect of Plasmonic Heating and Ag+ Release. *J. Mater. Chem. B* **2015**, *3*, 6255–6260. [CrossRef] [PubMed]

253. Chen, W.-Y.; Lin, J.-Y.; Chen, W.-J.; Luo, L.; Wei-Guang Diau, E.; Chen, Y.-C. Functional Gold Nanoclusters as Antimicrobial Agents for Antibiotic-Resistant Bacteria. *Nanomedicine* **2010**, *5*, 755–764. [CrossRef]

254. Boomi, P.; Prabu, H.G.; Mathiyarasu, J. Synthesis and Characterization of Polyaniline/Ag–Pt Nanocomposite for Improved Antibacterial Activity. *Colloids Surf. B Biointerfaces* **2013**, *103*, 9–14. [CrossRef]

255. Adams, C.P.; Walker, K.A.; Obare, S.O.; Docherty, K.M. Size-Dependent Antimicrobial Effects of Novel Palladium Nanoparticles. *PLoS ONE* **2014**, *9*, e85981. [CrossRef]

256. Wang, Z.; Dong, K.; Liu, Z.; Zhang, Y.; Chen, Z.; Sun, H.; Ren, J.; Qu, X. Activation of Biologically Relevant Levels of Reactive Oxygen Species by Au/g-C3N4 Hybrid Nanozyme for Bacteria Killing and Wound Disinfection. *Biomaterials* **2017**, *113*, 145–157. [CrossRef]

257. Liu, Z.; Wang, F.; Ren, J.; Qu, X. A Series of MOF/Ce-Based Nanozymes with Dual Enzyme-like Activity Disrupting Biofilms and Hindering Recolonization of Bacteria. *Biomaterials* **2019**, *208*, 21–31. [CrossRef] [PubMed]

258. Zhao, Y.; Li, H.; Wang, Y.; Wang, Y.; Huang, Z.; Su, H.; Liu, J. CeO2 Nanoparticle Transformation to Nanorods and Nanoflowers in Acids with Boosted Oxidative Catalytic Activity. *ACS Appl. Nano Mater.* **2021**, *4*, 2098–2107. [CrossRef]

259. Zhu, W.; Wang, L.; Li, Q.; Jiao, L.; Yu, X.; Gao, X.; Qiu, H.; Zhang, Z.; Bing, W. Will the Bacteria Survive in the CeO2 Nanozyme-H2O2 System? *Molecules* **2021**, *26*, 3747. [CrossRef] [PubMed]

260. Filippi, A.; Liu, F.; Wilson, J.; Lelieveld, S.; Korschelt, K.; Wang, T.; Wang, Y.; Reich, T.; Pöschl, U.; Tremel, W.; et al. Antioxidant Activity of Cerium Dioxide Nanoparticles and Nanorods in Scavenging Hydroxyl Radicals. *RSC Adv.* **2019**, *9*, 11077–11081. [CrossRef]

261. Tammina, S.K.; Wan, Y.; Li, Y.; Yang, Y. Synthesis of N, Zn-Doped Carbon Dots for the Detection of Fe3+ Ions and Bactericidal Activity against Escherichia Coli and Staphylococcus Aureus. *J. Photochem. Photobiol. B Biol.* **2020**, *202*, 111734. [CrossRef] [PubMed]

262. Sun, D.; Pang, X.; Cheng, Y.; Ming, J.; Xiang, S.; Zhang, C.; Lv, P.; Chu, C.; Chen, X.; Liu, G. Ultrasound-Switchable Nanozyme Augments Sonodynamic Therapy against Multidrug-Resistant Bacterial Infection. *ACS Nano* **2020**, *14*, 2063–2076. [CrossRef] [PubMed]

263. Sang, Y.; Li, W.; Liu, H.; Zhang, L.; Wang, H.; Liu, Z.; Ren, J.; Qu, X. Construction of Nanozyme-hydrogel for Enhanced Capture and Elimination of Bacteria. *Adv. Funct. Mater.* **2019**, *29*, 1900518. [CrossRef]

264. Zhang, L.; Liu, Z.; Deng, Q.; Sang, Y.; Dong, K.; Ren, J.; Qu, X. Nature-Inspired Construction of MOF@ COF Nanozyme with Active Sites in Tailored Microenvironment and Pseudopodia-Like Surface for Enhanced Bacterial Inhibition. *Angew. Chem. Int. Ed.* **2021**, *60*, 3469–3474. [CrossRef]

265. Roberts, R.E.; Hallett, M.B. Neutrophil Cell Shape Change: Mechanism and Signalling during Cell Spreading and Phagocytosis. *Int. J. Mol. Sci.* **2019**, *20*, 1383. [CrossRef]

266. Gao, L.; Fan, K.; Yan, X. Iron Oxide Nanozyme: A Multifunctional Enzyme Mimetics for Biomedical Application. *Nanozymology* **2020**, 105–140. [CrossRef]

267. Qin, T.; Ma, R.; Yin, Y.; Miao, X.; Chen, S.; Fan, K.; Xi, J.; Liu, Q.; Gu, Y.; Yin, Y. Catalytic Inactivation of Influenza Virus by Iron Oxide Nanozyme. *Theranostics* **2019**, *9*, 6920. [CrossRef] [PubMed]

268. Qin, T.; Ma, S.; Miao, X.; Tang, Y.; Huangfu, D.; Wang, J.; Jiang, J.; Xu, N.; Yin, Y.; Chen, S.; et al. Mucosal Vaccination for Influenza Protection Enhanced by Catalytic Immune-Adjuvant. *Adv. Sci.* **2020**, *7*, 2000771. [CrossRef]

269. Ravishankar Rai, V. Nanoparticles and Their Potential Application as Antimicrobials. 2011.

270. Galdiero, S.; Falanga, A.; Vitiello, M.; Cantisani, M.; Marra, V.; Galdiero, M. Silver Nanoparticles as Potential Antiviral Agents. *Molecules* **2011**, *16*, 8894–8918. [CrossRef]

271. Fouad, G.I. A Proposed Insight into the Anti-Viral Potential of Metallic Nanoparticles against Novel Coronavirus Disease-19 (COVID-19). *Bull. Natl. Res. Cent.* **2021**, *45*, 1–22.

272. Lin, N.; Verma, D.; Saini, N.; Arbi, R.; Munir, M.; Jovic, M.; Turak, A. Antiviral Nanoparticles for Sanitizing Surfaces: A Roadmap to Self-Sterilizing against COVID-19. *Nano Today* **2021**, 101267. [CrossRef] [PubMed]

273. Vazquez-Munoz, R.; Lopez-Ribot, J.L. Nanotechnology as an Alternative to Reduce the Spread of COVID-19. *Challenges* **2020**, *11*, 15. [CrossRef]

274. Vahedifard, F.; Chakravarthy, K. Nanomedicine for COVID-19: The Role of Nanotechnology in the Treatment and Diagnosis of COVID-19. *Emergent Mater.* **2021**, *4*, 75–99. [CrossRef] [PubMed]

275. Huang, X.; Li, M.; Xu, Y.; Zhang, J.; Meng, X.; An, X.; Sun, L.; Guo, L.; Shan, X.; Ge, J.; et al. Novel Gold Nanorod-Based HR1 Peptide Inhibitor for Middle East Respiratory Syndrome Coronavirus. *ACS Appl. Mater. Interfaces* **2019**, *11*, 19799–19807. [CrossRef]

276. Antoine, T.E.; Mishra, Y.K.; Trigilio, J.; Tiwari, V.; Adelung, R.; Shukla, D. Prophylactic, Therapeutic and Neutralizing Effects of Zinc Oxide Tetrapod Structures against Herpes Simplex Virus Type-2 Infection. *Antivir. Res.* **2012**, *96*, 363–375. [CrossRef]

277. Tabish, T.A.; Hamblin, M.R. Multivalent Nanomedicines to Treat COVID-19: A Slow Train Coming. *Nano Today* **2020**, *35*, 100962. [CrossRef]

278. Zhao, S.; Duan, H.; Yang, Y.; Yan, X.; Fan, K. Fenozyme Protects the Integrity of the Blood–Brain Barrier against Experimental Cerebral Malaria. *Nano Lett.* **2019**, *19*, 8887–8895. [CrossRef] [PubMed]

279. Zhang, R.; Fan, K.; Yan, X. Nanozymes: Created by Learning from Nature. *Sci. China Life Sci.* **2020**, *63*, 1183–1200. [CrossRef] [PubMed]

280. Guo, F.F.; Yang, W.; Jiang, W.; Geng, S.; Peng, T.; Li, J.L. Magnetosomes Eliminate Intracellular Reactive Oxygen Species in Magnetospirillum Gryphiswaldense MSR-1. *Environ. Microbiol.* **2012**, *14*, 1722–1729. [CrossRef] [PubMed]

281. Jiang, B.; Fang, L.; Wu, K.; Yan, X.; Fan, K. Ferritins as Natural and Artificial Nanozymes for Theranostics. *Theranostics* **2020**, *10*, 687–706. [CrossRef] [PubMed]

282. Tang, Z.; Wu, H.; Zhang, Y.; Li, Z.; Lin, Y. Enzyme-Mimic Activity of Ferric Nano-Core Residing in Ferritin and Its Biosensing Applications. *Anal. Chem.* **2011**, *83*, 8611–8616. [CrossRef] [PubMed]